UNIVERSITY OF TEXAS ARLINGTON

TxDOT Report 0-6872-01-1

# Use of Geothermal Energy for De-Icing Approach Pavement Slabs and Bridge Decks – Phase II


Xinbao Yu
Anand Puppala
Gang Lei
Punee Bhaskar
Alireza Fakhrabadi
Aditya Deshmukh



| | |
|---|---|
| Report Publication Date: | Submitted: September 2024<br>Published: February 2025 |
| Project: | 0-6872-01 |
| Project Title: | Use of Geothermal Energy for De-Icing Approach Pavement Slabs and Bridge Decks – Phase II |

Technical Report Documentation Page

| 1. Report No.<br>FHWA/TX-25/0-6872-01-1 | 2. Government Accession No. | 3. Recipient's Catalog No. |
|---|---|---|
| 4. Title and Subtitle<br>Use of Geothermal Energy for Deicing Approach Pavement Slabs and Bridge Decks | | 5. Report Date<br>Submitted: 09/2024<br>6. Performing Organization Code |
| 7. Author(s)<br>Xinbao Yu; Ph.D., P.E., M. ASCE, Orcid ID: 0000-0002-5681-0390. Anand J. Puppala, Ph.D., P.E., D.GE., F-ICE, Dist. M. ASCE, Orcid ID: 0000-0003-0435-6285. Alireza Fakhrabadi; M.S., S.M. ASCE, Orcid ID: 0009-0003-1982-6267. Aditya Deshmukh; M.S., EIT, S.M. ASCE, Orcid ID: 0000-0001-7855-3703. Gang Lei; Ph.D., A.M. ASCE, Orcid ID: 0000-0002-5144-0458. Puneet Bhaskar, Ph.D., A.M. ASCE, Orcid ID: 0009-0008-0973-9879. | | 8. Performing Organization Report No.<br>0-6872-01 |
| 9. Performing Organization Name and Address<br>Department of Civil Engineering<br>The University of Texas at Arlington<br>P.O. Box 19308<br>Arlington, TX 76019 | | 10. Work Unit No. (TRAIS)<br>11. Contract or Grant No.<br>0-6872-01 |
| 12. Sponsoring Agency Name and Address<br>Texas Department of Transportation<br>Research and Technology Implementation Division<br>125 E. 11th Street<br>Austin, TX 78701 | | 13. Type of Report and Period Covered<br>Technical Report<br>October 2020 – August 2024<br>14. Sponsoring Agency Code |

15. Supplementary Notes
Project performed in cooperation with the Texas Department of Transportation and the Federal Highway Administration.

16. Abstract
Bridges in many parts of Texas are prone to icing on the bridge deck during winter events, which poses severe travel disruptions and potential accidents to the drivers. Therefore, bridge deicing is critical to ensure roadway safety, mobility, and productivity reasons. This study tested and implemented a geothermal bridge deicing system (GBDS) as a sustainable solution to prevent ice accumulation on bridge decks. The lab and field study included laboratory-scale heated slab tests, the development of a mock-up geothermal bridge, and the implementation of an in-service pilot geothermal bridge. Finite Element Method (FEM) simulations were performed to optimize system design, including heat flux analysis, hydronic heating loops, and ground loop heat exchangers. The pilot geothermal bridge's performance was assessed under real-world winter conditions by monitoring and collecting field performance data. Additionally, a life cycle cost-benefit analysis was performed to assess the economic viability of geothermal deicing compared to conventional methods, considering installation, maintenance, and operational costs alongside benefits such as corrosion prevention, improved safety, and enhanced traffic flow. Finally, an operational manual was developed regarding the control, maintenance, and monitoring of the pilot geothermal bridge deicing system. The findings have shown that geothermal bridge deicing is an effective and cost-efficient alternative for winter road maintenance, enhancing transportation safety while reducing reliance on chemical deicers.

| 17. Key Words | 18. Distribution Statement |
|---|---|
| Bridge deicing, pavement deicing, in-service bridge, full-scale, shallow geothermal, externally heated bridge deck, heated bridge technology, renewable energy. | No restrictions. This document is available to the public through the National Technical Information Service, Alexandria, Virginia 22312; www.ntis.gov. |

| 19. Security Classif. (of report) | 20. Security Classif. (of this page) | 21. No. of pages | 22. Price |
|---|---|---|---|
| Unclassified | Unclassified | TBD [Total count excl. cover] | |

Form DOT F 1700.7 (8-72) Reproduction of completed page authorized

# USE OF GEOTHERMAL ENERGY FOR DE-ICING APPROACH PAVEMENT SLABS AND BRIDGE DECKS

# PHASE II

By

Xinbao Yu
Professor
Department of Civil Engineering
The University of Texas at Arlington

Anand Puppala
Professor
Texas A&M Transportation Institute
College Station, TX

Graduate Research Assistants: Alireza Fakhrabadi, Aditya Deshmukh

Post-docs: Gang Lei, Puneet Bhaskar

Project Number 0-6872-01
Research Project Title: Use of Geothermal Energy for Deicing Approach Pavement Slabs and Bridge Decks-Phase II

Sponsored by the
Texas Department of Transportation

September 26, 2024

Department of Civil Engineering
The University of Texas at Arlington
P.O. Box 19308
Arlington, TX 76019

## Disclaimers

**Author's Disclaimer**: The contents of this report reflect the views of the authors, who are responsible for the facts and the accuracy of the data presented herein. The contents do not necessarily reflect the official view or policies of the Federal Highway Administration or the Texas Department of Transportation (TxDOT). This report does not constitute a standard, specification, or regulation.

**Patent Disclaimer**: There was no invention or discovery conceived or first actually reduced to practice in the course of or under this contract, including any art, method, process, machine manufacture, design or composition of matter, or any new useful improvement thereof, or any variety of plant, which is or may be patentable under the patent laws of the United States of America or any foreign country.

## Engineering Disclaimer

NOT INTENDED FOR CONSTRUCTION, BIDDING, OR PERMIT PURPOSES.

Project Engineer: Xinbao Yu
Professional Engineer License State and Number: Texas No.110438
P.E. Designation: Research Supervisor

## Acknowledgments

The authors express appreciation to project managers Tom Schwerdt, Shelley Pridgen, James Kuhr, Sonya Badgley, and Chris Glancy, and the project advisor board, Andres Gonzalez, Cynthia Saldana, Danny Henderson, Frank Estrada III, Justin Thomey, Richard Williammee, Kevin Pruski, Manuel Padron Jr, Mark Burwell, Robert Moya III, Elijah Zelenov, Justin Derden, Philip Hempel, for their assistance throughout the project. The authors also acknowledge the pivotal role of the TxDOT Fort Worth office in supporting field construction activities. The authors are also thankful to Howard Newton of Image Engineering Group, Ltd., William McPike of Geothermal Drilling, Inc., Stephen Hamstra, Tom Weatherspoon, UTA facility office, and Pile Dynamics for their consultant, fieldwork, and technical support, respectively, during the execution of the field study.

# TABLE OF CONTENT

# List of Figures

## List of Tables

# CHAPTER 1

# INTRODUCTION

## 1.1. Project Background

Ice and snow cause hazardous driving conditions, especially on bridge decks where the cold air above and below the superstructure makes them the first to freeze before pavements. Texas, particularly the northern state, has an average winter season of more than three months and an average snowfall of more than 2 inches (Cui et al., 2017). About half of the state of Texas is involved in snow and ice removal each winter season. Texas Department of Transportation (TxDOT) maintenance forces are summoned to maintain open, passable roadways. Texas ranks 30$^{th}$ among all the states, with an average cost for snow and ice removal of $17.4 million/year (Cui et al., 2017). During the deicing operations, the winter maintenance crews are exposed to an undesirable safety hazard. Typical deicing methods include sand and salts applied before and during winter storms. Sand provides traction until the roadway is dry, and then it causes the potential for skidding; it must be cleaned up after the winter event. Salt is corrosive and eventually penetrates down to the reinforcing steel. When it corrodes, the bridge life will be reduced. In Texas, there are a large number of overpass bridges that are severely affected by the freezing conditions each year.

Due to the growing concern about conventional methods to deice roadways and bridges, alternatives such as the use of geothermally heated bridges are increasing in demand. Geothermal energy is a reliable energy source that can provide power 24 hours a day, 365 days a year, and independent of weather conditions. Current estimation by the United States Department of Energy (DOE) shows that geothermal energy has the potential to satisfy more than four-fifths of our nation's energy needs. As a result, many geothermal projects have been the focus of many projects for generating additional energy at a given location for various operations. This research explores a green and sustainable bridge/road deicing alternative system by harnessing geothermal energy from subsurface to deice bridge decks and roads during severe winter hazards.

The geothermal energy used for bridge and pavement deicing is usually from the earth at a shallow depth of less than several hundred feet, and it is referred to as shallow geothermal energy. Below a ground depth of 25-30 ft., the ground temperature remains relatively constant during all seasons. This temperature is less than the ambient temperature during summer and higher than that during winter. As a result, thermal energy can be extracted from the ground during the winter for heating purposes or injected into the ground during summer for cooling purposes. Based on this principle, geothermal energy has been recently used for bridge and pavement deicing with closed hydronic loops, as shown in Figure 1.1 In the geothermal bridge deicing system, flow pumps are used to move the heat carrier fluid to extract heat from the ground via ground loop heat exchangers (GLHE) and carry it to the hydronic loops installed in the bridge deck. Heat is transferred from the

hydronic loops to the bridge deck surface and provides the heat to melt the ice and snow on the deck surface. The fluid temperature out of the ground is usually less than 70 ºF, depending on the location. If this temperature meets the deicing needs, the ground loops can be directly connected to bridge heating loops. For higher fluid temperatures of 100 ºF, ground source heat pumps (GSHPs) are utilized to provide extra heat energy.

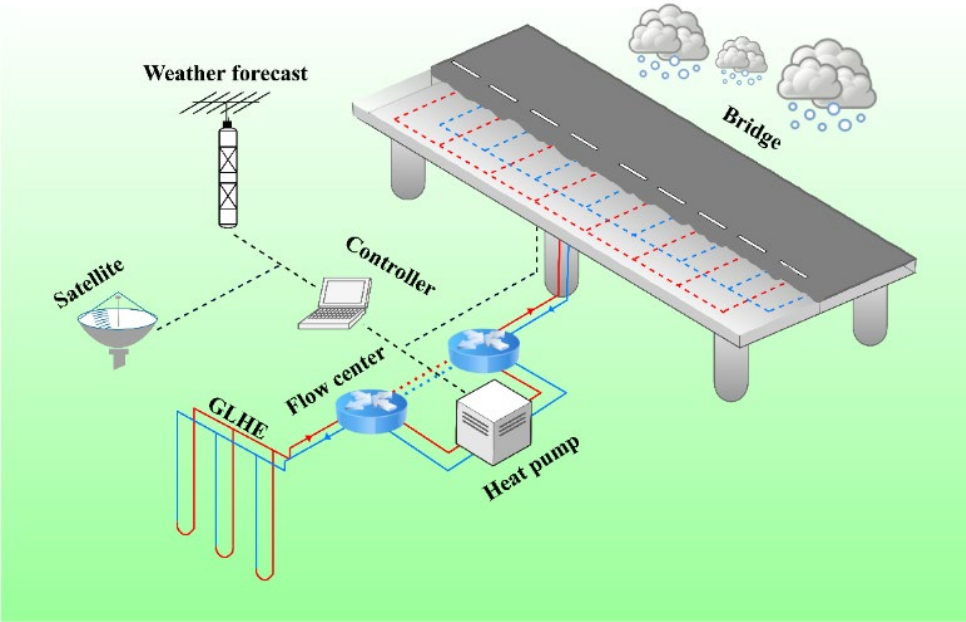


Figure 1.1 Conceptual diagram of the geothermal heat pump de-icing system (GHDS) (Habibzadeh-Bigdarvish et al. 2019)

This research project consists of two phases, and phase I was completed in 2016. In phase I, a synthesis study was performed to 1) investigate the current state of the art on the development of a geothermal system for Texas to store and reuse the temperatures collected into an underground soil system to keep the roadway pavements above the freezing point, and 2) collect the available knowledge base on the Underground Thermal Energy Storage (UTES) technology and determine the effectiveness in reducing the bridge deck and pavement freezing areas. In phase II, the focus is to develop, test, and optimize a geothermal bridge deck deicing system that can be installed onto in-service bridges through retrofitting. To meet the installation and bridge inspection challenges, the research team tested various bridge heating loop designs considering heating fluids (water-based vs. CO2), insulation materials (spray-on polyurethane vs. geofoam), and loop configurations (geometry and insulation coverage). Prototypes of various bridge heating loops were evaluated and tested at different scales both in the laboratory and field under simulated and real winter weather scenarios. Selected bridge heating loop designs were tested on a mock-up model bridge constructed in Fort Worth with one geothermal borehole in the 2019, 2020, and 2021 winter events. Following the successful deicing performance of the mock-up geothermal bridge, the geothermal bridge deicing system was implemented on an 8-span, in-service flat-slab concrete bridge with 16 geothermal boreholes in Fort Worth as a pilot geothermal bridge and tested successfully in the

2024 winter events. Besides, the environmental impact and cost-benefit of the geothermal bridge deicing system were also analyzed using both historical and newly collected data on geothermal bridges. This report documents the major results and findings of the phase II research, specifically on the pilot geothermal bridge and its life cost-benefit analyses.

### 1.2. Scope and Objectives

Using geothermal energy for deicing can provide a better alternative than the existing method of deicing sand and/or salt. However, the usage of geothermal energy is limited in the U.S. due to the lack of research in practical studies, including field demonstrations. This research project is an attempt to address this topic with a primary focus on field demonstration of the geothermal bridge deicing technology. The research goal was to develop an energy-efficient and environmentally friendly method of using shallow geothermal energy for bridge/road snow removal and deicing. The developed technology utilizes shallow geothermal energy, which is extracted through closed-pipe loops embedded under the ground. A heat-carrying fluid circulates inside the loop and carries the underground heat to the bridge, and the heat can be further enhanced through a geothermal heat pump. The warm fluid circulates inside a pipe network attached to the bridge deck bottom, which heats the bridge deck and melts snow and ice on the bridge surface. The developed new bridge deck heating system can be implemented on existing bridges.

The following are the main objectives of the Phase II project:

1. Design, construct, and test prototype geothermal bridge deicing system built on an element and panel scale of the concrete bridge deck in the laboratory environment.
2. Design and construct a field-scale mock-up geothermal heated bridge and monitor its temperature/heat transfer behavior in winter storms.
3. Test the developed geothermal de-icing system on an in-service bridge at operational traffic conditions during winter weather events.
4. Assess the economic viability of geothermal heated bridge technology using life cycle cost-benefit analyses.
5. Recommend installation, operation, and maintenance guidelines for the geothermal bridge deicing system.

The major benefit of this study is that it enhances the safety of the traveling public by alleviating treacherous road conditions during winter. Over the last three years, severe winter conditions, including snowstorm events, have resulted in the closure of bridges and pavements due to icing conditions. These cold conditions have caused the closure of roads and bridges, as icy road conditions result in accidents, including those in which human lives are lost. This geothermal technology can potentially alleviate this concern and enhance the safety of the traveling public by warming the roads and bridge decks so that the surface conditions are much more conducive to safe traveling.

### 1.3. Organization of the Report

This report documents the research tasks completed during phase II of the project from 2016 to 2024. During phase II, the technology of using geothermal energy to deice Texas bridges was studied, from laboratory environmental chamber tests to a mock-up geothermal bridge in the field and eventually on an in-service bridge. This report is organized as follows. Chapter 1 provides the background and objectives of the performed research. Chapter 2 provides a summary and highlights of tasks 1 and 2, which include laboratory tests of heated slabs in the environmental chamber, freezer box, outdoor, and mock-up geothermal bridge. Chapter 3 presents the design and construction of a mock-up geothermal externally heated bridge. Chapter 4 assesses the economic viability of the geothermal bridge deicing using a life-cycle cost-benefit analysis (LCCBA) for the pilot geothermal bridge in Fort Worth, Texas. Chapter 5 presents the economic viability of the geothermally heated bridge using life-cycle cost-benefit analysis (LCCBA). Chapter 6 summarizes and outlines the control system for the pilot bridge deicing system using Tekmar 519. It also details the system's operation manual, inspection, and maintenance.

# CHAPTER 2

# Summary and Highlights of Laboratory Heated Slab Tests and the Mock-up Geothermal Bridge

## 2.1. Laboratory Tests of Heated Slabs

Texas Department of Transportation (TxDOT) owns many overpass bridges that are in critical need of bridge deicing. Approximately 85 percent of the bridges in Texas were constructed using CIP-PCP bridge decks, which consist of precast, prestressed concrete panels (PCPs) and a cast-in-place (CIP) concrete deck (Habibzadeh-Bigdarvish et al., 2021). Therefore, this heated bridge deck design is intended to be used on the CIP-PCP bridge decks. Deicing of bridge decks for existing bridges requires an external heating source, which is only possible by supplying heat from two sides of the bridge deck. For the convenience of installation, heat supply from the bottom of the bridge deck is a reasonable choice, although its heating efficiency is not optimum compared to internal heating. Figure 2.1 presents a schematic of the attached hydronic heating loop design for a heated bridge deck, which consists of hydronic pipes and foam insulation materials. For bridges at service (Figure 2.1, right), the hydronic pipes are attached to the bottom of the bridge deck through U-shape fixtures. Insulation foam (polyurethane or geofoam) is installed to encapsulate the heat pipes and minimize the heat loss from the bottom. Warm fluid (typically a water and antifreeze mixture)) supplied from GLHEs or GSHPs provides a heat source to warm the bridge deck surface above with minimal heat loss due to the high thermal resistance of the underneath insulation.


Figure 2.1 Concept design of externally heated bridge deck, i.e., attached hydronic loop (left), and a photo of PEX pipe attachment to a concrete slab (right) (Yu et al. 2020)

The hydronic loops are attached to the bottom of a bridge deck and are encapsulated inside thermal insulation materials such as geofoam and polyurethane foam. A total of three heated slab tests were fabricated and tested. The first two slabs are 4 ft wide, 6 ft long, and 4 in. thick. A cross-linked polyethylene (PEX) tubing with a 0.5-inch internal diameter and 6-inch spacing was attached to the bottom of the first slab. The PEX pipe loop was encapsulated inside a geofoam layer. The first heated bridge slab was tested in an environmental chamber under various room

temperatures (above 40 °F). A water tank supplied the heat to the slab at a controlled water temperature to simulate various geothermal ground loop outputs. The supplied heat was able to travel upward to warm the bridge deck surface due to the high thermal resistance of the underneath insulation. Various winter scenarios, including wind, freezing, and icing, were created by placing a foam box of controlled environments on the top of the heated slab. To test the heated slab performance during a winter storm, a second slab with the same design as the first one, except the insulation material replaced with spray-on polyurethane foam, was fabricated and tested outdoors. The heating performance was observed for two winter events and one simulated snow/ice event. The third slab, half the size of the first two slabs and 8-inch thickness, was tested in a freezer box, which provides a controlled temperature below freezing.

For the third and fourth heated slab tests, a walk-in freezer box with a minimum temperature of 20 °F was obtained to create freezing test environments. The third slab, cast at UTA, was 8 inches thick to replicate a bridge deck with the same thickness as in-service bridges. It was tested with hydronic loops installed in the same way as the second slab test and a new water bath with precise temperature control. In the fourth heated slab test, CO2 heat pipes were evaluated as an alternative heating method to the hydronic PEX loops (Lei et al. 2020).

### 2.1.1. Slab 1 (Environmental Chamber >40 F)

A heated bridge deck slab was designed and fabricated in the laboratory. The hydronic loops consist of nine (9) loops encapsulated inside a geofoam. A series of environmental chamber tests were performed to evaluate the heating response under different environmental conditions, i.e., ambient and supplied water temperature. The heated bridge deck can be heated efficiently with supplied warm water, which simulates warm water supplied from underground loops. In the test environments, it typically took 20 to 30 hours to reach the thermal equilibrium. A temperature prediction equation was presented to predict the steady-state temperature of the concrete slab. The heat transfer inside the heated deck can be assumed to be one dimension upward with reasonable accuracy. In the testing environment, approximately 60 percent of the supplied heat from the attached loop is transferred to the concrete slab surface at a steady state. More tests under freezing and various wind conditions should be conducted so that the model can be applied to winter event scenarios.

A new hydronically heated bridge deck design with attached hydronic loops was presented, which can be implemented on existing bridges using geothermal energy as the heating source. A heated bridge deck slab was designed and fabricated in the laboratory. The hydronic loops consist of nine (9) loops encapsulated inside geofoam. Environmental chamber tests were performed to evaluate the heating response under different environmental conditions, i.e., ambient (>4.4 °C, >40 °F) and supplied water temperatures. The concrete slab can be heated efficiently with the supplied warm water, which simulates warm water supplied from GLHEs and GSHPs. In the test environments, it typically took 20 to 30 hours to reach the thermal equilibrium. A temperature prediction equation was presented to predict the steady-state temperature of the concrete slab. The

heat transfer inside the heated deck can be assumed to be one-dimensional and upward to estimate the heat flux with reasonable accuracy. The heated deck can provide enough heat flux required for deicing. At the testing environment, approximately 60 percent of the supplied heat from the attached loop is transferred to the concrete slab surface at steady state. The prediction method for the slab temperature was validated with localized subfreezing tests, and it can be extrapolated to subfreezing conditions without consideration of snow/ice melting. More tests at freezing, snow/ice, and various wind conditions should be conducted to evaluate the heating performance to remove ice/snow under winter event scenarios.

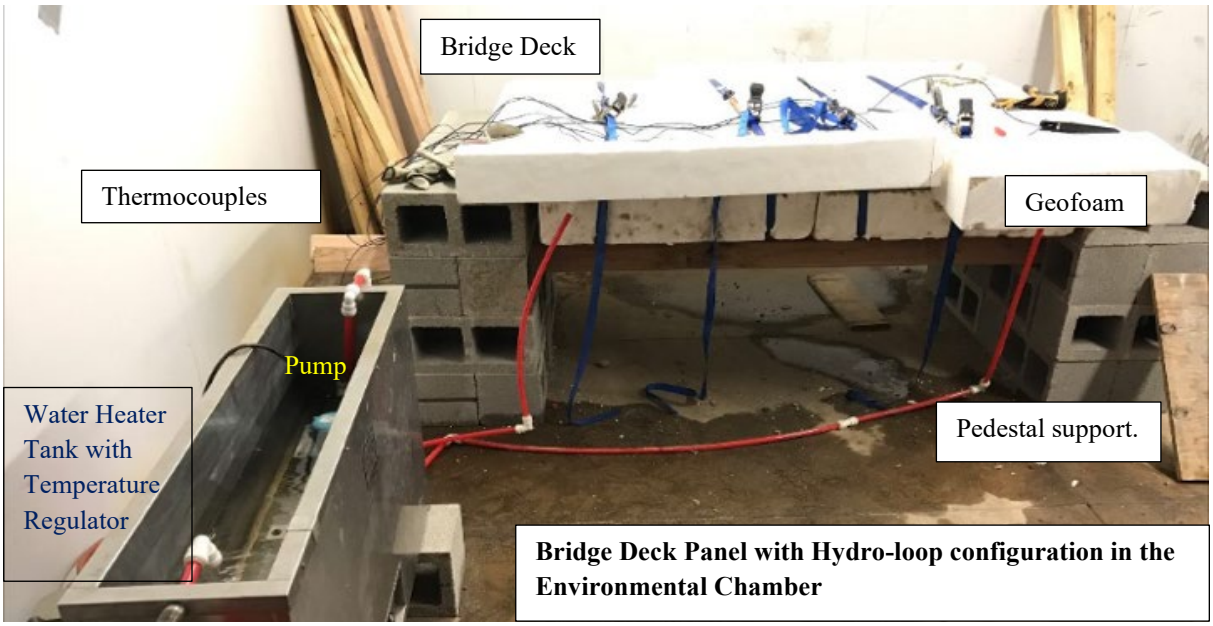


Figure 2.2 Laboratory scale test setup.

### 2.1.2. Slab 2 (outdoor test)

To determine the effectiveness of a geothermally driven de-icing system, an experimental model must precede its implementation in the field. Thus, a smaller-scaled model (6ft x 4ft x 4in. concrete slab) was placed outdoors to simulate the de-icing of bridge overpasses via geothermal energy. The second heated slab was placed outside and tested for two winter events and one simulated snow/ice event. The results of the simulated snow/ice event showed that the minimum required inlet temperature to keep the slab surface above freezing would be approximately 70 °F for a 4in. slab.

Figure 2.3 Creation of freezing mist via a snow gun

### 2.1.3. Slab 3 (Freezer Box)

The concrete slab is 8-inch thick, representing a full-scale bridge deck thickness in Texas. This slab was equipped with a simulated geothermal bridge de-icing system and tested inside a freezer subjected to sub-freezing controlled conditions. Various winter scenarios were applied to the system to determine its heating performance and how feasible it would be for the system to be transferred to the field. For example, with the supplied water at 25 *°C (*77 °F*)* and the freezer temperature of -3.3 °C (26 °F), the observed deck temperature dipped slightly below freezing at the surface of the slab, which implies that the inlet temperature must be greater than 77 ° *F* for effective de-icing. A prediction equation was developed to estimate the total energy reserves required to permit de-icing, and statistical analysis was performed and validated with test results. The slab surface heat flux was estimated to range from 27 $W/m^2K$ to 73 $W/m^2K$ from the heating test. The externally heated deck can be designed with the developed prediction equation for snow melting.

Figure 2.4 Wooden framework utilized to Conceal Spray Foam

### 2.1.4. Slab 4: $CO_2$ Heat Pipe

Heat pipes have been applied in many fields, like air conditioning and solar heating systems (Wan et al., 2007; Tundee et al., 2010). The $CO_2$ heat pipe works with $CO_2$ as the heat-transfer fluid. In a $CO_2$ heat pipe, heat transfer works by the phase change of the $CO_2$ between liquid and gas in a continuous endothermic and exothermic cycle. The heat-transfer medium $CO_2$ absorbs heat by evaporating. It releases heat by condensing. The allowed operating temperature range of a $CO_2$ heat pipe is from -50 to 30ºC, which enriches the feasibility of applications (Boydcorp Inc.; Chayadit et al. 2017). The research team also investigated the technology of heat pipes filled with $CO_2$ for potential use in heating bridges. The research team aimed to design a heat pipe suitable for bridge deicing and test its performance. Copper heat pipes were fabricated as the de-icing system, and the temperature responses of the lab-scale heated slab were measured under sub-freezing conditions.

**Design and Testing of a Multiloop Heat Pipe:** A multiloop heat pipe made of copper was designed and fabricated by the research team (Figure 2.5). Parametric tests to investigate the performance of the pipe alone were conducted concerning various parameters, including different quantities of dry, inclinations, ambient temperatures, and water inlet temperatures. The test results show that the optimum quantity of dry ice is 300g, and the optimum inclination of the pipe is 5º. With the optimum heat-pipe design, it was found that when the ambient temperature was -2 ºC, the heat-pipe system could heat the bottom and top of a model deck to 5 and 1 ºC, respectively, indicating that the new heat pipe system has excellent de-icing capability.

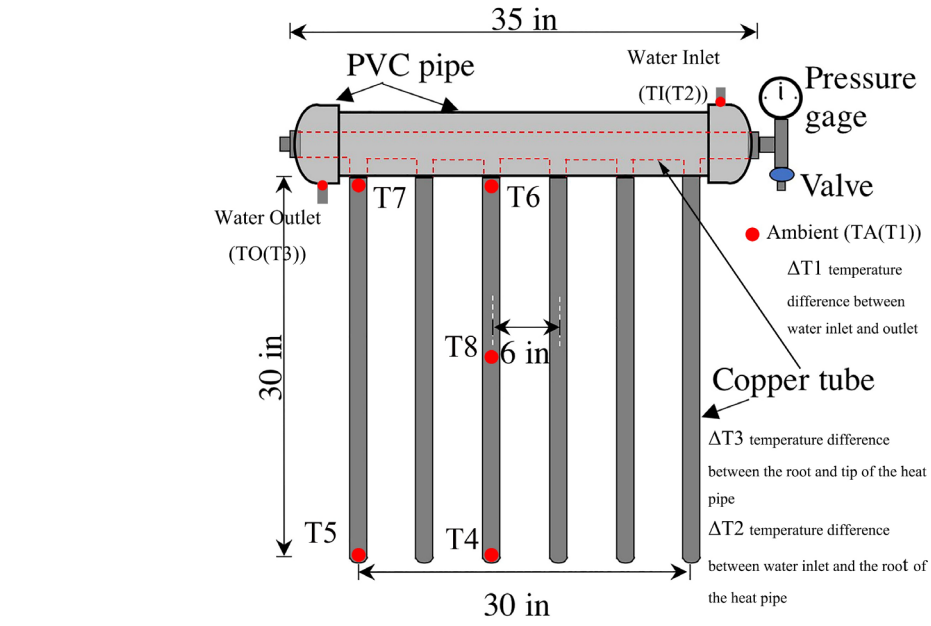


(a)

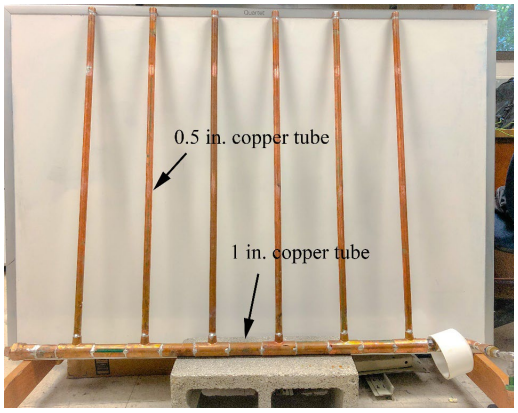


(b)


(c)

(d)

Figure 2.5. Schematic and assembled body of the heat pipe system with specific dimensions and thermocouples laying out.

**Performance Test of the Heated Slab Attached with the Heat Pipe under Sub-freezing Conditions:** Two heating tests were conducted to investigate the temperature response of the bridge deck attached with the designed heat pipe at 27 ºF and 25 ºF freezing temperatures (Figure 2.6). Both tests indicated the feasibility of the heat pipe system in deicing the bridge slab. It took approximately 10 hours for the slab top surface to reach a temperature above freezing. The average slab top surface temperature of tests 1 and 2 are 34.3 and 36.6 ºF, respectively. Additionally, thermal imaging studies were conducted, which also showed the slab top surface temperature was above zero at steady state during both tests. The research team also noticed that the heat pipe system needs careful handling and installation. No commercial products are found available for large-scale field implementation.

(a) (b)

Figure 2.6 Attachment of the heat pipe on the bottom surface of the slab

## 2.2. Design, Construction, and Winter Tests of Mock-up Geothermally Heated Bridge

The mock-up geothermally heated bridge shown in Figure 2.7 is located west of Arlington and adjacent to Fort Worth, TX. The site is on abandoned asphalt pavement along SH 180, which TxDOT uses to store RAP stockpiles. The subsurface of the bridge includes a relatively uniform 40 ft top layer of sandy clay with alternating sand and gravel seams. Groundwater was encountered at 15 ft. at the time of drilling. The bottom stratum is limestone extended to 60 ft., the bottom of the boring logs. The mockup bridge consists of a PCP-CIP bridge deck of 12 8 ft x 6 ft PCP panels and 4 in. CIP seated on two 39 ft I-beams supported on the LPCTBs.

Figure 2.9 illustrates the geothermal heating system, consisting of a) heating loops underneath the bridge deck, b) a geothermal heat pump, circulation pump, and control system, and c) a ground loop heat exchanger (GLHE). Glycol and water mixture (20%) were inside the underground and deck loops as the heat-carrying fluid. The heat transfer cycle in the geothermal heating system starts with the cold mixture fluid, which enters the ground at the GLHE inlet. After being circulated inside the U-shape vertical ground loop, the fluid becomes warm by absorbing heat from the surrounding soil. For mild winter events with less heating demand, the warm fluid from the ground loop enters the circulation pump and then the bridge deck loop. Under excessive

heating mode for severe winter events, a geothermal heat pump connecting the water pump and the bridge loops will be activated to provide extra heat for snow melting. The temperature of the fluids at the exit of the heat pump is further increased. The warm fluids are pumped to the bridge deck loops, which heat the bridge deck by providing enough heat flux at the bridge surface to melt snow and ice.


Figure 2.7 The geothermally heated mock-up bridge near Green Oaks BLVD and U.S. Highway 180 overpass bridge, Fort Worth, TX. The heating zone using the developed insulated PEX pipe channel is highlighted.

### 2.2.1. Heated Bridge Deck

The research team completed the initial construction of a mock-up geothermal bridge in the summer of 2018 and tested the geothermal bridge deicing system in a series of winter events in December 2018 and the spring months of 2019. The initial heated-bridge deck only included an internally heated section and an externally heated section, as shown in Figure 2.9. (a) and (b). In a project update meeting with TxDOT in the Spring of 2019, bridge engineers in TxDOT Fort Worth district raised concerns about bridge inspection for such geothermally heated bridges. To facilitate bridge inspection, the research team developed an insulated loop channel design, i.e., prefabricated insulated hydronic heating channels for PEX pipes, which were installed on the mockup bridge in March 2020.

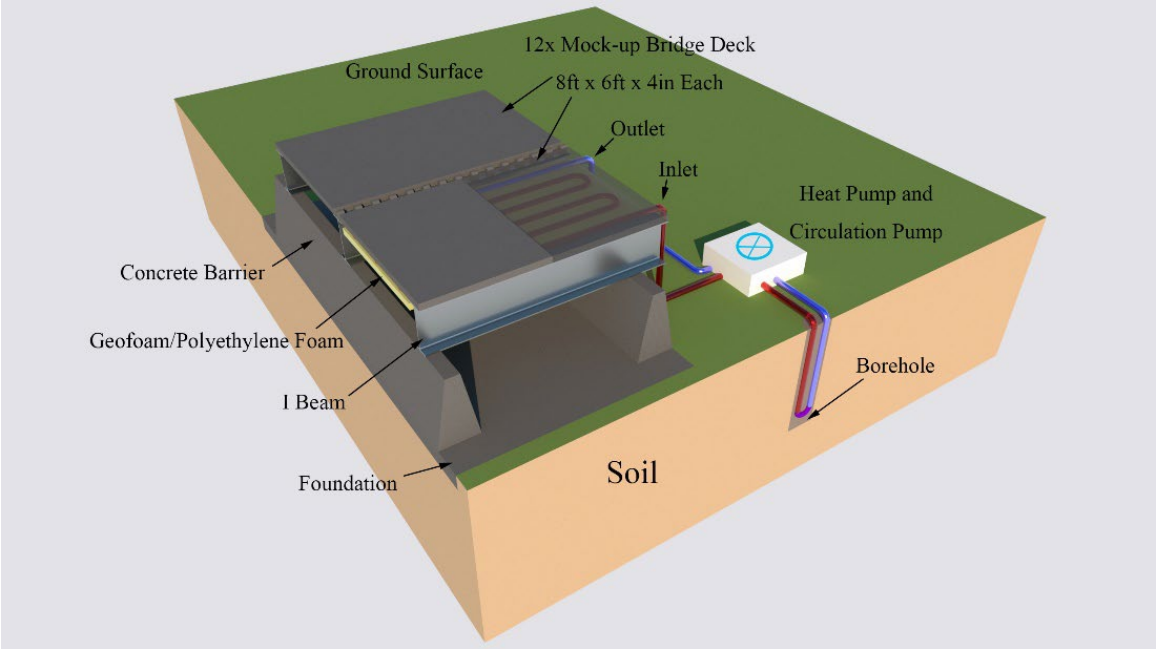


Figure 2.8 Schematic design of external bridge de-icing system

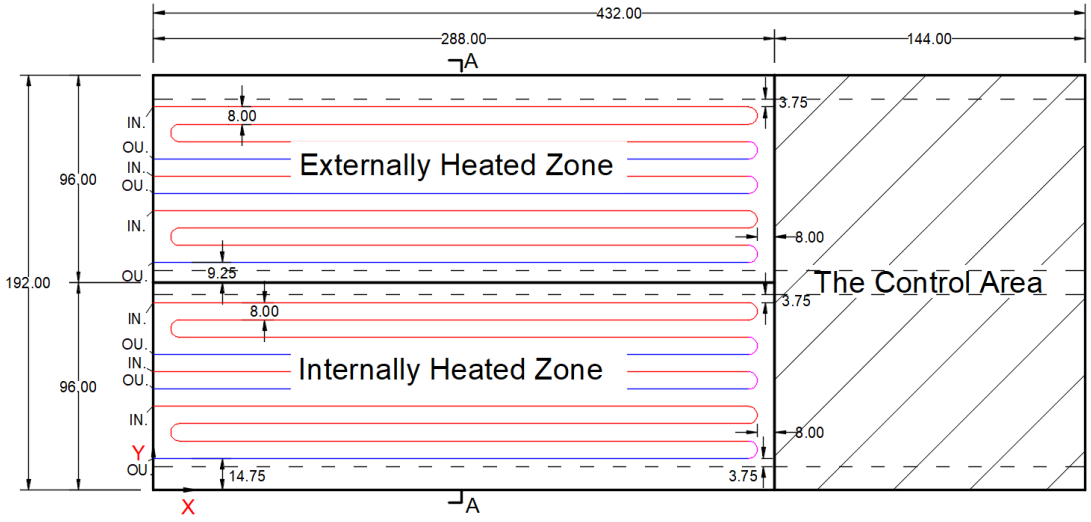


(a)

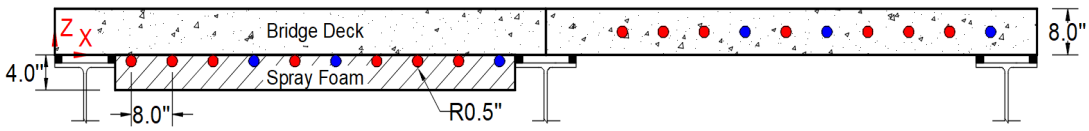


(b)

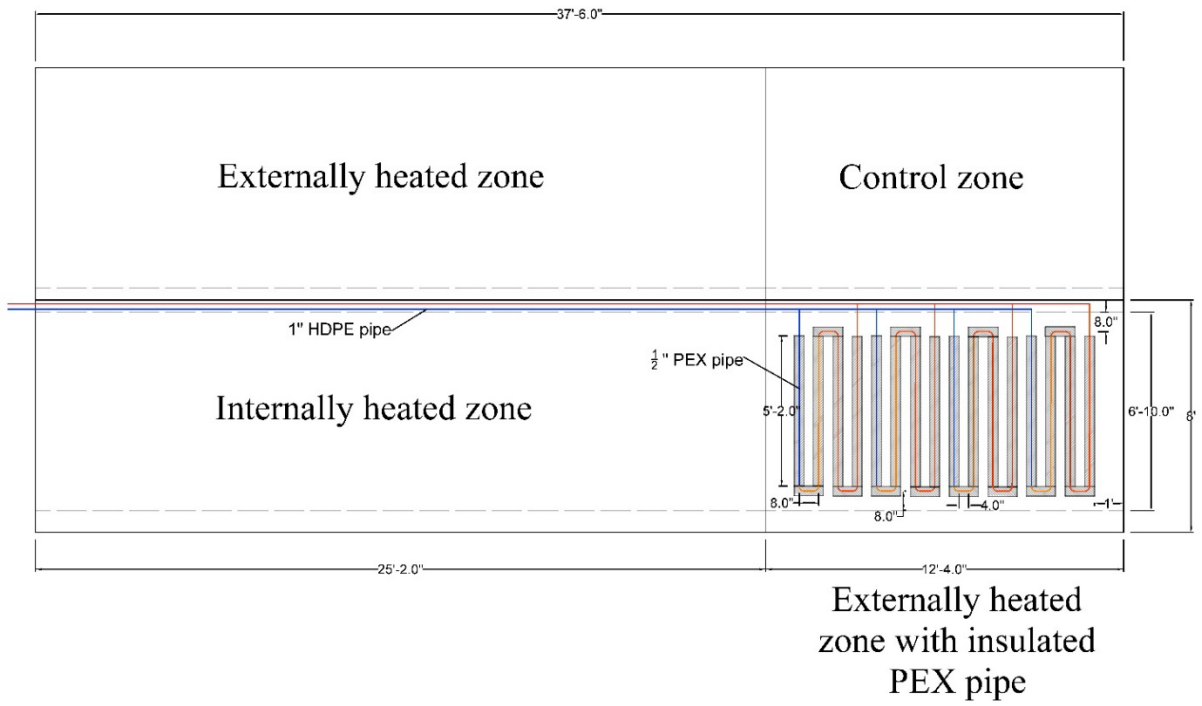


(c)

Figure 2.9 (a) Initial layout of the heated bridge deck; (b) cross-section view of the bridge deck, left: external heating zone and right internal heating zone (unit: in.); (c) final layout of the heated bridge deck with insulated loop section added in

### 2.2.2. Design of the GLHE and Construction

The historical winter snow data of the construction site were analyzed, and several winter snow scenarios were analyzed and used to calculate the required heat fluxes. By synthesis of calculation results and previous design cases, the final design heat flux of 340 w/m$^2$ was selected as the required snow-melting heat flux. Four concrete panels were designed for geothermal heating. The ground loop heat exchanger (GLHE) was analyzed based on the resulting total heating load to determine the required geothermal heat pump capacity and GLHE heat extraction. A 3.5-ton GeoComfort water-to-water geothermal heat pump and two double U ground loops with 180 ft depth were selected. Table 2.1 shows the required heating load for the mock-up bridge, and Table 2.2 shows GLHE design parameters. Table 2.3 summarizes the final design of the GLHE.

The model bridge was constructed during February and March of 2018. Twelve standard PCP panels, 3 I-beams, and two standard CTBs were used. The bridge deck follows the CIP-PCP construction sequence. The PCP panels are 4 inches thick, and the design thickness of the CIP layer is also 4 inches. The 16 ft wide and 36 ft long bridge deck was divided into three zones. Two parallel zones of 8 ft wide and 24 ft long along the length direction were used for internal heating with embedded PEX pipes and external heating with attached pipes, respectively. The installation of internal heating was decided to compare the heating performance of the two heating systems. The third zone at the other end is a square of 16 ft by 16 ft, used for baseline performance of

unheated bridge decks. Instrumentations of point thermocouples and thermal string sensors were installed inside the CIP layer and the PCP layers to obtain three-dimensional temperature distribution along the heat transfer paths of the PEX pipes.

The construction and installation of the geothermal systems started at the end of July and was completed at the end of August. The underground works include one geothermal borehole (GB) and five temperature monitoring borehole (TMB). Although only one geothermal well was designed, five more boreholes were drilled and equipped with temperature sensors to monitor the temperature field at different distances concerning the geothermal borehole. A control room was built to house the flow center and control the geothermal heating system and the data acquisition system. A thermal conductivity test of the geothermal well was performed before constructing the horizontal trench.

Table 2.1 Required Heating Load of the Bridge

| Required Heat Flux (Btu/h.ft$^2$) | Area of Snow Melting (ft$^2$) | Peak Hourly Heating (Btu/ h) | Monthly Snow Hours (h) | Total Monthly Heating(Btu) |
|---|---|---|---|---|
| 108 | 192 | 20736 | 21.3 | 441677 |

Table 2.2 GLHE Design Parameter

| | |
|---|---|
| **$EWT_{min}$** = 35 °F | **$K_{grout}$** = 0.43 Btu/h.ft.°F |
| **$EWT_{max}$** = 90 °F | **$D_{bore}$** = 5 in |
| **Flow Rate** = 9 gal/min | **$D_{pipe}$** = ¾ in |
| **$T_g$** = 68 °F | **Flow Regime** = Turbulent |
| **$K_{soil}$** = 1.4 Btu/h.ft.°F | **Bore Layout** = 1 x 2 |
| **Heat Pump** = GeoComfort GWS 036 (COP 3.2 @ EWT = 30 °F) | |
| **Fluid** = Propylene Glycol/ Water with 20% concentration | |

Table 2.3 The final design of the GLHE

| | |
|---|---|
| Borefield Layout | 2 bores - 10' min. c-c spacing |
| Depth (Below Header Trench) | 210 ft [217 ft below surface] |
| Borehole Diameter | 5" |
| Double-U Pipe Diameter | DR-11- 3/4" |
| Header Pipe Diameter | DR-11- 1 1/4" |
| **Grout Thermal Conductivity** | 0.43 Btu/hr ft °F |

### 2.2.3. Winter Tests of the Mockup Bridge Heated with the Original Insulated PEX Pipe Panels during 2019-20 Winter Events

The research team closely monitored the winter climatic conditions from November 2019 to March 2020, and the geothermal system was operated when a cold front with below-freezing temperatures was forecasted. The internal and external heated zones were operated independently by a control valve, and the system was operated in several modes, full-load and bypass, depending on the operational condition of the geothermal heat pump and the heated deck. In the full-load operation mode, the control valves at the heat pump were closed, and the flow went through the heat pump, which was turned on and provided more heat to the bridge deck surface for snow/ice melting. The geothermal heat pump was allowed to be off when the winter event was mild, and the heat demand was less. The geothermal heat pump was not active in bypass mode, and the heat carrier fluid circulated through the bypass into the hydronic loops on the bridge site and back to the ground loop. All the winter tests focused on testing the heating performance of the externally heated zone, the new geothermal bridge deck design. Therefore, most of the tests were operated with the external heating zone turned on only by closing the control valve of the internally heated zone. Seven tests were conducted to melt the ice on the bridge deck surface.

Table 2.4 summarizes the seven winter tests performed in the winter of 2019-20. The start and end time is the operation period of the geothermal system. The freezing hours were determined from the air temperature measured by the thermocouple installed at the bridge site. The freezing hours, minimum air temperature, and average air temperature during the freezing period were obtained to characterize the winter events. The average surface temperature, minimum surface temperature, and the number of freezing hours of surface temperature for the heated zone were obtained from a sensor installed on the top surface of the externally heated zone (Figure 2.9). This sensor was selected as a representative temperature response of the bridge deck during the coldest period of the winter test. The last column in Table 2.4 describes the operation of the geothermal system during each winter test. Table 2.4 shows that the system was able to maintain the temperature of the deck surface above freezing during all the heating tests. Test #5 was selected as an example of the winter tests. A detailed discussion of the system's performance is presented below.

Test #5 spanned from 3:37 p.m. on 2/13/2020 to 2:32 p.m. on 2/14/2020. The geothermal system was turned on at 3:37 p.m. on 2/13/2020 to provide 10.5 hours of pre-heating before the bridge began to experience the freezing temperature at 1:00 a.m. on 2/14/2019. The geothermal system was operated in a bypass mode, and only the external heating hydronic system was active. As no precipitation was forecasted or experienced, the project team made snow/ice on the bridge deck surface using a snow gun. It was an excellent opportunity for the application of snowmaking devices due to the low ambient temperature of 26.1 °F, a temperature suitable for making snow; however, the snowmaking was not successful due to the high humidity. The water drops became ice pellets, and a uniform ice layer was observed on the non-heated zone surface. Figure 2.10 shows the different stages of the de-icing test.

Table 2.4 Summary of the 2019-2020 winter tests and performance

| Test # | Start | End | # Hrs. of freezing ambient | Average ambient (˚F) | Minimum ambient (˚F) | # Hrs. of freezing surface | Average surface (˚F) | Minimum surface (˚F) | Test description |
|---|---|---|---|---|---|---|---|---|---|
| 1 | 11/11/19 10:00 | 11/14/19 17:25 | 25.0 | 25.5 | 21.4 | 0.0 | 39.0 | 35.3 | Bypass mode operation for externally & internally heated zone |
| 2 | 12/9/19 17:30 | 12/12/19 9:50 | 8.0 | 29.4 | 26.7 | 0.0 | 39.1 | 37.5 | Bypass mode operation for externally heated zone |
| 3 | 12/18/19 23:30 | 12/19/19 9:15 | 10.0 | 26.8 | 23.7 | 6.5 | 31.7 | 27.8 | No heating test |
| 4 | 2/5/20 12:08 | 2/8/20 15:58 | 6.7 | 29.9 | 27.4 | 0.0 | 38.8 | 36.8 | Full load heating mode operation for the externally & internally heated zone. A de-icing test was conducted on the pre-heated deck |
| 5 | 2/13/20 15:37 | 2/15/20 14:32 | 7.0 | 28.1 | 26.1 | 0.0 | 34.8 | 33.3 | Bypass mode operation for the externally heated zone; de-icing test conducted on the pre-heated deck |
| 6 | 2/20/20 16:50 | 2/22/20 18:46 | N/A | N/A | N/A | N/A | N/A | N/A | Full load heating mode operation for the externally heated zone with set Tin= 85 ˚F |
| 7 | 2/26/20 17:57 | 2/28/20 11:00 | N/A | N/A | N/A | N/A | N/A | N/A | Full load heating mode operation for the externally heated zone with set Tin= 75 ˚F |

[1] For this test, the surface temperature data was obtained from a sensor that was approximately 1 inch below the surface.

[2] The geothermal de-icing system was not active during this test. Only the thermal response of the concrete deck during the cold temperature was observed.

[3] The monitoring system malfunctioned during this test, and the data is not available.

(a)

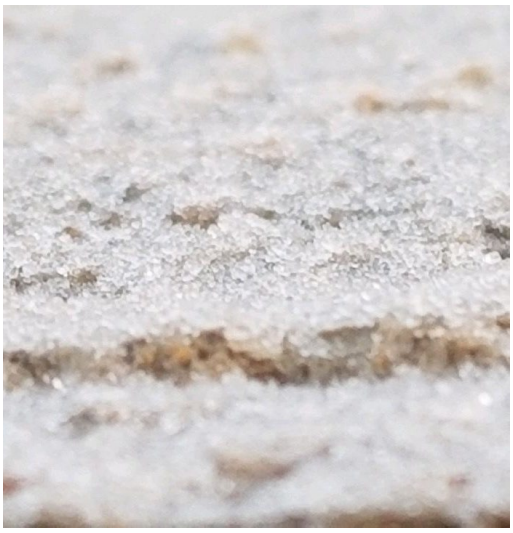

(b)

(c)

Figure 2.10 De-icing Test: (a) snow gun operation, (b) ice formation on the bridge deck, (c) bridge deck surface condition after the snow gun operation.

### 2.2.4. Deicing Tests of Insulated Heating Loops

The insulated heating loops, as shown in Figure 2.11, were tested during the winter of 2020- 2021.

Figure 2.11 Installed insulated PEX pipe channel (bottom view of the bridge deck, the insulated loop section in Figure 2.9 (c)

The research team monitored winter weather conditions from November 2020 to March 2021, operating a geothermal system in various de-icing modes based on the geothermal heat pump's operational condition and the activated heating zone. The system was operated in full-load and bypass operation, with the heat pump on and control valves closed for full-load operation and heat carrier fluid circulating through the bypass, hydronic loops, and ground loop. The goal was to maintain the heated surface temperature above freezing and melt snow/ice on the bridge deck surface.

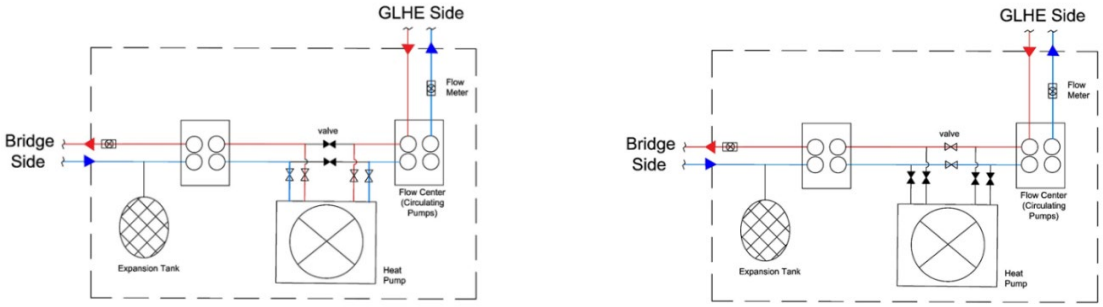


Figure 2.12 System operation modes: (a) full load operation mode for higher heating temperature (greater than 100 $^{o}$F); (b) bypass operation mode for moderate heating temperature (around 70 $^{o}$F)

Table 2.5 presents six winter tests conducted in 2020-2021, analyzing the operation period, freezing hours, minimum and average air temperatures, and temperature responses of the bridge deck. The thermocouple installed at the bridge site measured the number of freezing hours, minimum and average temperatures, and the average surface temperature for the externally heated zone. The system was found to keep the deck surface temperature above freezing, with Winter Test #6 having the most prolonged freezing hours.

Table 2.5 Summary of the 2020-2021 winter tests and performance for heated bridge deck with insulated PEX pipe channels

| Test # | Start | End | # Hrs of freezing | Average of ambient temperature (˚F) | Minimum ambient temperature (˚F) | Average surface temperature (˚F) | Minimum surface temperature (˚F) | # Hrs of freezing heated surface | Test description |
|---|---|---|---|---|---|---|---|---|---|
| 1 | 11/30/20 17:52 | 12/5/20 18:35 | 24.4 | 28.2 | 23.9 | 52.3 | 43.7 | 0.0 | Full-load heating mode (inlet: 100 °F) |
| 2 | 12/15/20 19:55 | 12/19/20 16:08 | 12.3 | 27.9 | 25.6 | 53.5 | 51.5 | 0.0 | Full-load heating mode (inlet: 100 °F) |
| 3 | 12/23/20 18:41 | 12/27/20 21:06 | 16.2 | 29.4 | 25.2 | 48.1 | 42.7 | 0.0 | Full-load heating mode (inlet: 80 °F) |
| 4 | 12/30/20 11:10 | 1/4/21 12:10 | 3.2 | 31.5 | 29.5 | 56.8 | 55.7 | 0.0 | Full-load heating mode (inlet: 100 °F) |
| 5 | 1/8/21 16:00 | 1/13/21 10:33 | 29.7 | 28.3 | 24.0 | 55.0 | 51.4 | 0.0 | Full-load heating mode (inlet: 100 °F) |
| 6 | 2/10/202 9:55 | 2/20/2021 12:11 | 209.0 | 22.6 | -3.1 | 40.9 | 31.3 | 1.3 | Mixed operation strategy (Full-load and Bypass) |

Note: the data presented in this table was obtained when the air temperature was below freezing. The surface temperature was obtained from the thermocouples attached to the surface.

**Winter Test #6 during Record Texas Winter Storm:** Winter test six was chosen due to record snowstorms and low temperatures of -3 ˚F. The test occurred from February 10th to February 20th, 2021, with snowstorms causing ice accumulations up to 0.5 inches across Central Texas. Two snowfall events occurred on February 14-15th and 16-17th, with the DFW International Airport weather station recording 4 inches of snowfall. The geothermal heating system used a mixed operation strategy to minimize electricity consumption and achieve optimal results. The test began in bypass mode, with the geothermal heat pump operating in Bypass mode.

The study collected weather data from thermocouple measurements and on-site Vaisala WXT530 weather station. The onsite thermocouple closely matches the stations' data. Historical data from the DFW metroplex area showed 209 hours of freezing temperatures during Test #6, with an average of 22.6 ˚F and a minimum ambient temperature of -3 ˚F.

Table 2.6 Climate stats and new records for DFW airport (Source: National Weather Service, 2021)

| Date | Max / Min Temps | Records Broken |
|---|---|---|
| Feb 14, 2021 | **22 / 9** | Record Low Temp of 9 degrees Previous: 15 in 1936 and 1909)<br>*Record Snowfall of 4" (Previous: 3.0" in 1935)*<br>Record Low Max/High Temp of 22 degrees (Previous: 27 in 1951) |
| Feb 15, 2021 | **14 / 4** | Record Low Temp of 4 degrees (Previous: 15 in 1909)<br>Record Low Max/High Temp of 14 degrees (Previous: 31 in 1909) |
| Feb 16, 2021 | **18 / -2** | Record Low Temp of -2 degrees (Previous: 12 in 1903)<br>Record Low Max/High Temp of 18 degrees (Previous: 21 in 1903) |
| Feb 17, 2021 | **27 / 18** | Tied Record Low Max/High Temp of 27 degrees (Previous 1936 and 1910) |

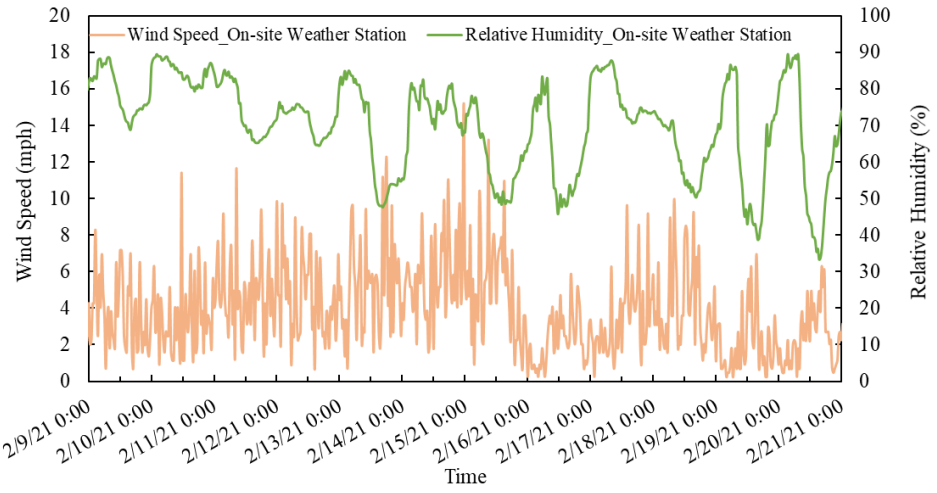


Figure 2.13 Wind speed and relative humidity during test #6

The temperature response of a new externally heated zone using insulated heating loops during Test #6 was examined. The geothermal heating system used a mixed operation strategy,

with the bridge deck heated using heating fluid from a single U-tube borehole heat exchanger. The temperature varied between stages, with the inlet and outlet fluid temperatures recorded at 104.3 ˚F and 102.2 ˚F, respectively. The operation electricity cost was estimated at approximately $50.

Table 2.7 Timeline of operation modes during heating test #6

| Stage | Action | Date/Time | Operation Mode |
|---|---|---|---|
| #1 | System On | 2/10/2021 9:55 | Bypass |
| #2 | Mode Change | 2/12/2021 17:23 | Full-load with set supplied fluid temperature = 85 ˚F |
| #3 | Mode Change | 2/13/2021 17:55 | Full-load with set supplied fluid temperature = 100 ˚F |
| #4 | System Off | 2/20/2021 12:11 | N/A |

Figure 2.14 compares the surface temperature variation of the new externally heated zone and non-heated zone using thermocouples. The heated zone's temperature increases after circulating pumps, while the non-heated zone remains close to ambient temperature. After the test, the heated zone's temperature drops and merges with the non-heated zone. The heating system maintains a temperature above freezing during the entire period, except for 1.3 hours during stage #3 when low ambient temperatures reached -3 ˚F.

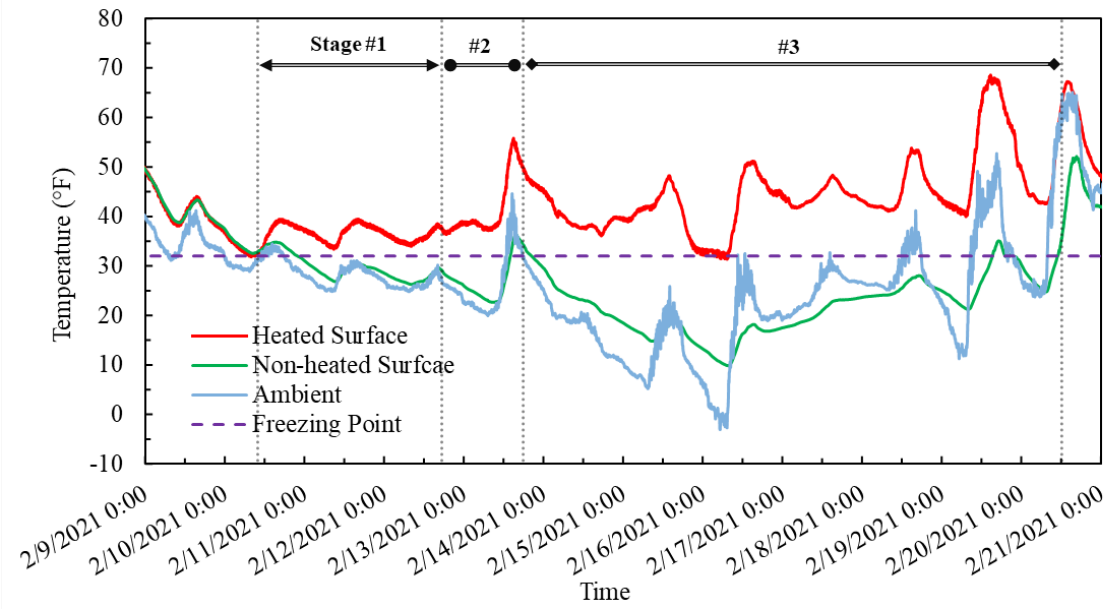


Figure 2.14. Comparison of the heated and non-heated zone temperature variation during Test #6

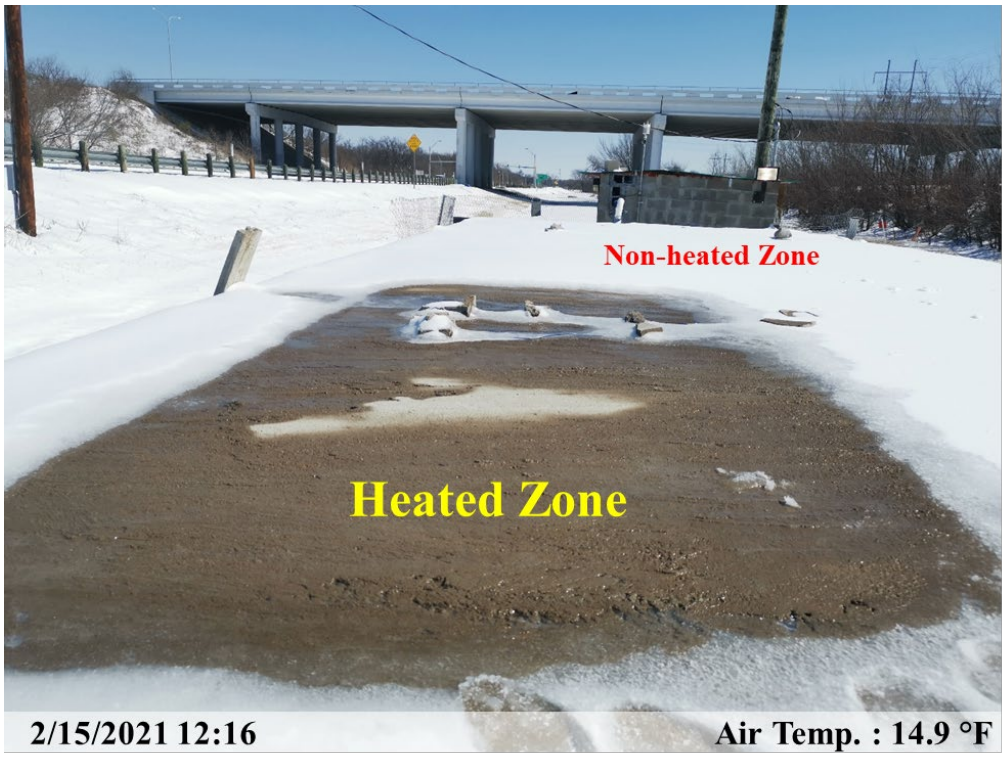


Figure 2.15 Bridge deck condition on February 15th

**Observation of the Bridge Deck Condition:** The bridge deck experienced 4 inches of snowfall on February 14th and 15th, 2021. The geothermal de-icing system was operated at maximum capacity, and the heated zone was pre-heated. Snow accumulation began in the non-heated zone, while the heating system did not allow snow accumulation in the heated zone. The temperature dropped to 10˚F, and snowfall resumed with extreme intensity. The heated zone experienced snow-free conditions when snowfall was low and snow-covered surfaces when it was extremely high. The handheld infrared thermometer was used for surface temperature measurements, showing a good correspondence between the handheld thermometer and surface sensor readings.

The study used a thermal imager to visually illustrate temperature variation across a large area, comparing it to an infrared thermometer. The images showed temperature changes on the bridge deck and borderline between heated and non-heated zones. The handheld infrared thermometer also measured surface temperature, showing a good correlation with the surface sensor. The exposed bottom surface of the heated zone was recorded as 46.2 ˚F.

**Findings:** This report documents six winter tests performed during the winter of 2020-2021 on the mock-up geothermally heated bridge, which is equipped with a geothermal heat pump de-icing system. It reports the heating performance of the bridge deck and its response in the winter events. The main findings from these winter tests are summarized as follow:

- The outputs of the test results show that the system was successful in maintaining the surface temperature of the heated zone above freezing during the encountered six cold fronts except for 1.3 hours during Test#6 when the record low ambient temperature of -3 ˚F was reached and heated surface temperature recorded as 31.3 ˚F.
- The de-icing system successfully melted the snow/ice on the surface and maintained snow and ice-free deck surface most of the time during the severe winter storm except for during the peak snowfall, 4 inches of snow over 8 hours, coincided with air temperature below 10˚F.
- The weather data was extracted from two sources, namely: thermocouple measurement on-site and on-site weather station which is in good agreement with each other with slight differences. Overall, the data shows the system experienced about 295 hours of freezing temperature with the minimum ambient temperature recorded as -3˚F which was the second-lowest minimum temperature recorded in the history of the DFW metroplex.
- De-icing operation using bypass operation was proved to be applicable for the mild winter weather condition with an ambient temperature of around 25˚F in which the bridge deck was heated with about 63.5˚F fluid by using circulating pump only.
- In one of the most severe snowstorms of North Texas, the de-icing system consumed around 40 kWh of electricity per day employing the mixed operation strategy.

# CHAPTER 3

# Pilot Geothermal Bridge

## 3.1. Introduction

This project focuses on developing and implementing a geothermal deicing system for existing bridges, offering a more sustainable alternative to traditional de-icing methods like sands and salts. The research has progressed through several phases, beginning with lab-scale experiments, and culminating in the successful testing of a geothermal deicing system on a mock-up bridge during multiple winter events, including those with record low temperatures. The system demonstrated excellent performance, and a prototype with insulated PEX pipe channels was developed to address concerns about bridge inspection. The geothermal system was subsequently implemented on an in-service bridge and tested during the 2023-2024 winter events, showing promising results. This project aims to refine the system further, develop design and construction guidelines, and assess its broader application across North Texas. The final report includes detailed designs, installation and construction, deicing performance, and cost-benefit analyses.

## 3.2. Selection of the Pilot Bridge

A list of bridges suitable for the installation of the external geothermal de-icing system was provided to the research team by TxDOT (Table 3.1). A comprehensive assessment was conducted to select the ideal bridge for the installation of the geothermal deicing system during the research phase. The following criteria were investigated in the selection process:

- Easy access
- Two or three spans and one/two lanes
- Low to moderate traffic
- Electric supply access
- Sufficient ROW space for placement of geothermal accessories
- Bridge height feasible for construction and installation
- Ideal for a bridge crossing a small creek for pilot-scale study.

The outcome of the analysis shows bridge #7 has the highest potential for installation of the de-icing system. Bridge #7 is a low-height bridge situated on a large site that provides convenient access to the site and bridge deck bottom surface. The bridge structure, site, and location make it an appropriate case for the installation of the geothermal de-icing system.

### Pilot bridge: Bridge #7

This bridge is on SH 180 and was designed for West Village Creek relief. It is located in the Dallas/Fort Worth Metroplex in North Texas (Figures 3.1 and 3.2). The bridge consists of 8 spans and has 2 lanes on each bound. It is 200 ft. long and 48 ft. wide, and the bridge deck is 18 in. thick. The total bridge deck area is 9,600 $ft^2$; however, the bottom surface of the deck, which would be

used for the installation of the hydronic heating loops, has an area of about 8,650 $ft^2$. The bottom surface on girders and other supports is not suitable for heating because hydronic loops cannot be installed in those areas. In 2019, the Texas Department of Transportation estimated the average annual daily traffic (AADT) at 11,000 vehicles (Texas Department of Transportation, 2019). Table 3.2 summarizes the details of the bridge.

Table 3.1 List of potential candidate bridges.

| Bridge # | Description |
|---|---|
| 1 | 02-220-0-0008-06-483 – SH 180 @ Village Creek<br>(3 - Span, 210', PS I-Beam), 32.73145952 - -97.17721075 |
| 2 | 02-220-0-3559-02-001 – SH 170 EB SFR @ Trib. Of Henrietta Creek<br>(2 – Span, 95', PS I-Beam), 32.96629488 - -97.2924543 |
| 3 | 02-220-0-3559-02-002 – SH 170 WB NFR @ Trib. Of Henrietta Creek<br>(2 – Span, 98', PS I-Beam), 32.96728485 - -97.29312432 |
| 4 | 02-127-0-0747-05-057 – FM 157 @ Mountain Creek<br>(2 – Span, 170', PS I-Beam), 32.49124613 - - 97.12344156 |
| 5 | 02-127-0-2762-01-002 – FM 2738 @ Mountain Creek<br>(1 – Span, 110', PS I-Beam), 32.451523 - -97.168954 |
| 6 | 02-127-0-1181-04-008 – FM 917 @ Walnut Creek<br>(1 – Span, 80', PS I-Beam), 32.47511902 - -97.22181614 |
| 7 | 02-220-0008-06-045 – SH 180 @ West Village Creek Relief<br>(8 – Span, 25', Continuous Concrete Flat Slab), 32.730044 - -97.186899 |
| 8 | 02-220-0008-06-046 – SH 180 @ West Village Creek Relief<br>(6 – Span, 25', Continuous Concrete Flat Slab), 32.731162 - - 97.179372 |

Table 3.2 Details of the pilot bridge.

| Item | Quantity |
|---|---|
| Coordinate | 32.730044, 97.186899 |
| Number of lanes | 4 |
| Average annual daily traffic | 11,000 Vehicles |
| Number of spans | 8 |
| Deck area | 9,600 $ft^2$ |
| Exposed bottom surface area (heated area) | 8,650 $ft^2$ |

Figure 3.1 The selected pilot bridge on SH 180 at West Village Creek relief (Bridge #7): side view of the bridge

Figure 3.2 The selected pilot bridge on SH 180 at West Village Creek relief (Bridge #7): bottom view of the bridge deck

### 3.3. FEM Simulation of the Pilot Geothermal Bridge

To assess the feasibility of the deicing system on an 18 in. concrete bridge deck, numerical simulations were performed using COMSOL (COMSOL, 2016). This model was previously developed and verified with the experiments on a lab-scale concrete slab of 3 ft. × 4 ft. ×8 in. (Figure 3.3), which employed the hydronic heating system with insulated PEX pipe loops at 8 in. spacing to heat the bridge deck. However, the slab's thickness was modified to 18 in., and two cases of with and without asphalt layer were considered. For with asphalt case, the asphalt layer covers the top 3.5 in.

Constant ambient temperatures of 29 °F and 25 °F were considered for heating operation. The inlet temperature was set to 110 °F to heat the bridge deck. To further explore the preheating requirements of the system, a transient numerical study was performed.

Table 3.3 Summary of material properties considered in numerical simulations.

| Materials | Properties | Values | Units |
|---|---|---|---|
| Water (liquid) | Dynamic viscosity | 0.00273 | Pa·s |
| | The ratio of specific heat | 1.0 | - |
| | Heat capacity at constant pressure | 4180 | J/(kg·K) |
| | Density | 1000 | $kg/m^3$ |
| | Thermal conductivity | 0.61 | W/(m·K) |
| Concrete | Density | 2300 | $kg/m^3$ |
| | Thermal conductivity | 2.2 | W/(m·K) |
| | Heat capacity at constant pressure | 1000 | J/(kg·K) |
| | Surface emissivity | 0.91 | - |
| PEX pipe | Density | 938 | $kg/m^3$ |
| | Heat capacity at constant pressure | 950 | J/(kg·K) |
| | Thermal conductivity | 0.51 | W/(m·K) |
| Aluminum | Thermal conductivity | 205 | W/(m·K) |
| Spray Foam | Density | 21.6 | $kg/m^3$ |
| | Thermal conductivity | 0.028 | W/(m·K) |
| | Heat capacity at constant pressure | 1300 | J/(kg·K) |
| | Surface emissivity | 0.60 | - |

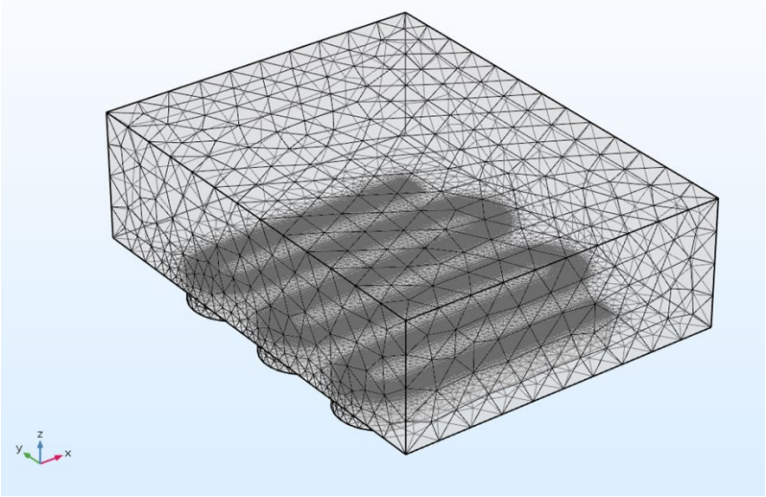

Figure 3.3 Overview of the finite element model

The numerical simulation outcomes show that despite the large thickness of 18 in., the system could still heat the bridge deck and raise the surface temperature above 32 °F as illustrated in Figure 3.4. For both cases with and without the asphalt layer, the system can heat up the bridge deck to avoid freezing conditions on the surface; however, it will take more time for the case with asphalt due to the lower thermal conductivity of asphalt in comparison to the concrete. Besides the increase of the inlet water temperature, to increase the heat supply to the bridge deck, it is suggested to reduce the hydronic loop spacing to 6 in. and employ better insulation at the bottom of the bridge deck.

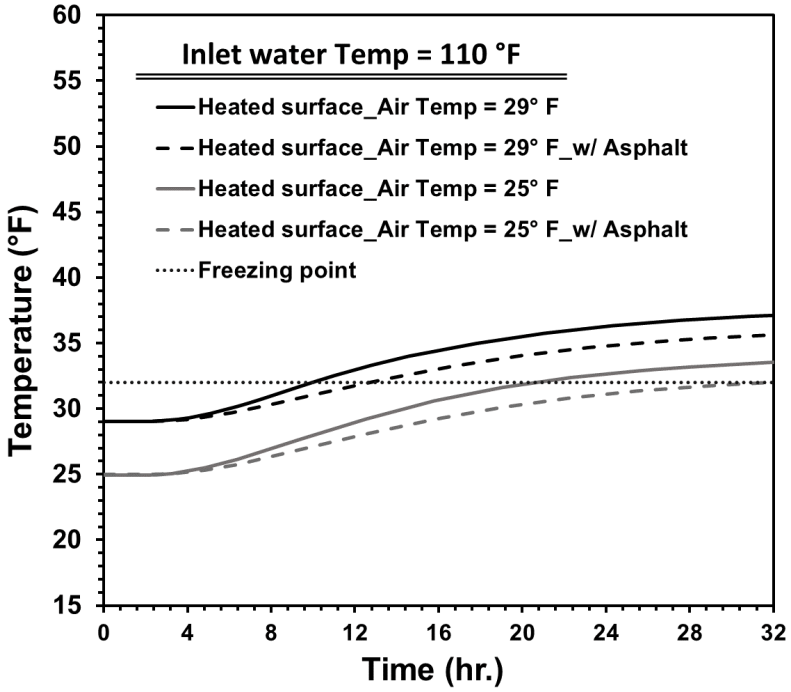


Figure 3.4. Numerical simulation result

### 3.4. Design of the Geothermal Bridge Deicing System

The design flow chart of the geothermal bridge deicing system is shown in Figure 3.5. In the following sections, the design heat flux is first determined, and then the design procedure for hydronic heating loops and the ground heat exchangers is introduced.

#### 3.4.1. Heat Flux Analysis

The required heat flux on the bridge deck surface is defined as the total heat flux maintained on the bridge deck surface in order to prevent snow/ice formulation under specified winter weather conditions. The required heat flux was determined based on the field data obtained during a deicing test on the geothermal mock-up bridge deck. Figure 3.6 shows the estimated surface heat flux on the geothermal mock-up bridge deck during a test in February 2019. The maximum surface heat flux of about 80 Btu/hr.ft$^2$ was determined on the heated surface while the ambient temperature was 25 °F. As the surface heat flux of 80 Btu/hr.ft$^2$ was found adequate for deicing the bridge deck surface, it is selected as a design heat flux for the geothermal deicing system in this report.

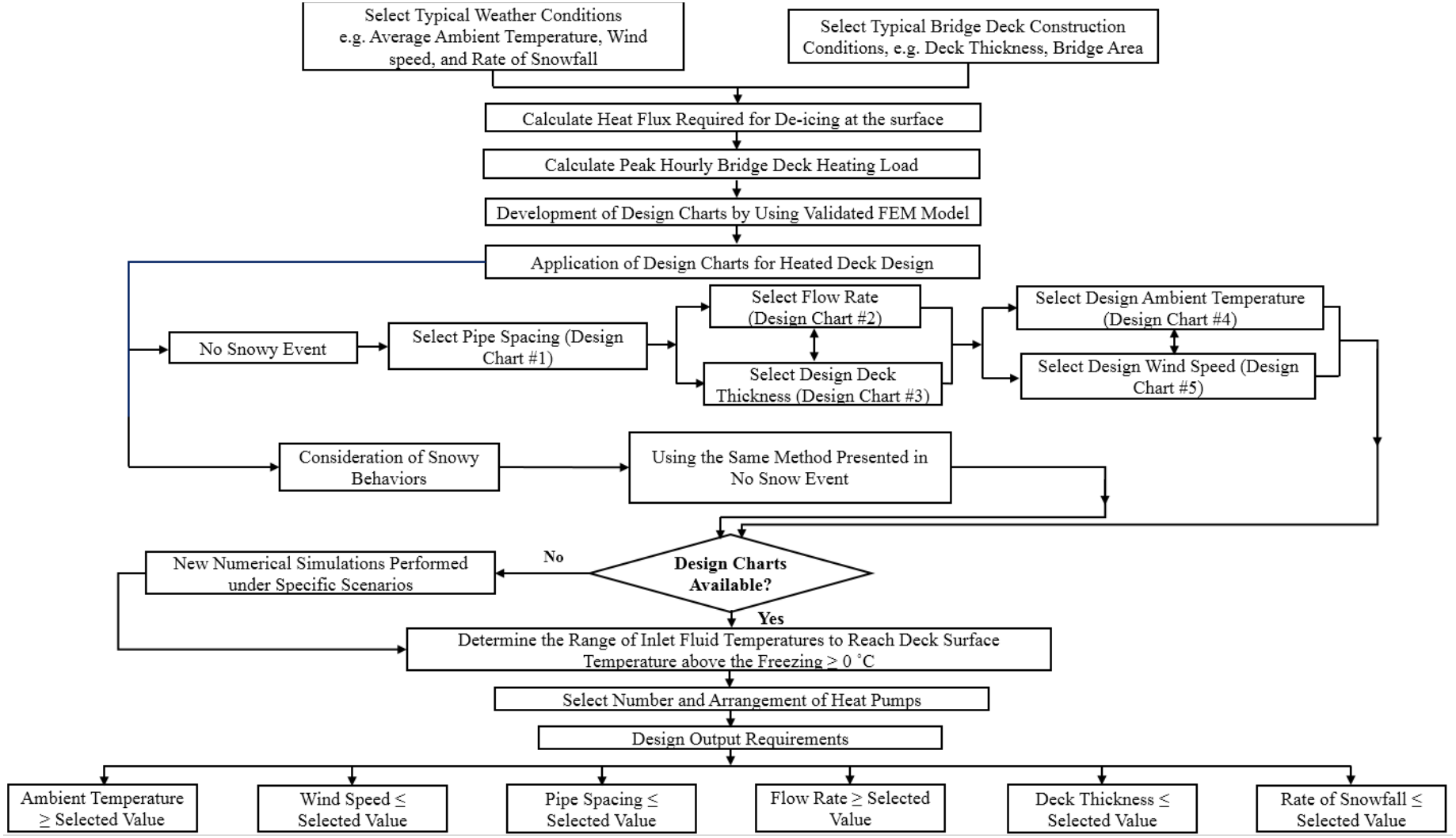


Figure 3.5 Flow chart of the design process for externally heated bridge decks, using a series of design charts developed from parametric studies

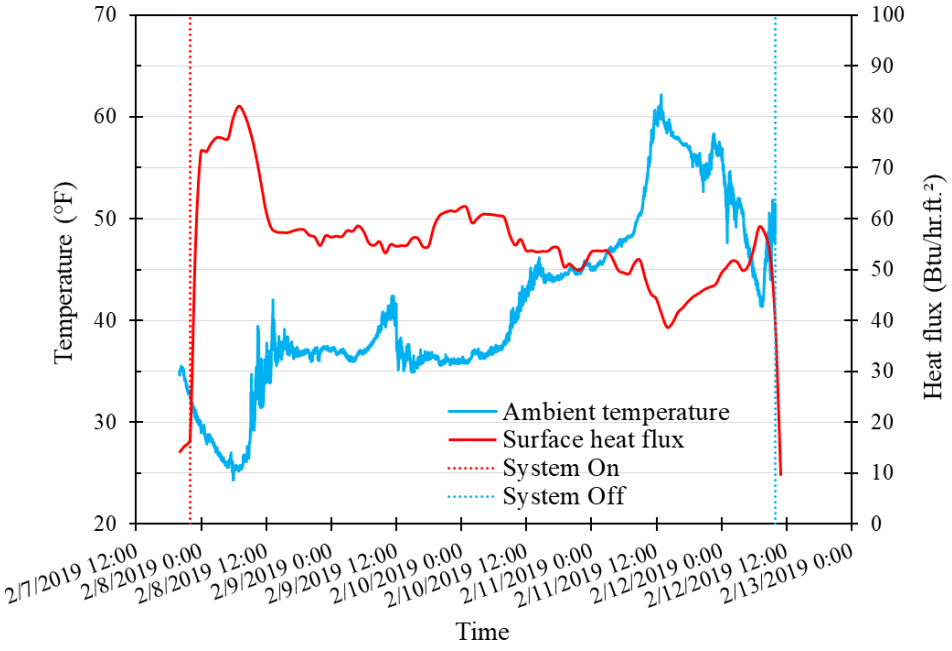


Figure 3.6 Surface heat flux variation during a deicing test on the geothermal mock-up bridge deck in February 2019 (Habibzadeh-Bigdarvish et al., 2021)

### 3.4.2. Design Procedure for Hydronic Heating Loops

The design procedure for externally heated bridge decks uses a series of design charts previously developed by FEM models accounting for various environmental and operational factors, including ambient temperature, wind speed, snowfall rate, bridge deck thickness, pipe spacing, and flow rate. The developed design charts are used to determine various parameters of the hydronic loops system. The design charts were created for a set of parameters defined in the FEM simulations. If the input values are not available in the charts, interpolation is needed to provide an estimated range of the outputs.

#### Pipe Spacing

Pipe spacing is one of the primary design factors that affect the efficiency of the heat transfer of an external system. In previous studies, pipe spacing of 6 to 12 inches was recommended. Figure 3.7 shows the steady-state temperature response curves under various pipe spacings, respectively. For the three pipe spacings, the minimum supplied inlet fluid temperatures required to keep the bridge deck surface above freezing are 64°F, 70 °F, and 78 °F, respectively.

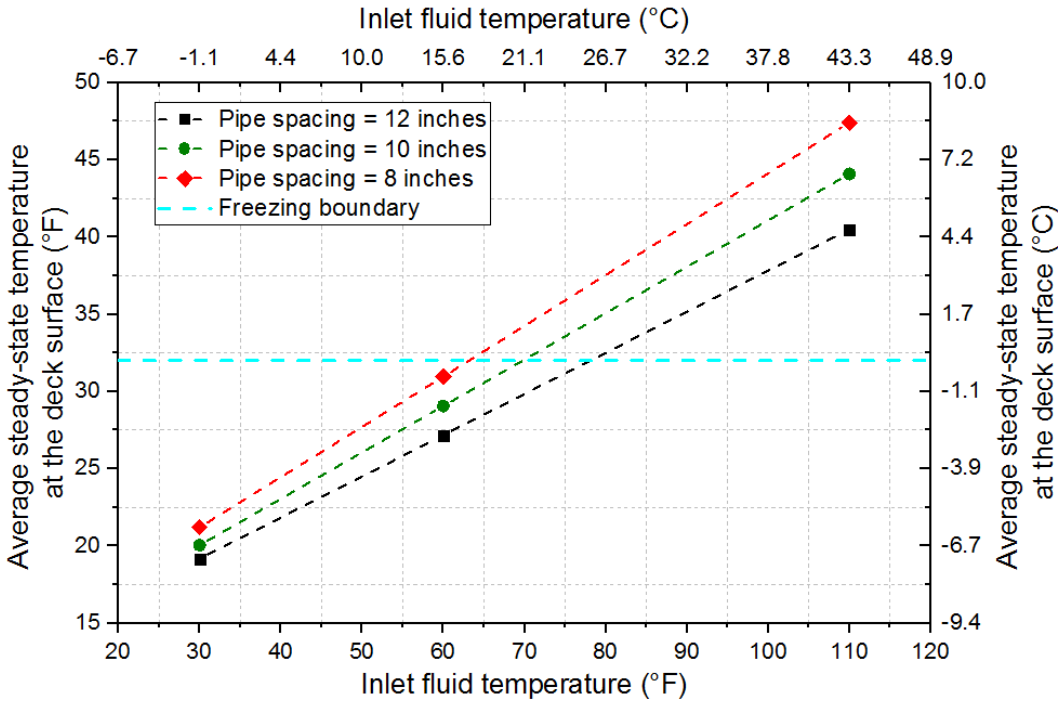


Figure 3.7 Interactions between inlet fluid temperatures and average steady-state temperatures at the deck surface under different pipe spacing.

In this design, typical weather and bridge deck conditions were selected. As mentioned previously, the system is designed for maximum heating capacity. Table 3.4 shows the design and weather conditions.

Table 3.4 Design weather and bridge conditions.

| Ambient Temperature (°F) | Wind Speed (mph) | Snowfall (in./hr) | Thickness of Bridge Deck (in.) |
|---|---|---|---|
| 25 | 6.7 | 0.8 | 18 |

The hydronic loop pipe spacing is a critical parameter in the de-icing system. To maximize the heat supply capacity, 6-inch pipe spacing is chosen. Based on previous experience, it is not usually feasible to install the pipe at smaller spacing than 6 in. as it might damage the loops during bending. The maximum outlet fluid temperature of the heat pump is selected as the system inlet fluid temperature and should be >110 °F according to the numerical simulations. The flow rate of the fluid in the hydronic heating system should be >5 gallons/min (GPM). The final proposed design requirements are listed in Table 3.5.

Table 3.5 Final proposed design output requirements.

| | |
|---|---|
| Pipe spacing | **≤ 6 in.** |
| Flow rate | **≥ 5 GPM** |
| Inlet fluid temperature | **≥ 110 °F** |

### Pipe Layout

Bridge span and deck configuration also play essential roles in designing externally heated bridge decks, which determine the length and layout of hydronic PEX loops.

### Pipe Material and Diameter

The recommended pipe material is the crosslinked polyethylene PEX pipe, which was used on the mock-up bridge. The pipe has 0.75 in. outer diameter and 0.5 in. of inner diameter. In addition, for heating performance enhancements, an aluminum plate and HDPE channel jacket filled with insulation foam are recommended.

### Flow Rate

Flow rate is another parameter that controls the heating system's performance since it can affect the convective flow contribution, accounting for the energy transport resulting from the fluid flow inside the hydronic loops. Figure 3.8 depicts the relationship between fluid inlet temperature and average steady-state temperatures on the deck surface under various flow rates. For studied flow rates, the flow rate has a negligible effect on the system's heating performance.

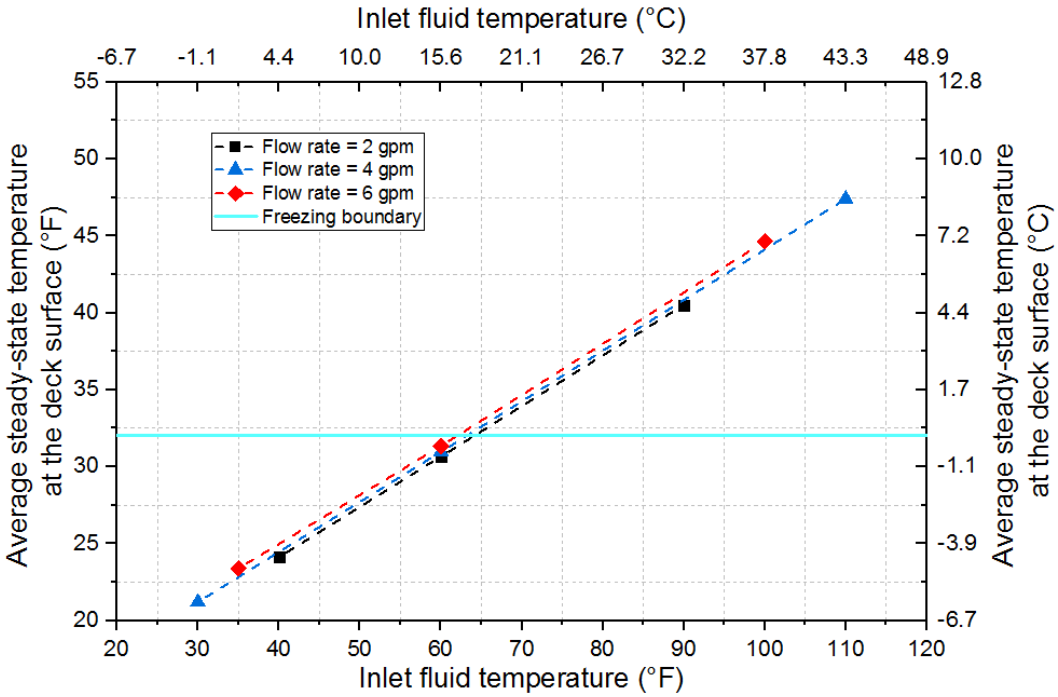


Figure 3.8 Interactions between inlet fluid temperatures and average steady-state temperatures at the deck surface under various flow rates

### Inlet Fluid Temperature

Ambient temperature has a dominant effect on the system's performance, as more heat energy is needed for the deck surface under lower ambient temperatures. Figure 3.9 shows the relationship between fluid inlet temperature and the average steady-state temperatures on the deck surface under different ambient temperatures and rates of snowfall.

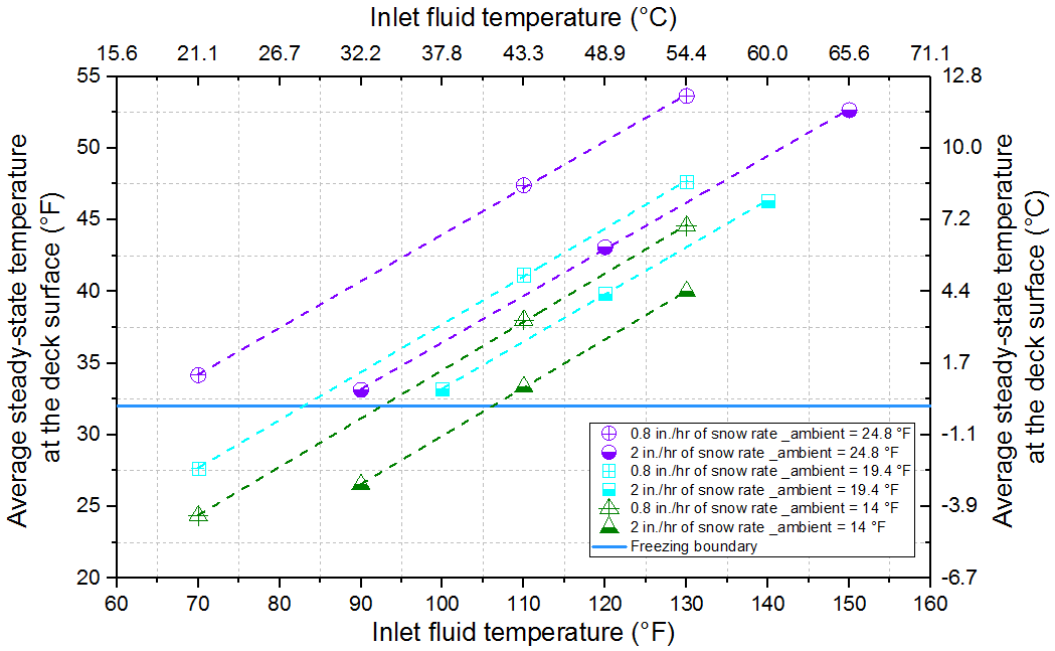


Figure 3.9 Interactions between inlet fluid temperatures and average steady-state temperatures at the deck surface under various ambient temperatures and rates of snowfall

Moreover, Figure 3.10 compares the average steady-state temperature at the deck surface under various wind speeds and snowy events.

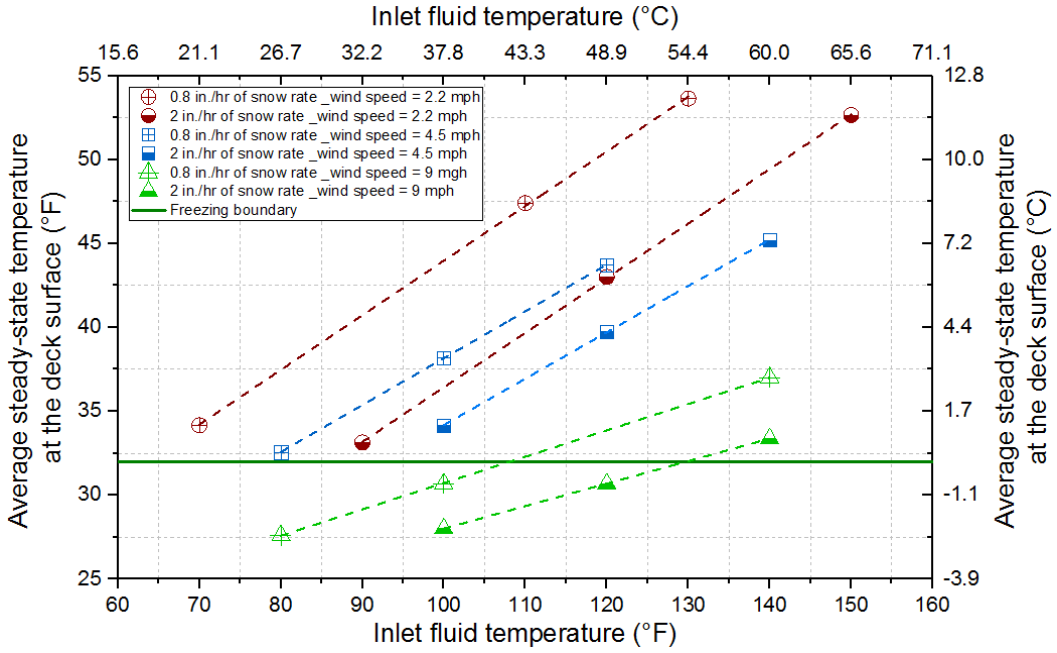


Figure 3.10 Interactions between inlet fluid temperatures and average steady-state temperatures at the deck surface under various wind speeds and rates of snowfall

For example, with an average snow rate of 0.12 in/hr, we can choose a middle line between the two green 9 mph wind speed lines to reach a fluid inlet temperature of 118 °F. In the end, the highest inlet fluid temperature would be the controlling temperature required to satisfy the steady-state surface temperature.

### 3.4.3. Design of the Ground Loop Heat Exchanger

A critical component of any Ground-Source Heat Pump (GSHP) system is the Ground Loop Heat Exchanger (GLHE). In order to obtain an appropriate system performance, the correct size of the bore field should be evaluated, including the length of GLHE and the spacing of boreholes. Furthermore, the system should be accurately designed since an undersized GLHE may cause performance failures, and on the other hand, oversizing results in an uneconomical system. In this report, the vertical ground heat exchangers were chosen to extract the energy from the ground and transfer it to the bridge deck for the deicing purpose. This section describes the design procedure of vertical ground heat exchangers.

A variety of geological formations complicate the design of vertical ground heat exchangers and eventually affect thermal performance. Figure 3.11 shows the design procedure for determining the proper size of the GLHE in this report. First, the design weather condition was chosen. In this step, weather data is collected, and the weather history of the region is investigated. Then the required heat flux for bridge deck snow/ice melting can be calculated based on the weather data. Then, the peak hourly and monthly heating loads are calculated according to the area of the bridge deck and snowfall hours, respectively. In the calculation of the monthly heating load, the number of hours of snowfall/ice event per year is used. Next, the heat pump unit is selected,

which is able to work in a system with the calculated heating load; Entering Water Temperature (EWT) and flow rates are specified, and heat pump and GLHE heating loads are selected from the heat pump heating performance datasheet. Afterward, the design and operational parameters are selected. If the required data are not available, a reasonable assumption can be made. Finally, all data are inputted to the design tool software, e.g., GLHEPro, and the GLHE size is calculated.

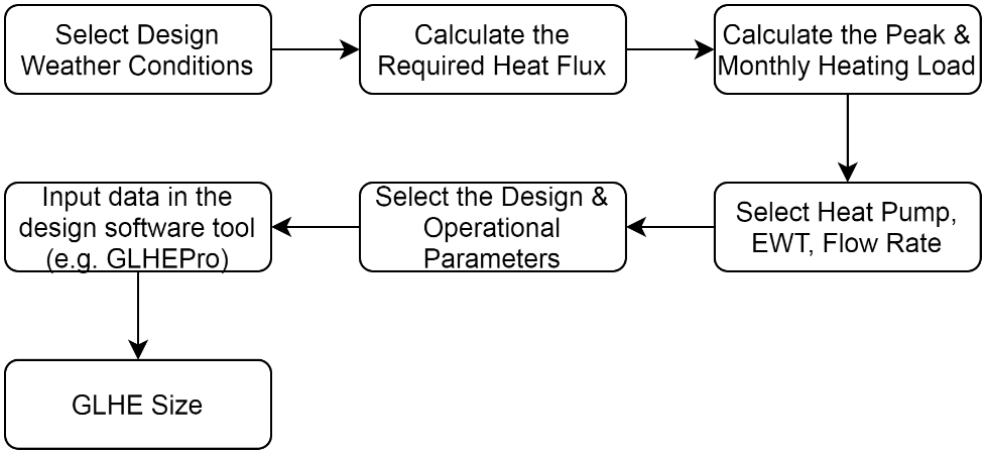


Figure 3.11 GLHE design diagram

For the design of the GLHE, first, we need to calculate the heat flux required for heating and de-icing at the surface. The heat flux required for heating and snow/ice melting on the bridge deck surface is selected based on previous de-icing test results of the external geothermal de-icing system on the mock-up bridge deck (Habibzadeh-Bigdarvish, 2021) and the design heat flux of 80 Btu/h.ft$^2$ is determined.

**Peak and Monthly Heat Load:** The snow melting systems are designed based on the design heat flux of 80 Btu/h.ft$^2$. The peak heating load and total monthly heating load are then calculated based on the bridge deck area and snowfall hours per year (20 hours of snow in each month of winter).

Table 3.6 Required heating load of the bridge.

| Design Heat Flux (Btu/h.ft$^2$) | Exposed Bottom Surface (ft$^2$) | Peak Heating (MBtu/h) | Monthly Snow Hours (h) | Total Monthly Heating (MBtu) |
|---|---|---|---|---|
| 80 | 4,325 | 346 | 20 | 6,920 |

**Heat Pump:**

Table 3.7 Heat pump heating performance data.

| **Heat Pump: 3 × GeoComfort Water-To-Water 10 Ton** | | | | | | |
|---|---|---|---|---|---|---|
| GPM | EWT(°F) | HYD LWT(°F) | CAP (MBtu/h) | PWR (KW) | COP | HE (MBtu/h) |
| 24 | 50 | 100 | 110.7 | 8.4 | 3.9 | 82.0 |

**GLHE Design Load:** A summary of the design GLHE and heat pump heating load is provided in Tables 3.8 and 3.9. The design peak heating load and the total monthly heating load are based on the performance data of the selected heat pump regarding heat extraction (HE) from the ground.

Table 3.8 Design heating load on GLHE

| GLHE loads | Month | Peak heating (MBtu/h) | Total heating (MBtu) | Percentage of annual heating load |
|---|---|---|---|---|
| | Jan | 246 | 4920 | 33.33% |
| | Feb | 246 | 4920 | 33.33% |
| | Mar | 0 | 0 | 0 |
| | … | … | … | … |
| | Nov | 0 | 0 | 0 |
| | Dec | 246 | 4920 | 33.33% |

Table 3.9 Design heating load on heat pump

| Heat pump loads | Month | Peak heating (MBtu/h) | Total heating (MBtu) | Percentage of annual heating load |
|---|---|---|---|---|
| | Jan | 86.1 | 1722 | 33.33% |
| | Feb | 86.1 | 1722 | 33.33% |
| | Mar | 0 | 0 | 0 |
| | … | … | … | … |
| | Nov | 0 | 0 | 0 |
| | Dec | 86.1 | 1722 | 33.33% |

**Ground Loop Heat Exchanger (GLHE):** The design parameters are essential to the proper design of the GLHE. Generally, the length of the heat exchanger that is required depends on three sets of data, namely soil properties, circulating fluid properties, and borehole specifications. In the following, the key parameters in designing the GLHE are described in Table 3.10, and the final recommended size for the GLHE is listed in Table 3.11 and illustrated in Figure 3.12.

Table 3.10 GLHE design parameters.

| | | | | | |
|---|---|---|---|---|---|
| $EWT_{min}$ | = | 50 °F | $k_{grout}$ | = | 0.8 Btu/h.ft.°F |
| Flow Rate | = | 24 gal/min | $D_{bore}$ | = | 6" |
| $T_g$ | = | 70.5 °F | $D_{pipe}$ | = | 1 1/4" |
| $k_{soil}$ | = | 1.15 Btu/h.ft.°F | Flow Regime | = | Turbulent |
| Heat Pump | = | 3 × GeoComfort Water-To-Water 10 Ton | | | |
| Fluid | = | Propylene Glycol/ Water with 20% concentration | | | |

Table 3.11 The final recommended size for the GLHE.

| | |
|---|---|
| # Boreholes | **16 (Spacing = 20 ft. & 6 ft.)** |
| Depth | **300 ft. [3055 ft. below surface]** |
| Borehole Diameter | **6"** |
| Single-U Pipe Diameter | **DR-11- 1 1/4"** |
| Header Pipe Diameter | **DR-11- 1 1/4"** |
| Grout Thermal Conductivity | **0.8 Btu/hr ft °F** |

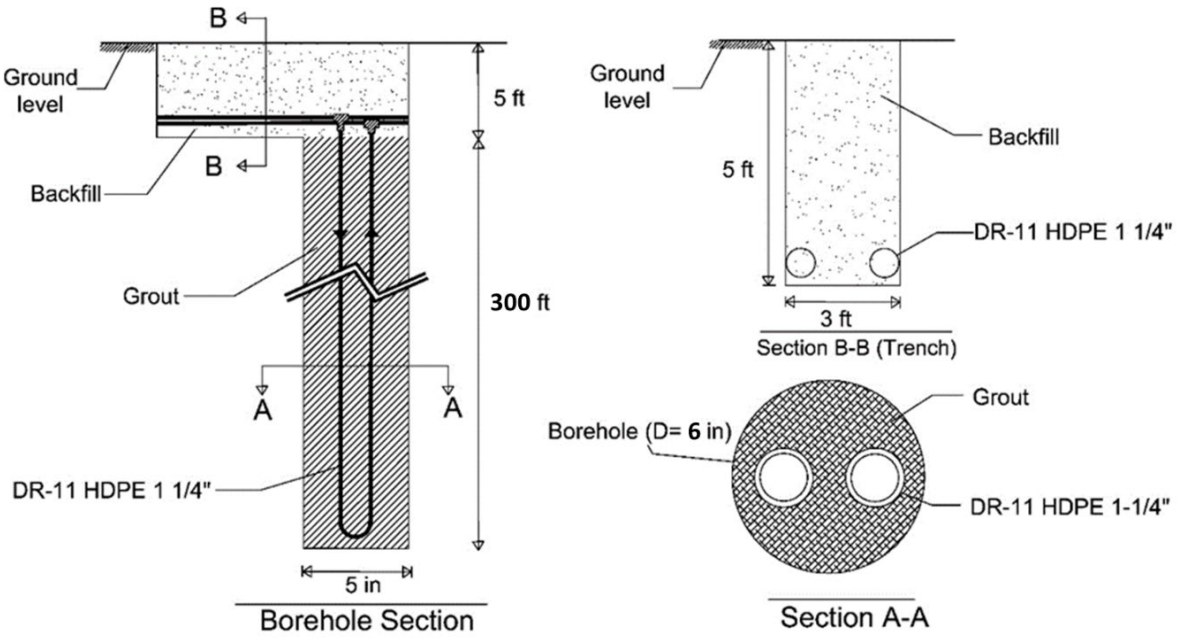


Figure 3.12 Borehole section detail

### 3.5. Pilot Bridge Deicing System

The deicing system, including ground heat exchangers, heat pumps and circulating pumps, bridge heating panels, etc., was installed onto an in-service bridge, as shown in Figure 3.13(a). The bridge consists of 8 spans and has 2 lanes on each bound. It is 200 ft. long and 48 ft. wide, and the bridge deck is 18 in. thick. Only the inner two lanes are designed for heating by the deicing system, as illustrated in Figure 3.13(b). Sixteen geothermal boreholes 300 feet deep (from ground level) were drilled, and five-feet deep trenches were excavated to connect the geothermal boreholes with the control room. Additionally, the system comprises four heat pumps, ten circulating pumps, two expansion tanks, 1 air dirt separator, and one storage tank, as shown in Figure 3.13(c). There are two types of bridge heating panels: spray-foam insulated panels and geofoam insulated panels. The spray foam insulated heating panels (Figure 3.13(d)) comprising aluminum plates, PEX pipes, and spray foam insulation were attached to the bottom of the pilot bridge. Geofoam blocks in 4 ft x 8 ft panels- 4 inches thick were secured (Figure 3.13(e)) with wooden cross beams (1/4 inch thick) at the bridge bottom surface.

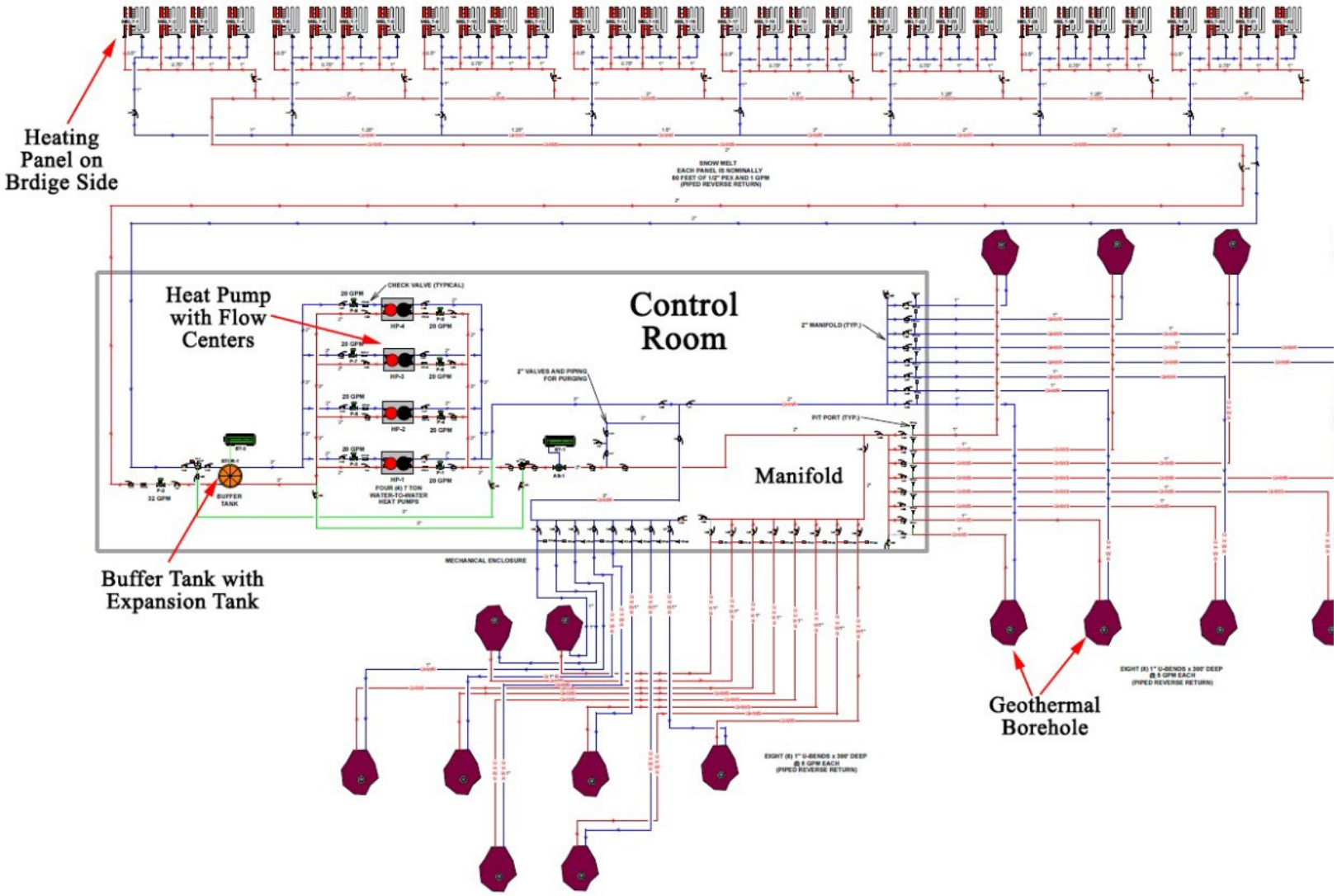
Heating Panel on Brdige Side
Heat Pump with Flow Centers
Control Room
Manifold
Buffer Tank with Expansion Tank
Geothermal Borehole
SNOW MELT
EACH PANEL IS NOMINALLY
60 FEET OF 1/2" PEX AND 1 GPM
(PIPED REVERSE RETURN)
CHECK VALVE (TYPICAL)
2" MANIFOLD (TYP.)
2" VALVES AND PIPING FOR PURGING
PIT PORT (TYP.)
BUFFER TANK
MECHANICAL ENCLOSURE
EIGHT (8) 1" U-BENDS x 300' DEEP @ 5 GPM EACH (PIPED REVERSE RETURN)

(a)


(b)

(c)

(d)

(e)

Figure 3.13 (a) design of the bridge deicing system; (b) the pilot bridge on SH 180 at West Village Creek relief; (c) geothermal heat pumps, flow centers, manifolds, and control system within the control room; (d) spray foam insulated panel; and (e) geofoam insulated panel.

Effective geothermal bridge deicing system operation relies on accurate sensors and a reliable data acquisition system. A network of sensors and monitoring devices is strategically deployed on the top and bottom surfaces of the bridge deck for essential data regarding temperature, fluid flow, and other appropriate parameters. These instruments play a critical role in ensuring the efficient functioning of the deicing system, allowing for real-time monitoring and control. This overview explores the instrumentation deployed on and beneath the bridge and the data acquisition system used to collect and analyze data for effective deicing operations.

To ensure the collection of all desired temperature data during the winter event, the UTA and TAMU team installed ten thermistor probes and two strain gauges on the bridge. The subsequent sections detail the installation process, locations, and specific sensor details.

### 3.5.1. Instruments and Data Acquisition System

The geothermal system and the bridge deck were instrumented with temperature sensors for heating performance evaluation. This section presents the sensors, data acquisition system, and instrumentation plan. Various temperature sensors, which are compatible with an LC-16 datalogger (GEOKON), were used in this project, including individual thermistors and thermistor strings (GEOKON) and type-T thermal probes (OMEGA). In addition, TEROS 10 moisture sensors (Meter Group) were installed within the geothermal boreholes (GHE) to monitor borehole moisture variations. In this report, only representative sensors on the bridge's surface are presented to demonstrate the performance of the de-icing system. All the sensors are calibrated internally in the data logger. Temperature outputs are recorded directly by the data logger. The following subsections detail the instruments and data acquisition system utilized for bridge and GHE.

#### 3.5.1.1. Instruments and Data Acquisition System on the Bridge Section

The geothermal system and the bridge deck were instrumented with temperature sensors for heating performance evaluation. This section presents the sensors, data acquisition system, and instrumentation plan. Various temperature sensors, which are compatible with an LC-16 datalogger (GEOKON), were used in this project, including individual thermistors and thermistor strings (GEOKON) and type-T thermal probes (OMEGA). In addition, TEROS 10 moisture sensors (Meter Group) were installed within the geothermal boreholes (GHE) to monitor borehole moisture variations. In this report, only representative sensors on the bridge's surface are presented to demonstrate the performance of the de-icing system. All the sensors are calibrated internally in the data logger. Temperature outputs are recorded directly by the data logger. The following subsections detail the instruments and data acquisition system utilized for bridge and GHE.

#### Surveying for Sensor Location

The successful completion of the bridge survey marks a significant milestone in our project. It signifies the accurate identification of locations for placing sensors at both the top and bottom sections of the bridge. This accurate surveying process ensured the sensors were strategically positioned for optimal data collection and analysis in the geothermal system evaluation.

To determine the optimal location for the sensors, the upper section of the bridge was precisely surveyed, considering variables including data collection efficiency, accessibility, and structural safety. In the same way, the lower portion was equally surveyed, with special care paid to important structural components to ensure precise sensor placement. Based on Figure 3.14, six sensors were located on the top of the bridge. Five thermistors were installed on the span insulated with spray foam at its bottom surface, called span 2, while one thermistor was placed on the span insulated with geofoam at its bottom surface, called span 1. The surveying of sensor locations is shown in Figure 3.15. Table 3.12 summarizes the temperature sensors installed on the bridge section.

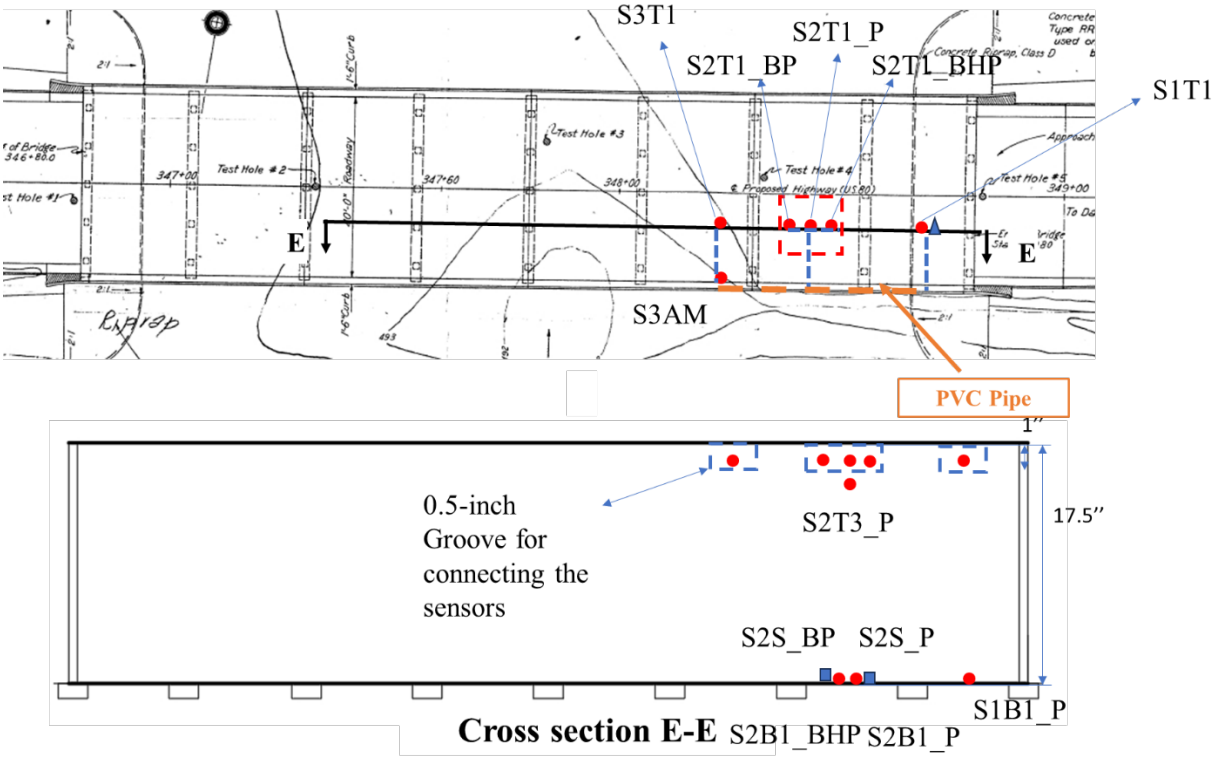


Figure 3.14 Plan view and cross-section view of temperature sensors for the bridge deck.

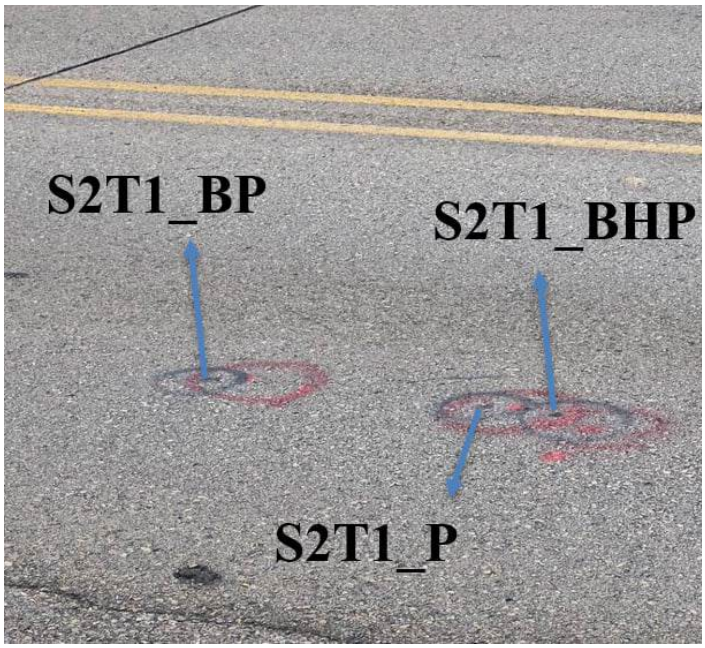


a) Top of the bridge

b) Surveying

Figure 3.15 Surveying the Bridge for sensor locations on the bridge deck surface.

Table 3.12 The identification and locations of all sensors.

| Logger Terminal | Sensor ID | Description | Location |
|---|---|---|---|
| T1 | S1T1 | Span 1 Top 1in | Span 1 |
| T2 | S1B1_P | Span 1 Bottom 1in above PEX | Span 1 |
| T3 | S2T1_BHP | Span 2 Top 1in Between Heat Transfer Plates | Span 2 |
| T4 | S2T1_P | Span 2 Top 1in above PEX | Span 2 |
| T5 | S2T1_BP | Span 2 Top 1in Between PEX | Span 2 |
| T6 | S2C | Span 2 Control | Span 2 |
| T7 | S2T3_P | Span 2 Top 3in above PEX | Span 2 |
| T8 | S2B1_P | Span 2 Bottom 1in above PEX | Span 2 |
| T9 | S2B1_BHP | Span 2 Bottom 1in Between Heat Transfer Plates | Span 2 |
| T10 | S3T1 | Span 3 Top 1in | Span 3 |
| T11 | S2S_P | Span 2 Strain Gauges above PEX | Span 2 |
| T12 | S2S_BP | Span 2 Strain Gauges Between PEX | Span 2 |

**Instruments on the Bridge Bottom Surface**

On the bridge deck bottom surface, three thermistor probes of model 3800 (GEOKON) and two strain gauges of type EA 4000B (GEOKON) were installed prior to the application of spray foam and geofoam insulation (Figure 3.16). Two of the three thermistors were positioned in the spray

foam insulated span, while the remaining one was installed on the geofoam insulated span. One of the thermistor probes was precisely placed at the interface between the bridge deck and the heat transfer plate to detect temperature variations. Additionally, the extra thermistor probes were inserted one and a half inches inside the bridge concrete to monitor temperature fluctuations within the concrete itself. Regarding the strain gauges, one was situated between two heating panels, while the other was positioned at the center of a panel. These strain gauges will monitor concrete deformation in both heated and unheated zones. All thermistors and strain gauge cables were enclosed within half-inch PVC pipes to safeguard the wires from heat generated by the spray foam.

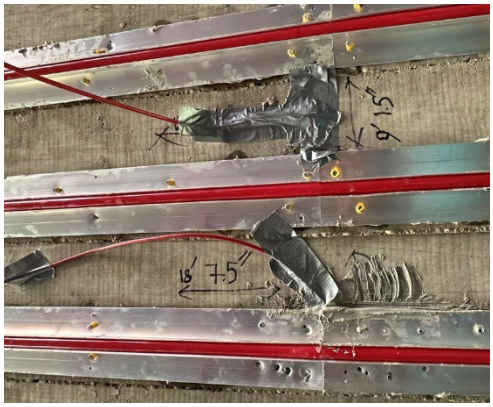


Figure 3.16 Sensor Installation: two thermistor probes.

Figure 3.17 shows the high-precision temperature sensors integrated into the inlet and outlet PEX loops in one spray foam-insulated span to measure the fluid temperature precisely. A data collection system was also implemented and connected to the temperature sensors to support real-time data collection. This monitoring system enables continuous monitoring of fluid temperature changes during the geothermal system's operational phases.

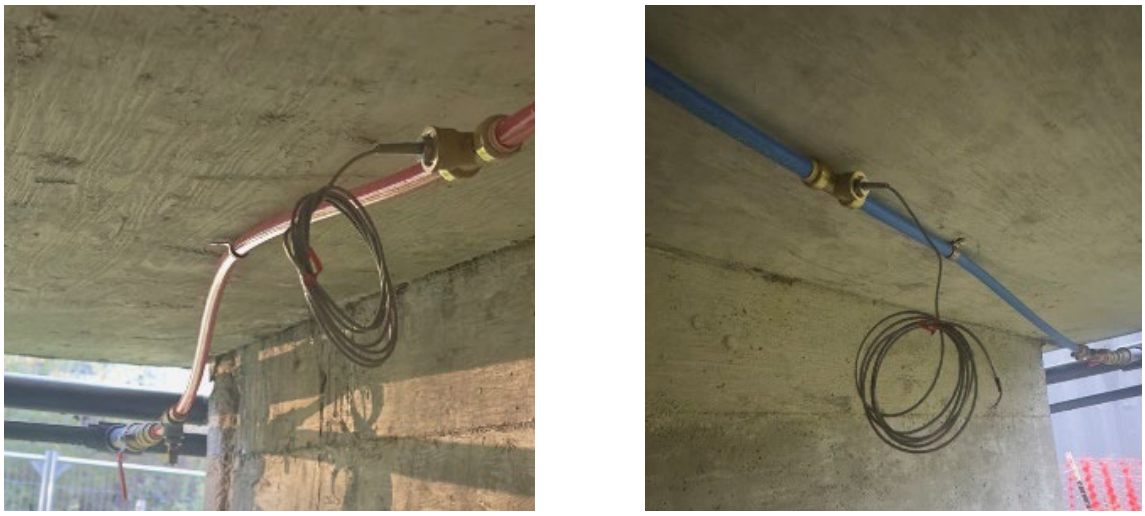

Figure 3.17 Installation of temperature sensors.

**Instruments on the Bridge's Top Surface**

With assistance from the TxDOT Fort Worth District, several thermistor probes were installed on the bridge's road surface to measure the bridge surface temperature response during winter events. Traffic control was implemented to establish a safe working environment for TxDOT and UTA teams during the bridge work. Grooves approximately 0.5 inches in width and depth were cut on the bridge surface, where thermistor probes were buried, and backfill was applied.

**Data Acquisition System**

As shown in Figure 3.18, an LC-16 (GEOKON) datalogger was installed underneath the bridge to collect temperature data from the thermistors installed on the bridge. An initial interval setting of 60 seconds was established to initiate the data collection process.

Figure 3.18 Sensor strings connection to the datalogger.

**3.5.1.2. Instruments and Data Acquisition System on GHE**

GHEs were installed at the bridge site to harness geothermal energy for de-icing operations. The installation involved drilling a soil borehole to the GHE design depth (300 ft), lowering an HDPE U-pipe, and grouting the drilled hole with thermal grout. The energy extraction will be performed by circulating cold water (temperature lower than the subsurface temperature) through the u-pipe (55 ˚F), which will heat up as it moves through the pipe. Figure 3.19 shows the plan view of GHEs installed at the site. Sixteen GHEs were installed on the project. Eight GHEs were installed in a conventional arrangement, where no thermal interaction is expected between the GHEs due to their substantial spacing (>20 ft), and the remaining eight were installed in proximity (<15 ft) to allow for thermal interactions during operation. The closely spaced GHE configuration was selected to study the efficiency of thermal heat storage in the summer, where the hot pavement of the bridge will be used as a solar collector, and the energy will be stored in the subsurface. It may improve the de-icing performance of the overall system. Four types of sensors were installed on the GHE system to assess the thermal efficiency of underground heat extraction. Figure 3.20 shows the locations of underground sensors.

- Three thermistor strings comprising thermocouples were installed on GHE pipes to measure the temperature around the u-pipe at distances 4, 11.5, and 14 ft from the geometric center of the installed GHEs. Each string has four sensors fabricated into a single wire, which read temperature data at set intervals. Each string was secured to the pipe with duct tape and zip-ties, as shown in Figure 3.21 and lined to the surface along the pipe to be connected to the data logger. The approximate elevations of the sensors have been presented in the cross-sectional view.
- Six moisture sensors were installed in the subsurface to measure moisture fluctuations over time. Four moisture sensors were installed in thermal measurement boreholes (T1 and T2), which were separately drilled holes around the GHE down to approximately the top of the rock, as the selected sensors are well suited for soil. In addition to moisture readings, these sensors also provide temperature readings. Since the thermal measurement boreholes did not have a U-pipe in the drill hole, a 20-foot deep, ½-inch diameter PVC pipe was utilized to install the sensors at their designated locations. The remaining two moisture sensors were installed in a GHE.
- A piezometer was also installed on T2 to observe seasonal groundwater movements on site.
- Two flow meters were installed on GHEs. Flow meters were installed (inline) to measure the flow rate through the u-pipes and the temperature of the moving fluid. One was installed in the conventional system's GHE, and the other was installed on the closely spaced GHE. These sensors help quantify the contribution of geothermal energy in bridge de-icing operations.

The data recorded from the sensors discussed above is presented in section 3.

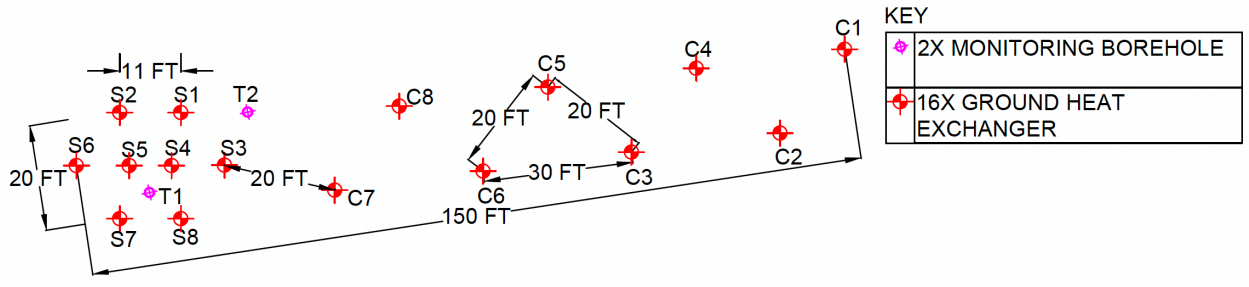


Figure 3.19 GHE plan view.

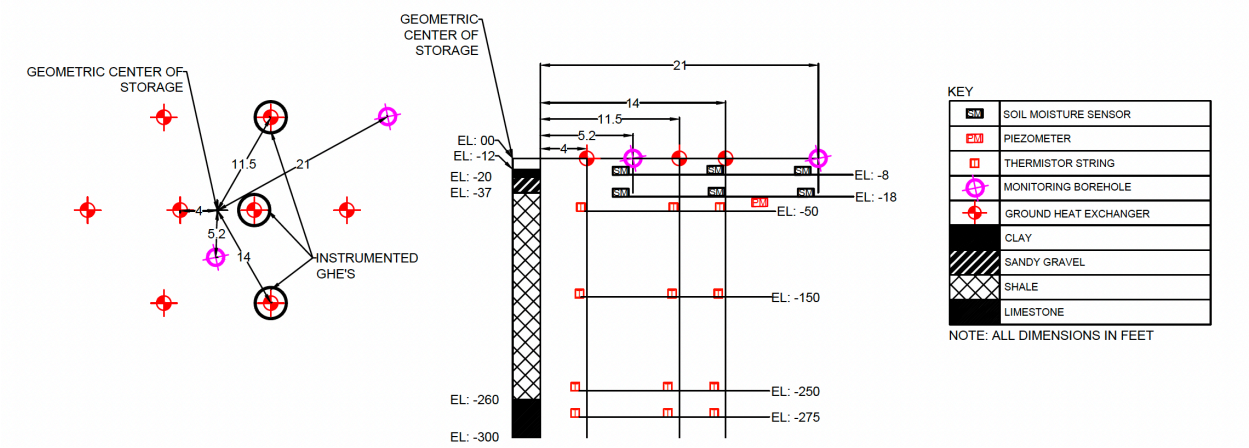


Figure 3.20 GHE instrumentation location plan view (left) and cross-sectional view (right).

(a) (b)

Figure 3.21 (a)Thermistor string installation. (b) Thermistor wire lined to the surface.

### 3.5.2. Control System

Four heat pumps and ten flow centers were applied for the new pilot bridge deicing system, forming a complicated flow system. Therefore, Tekmar Snow Melting Control 670, a programmable controller, was utilized for operating heat pumps and flow centers. The control operation relies on one temperature sensor embedded in the bridge deck and one outdoor temperature sensor to manage the system. The de-icing system has two operation modes: heat pump heating mode and bypass heating mode.

Since the Tekmar 670 control system experienced a connection issue and was unavailable this winter, four thermostats (Tekmar 519), as shown in Figure 3.22, were wired to the heat pumps to control the operation. Moreover, the thermostat was controlled by an external thermistor attached to the inlet pipe to the bridge deck inside the control room to measure the inlet heat carrier fluid temperature. However, it should be noted that the whole system, including the four circulating pumps, was turned on/off manually, and one 519 thermostats only controlled one heat pump when the power supply was activated.

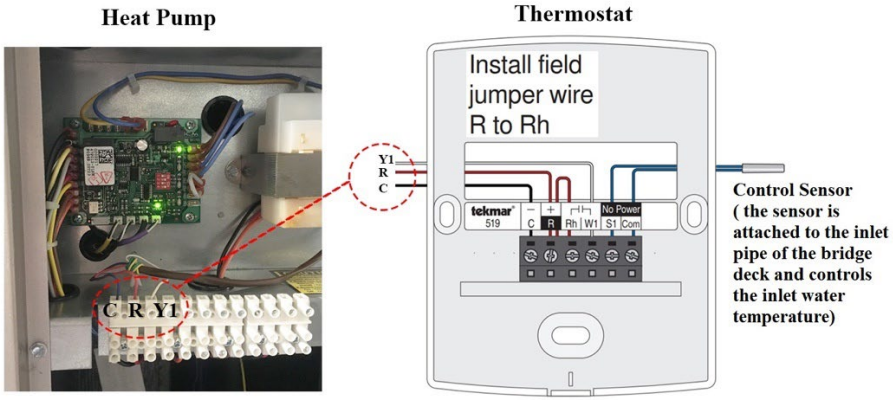


Figure 3.22 Control system: wiring diagram of the heat pump and thermostat (Tekmar 519).

### 3.6. Winter Test

A comprehensive overview of statistical weather data observed from November 2023 to February 2024 is summarized in Table 3.13. The first day of freezing temperature was observed on November 1, 2024, and the last day was February 18, 2024. The winter of 2023-24 was the 13$^{th}$ warmest winter on record. The type, duration, and precipitation of each winter event were analyzed using the data from the weather station at the DFW airport. According to the weather data, the area experienced a total of 15.5 hours of light snow in January 2024, which was the focus of the operation of the deicing system. The following section illustrates the performance of the pilot bridge deicing system during the January 2024 winter event.

Table 3.13 Summary of weather data from November 2023 to February 2024.

| Month | Winter Weather | Days of Occurrence | Hours of each event | Minimum temperature |
|---|---|---|---|---|
| Nov-2023 | Freezing | 2 | 5 hr | 30.9 °F to 28 °F |
| Dec-2023 | Freezing | 2 | 12 hr | 32 °F to 28 °F |
| Jan-2024 | Freezing | 8 | 48 hr | 23 °F to 15.1°F |
| | Freezing (Frigid) | 3 | 26 hr | 15.1 °F to 12.9 °F |
| | Light Snow; Mist | 1 | 8 hr | --- |
| | Light Snow | 1 | 7.5 hr | --- |
| Feb-2024 | Freezing | 1 | 20 hr | 30.9 °F to 28.9 °F |

#### 3.6.1. January 2024 Snow Event

The research team closely monitored the winter weather conditions from January 13$^{th}$ to 20$^{th}$, 2024. When a cold front with freezing temperatures was forecasted, the de-icing system was turned on a few hours before the freezing event. The system was operated with its full heating load, meaning that all four heat pumps were initiated, and the outlet fluid temperature of the heat pumps was set to 105 °F. The lowest local air temperature detected was 12.8 °F with approximately 0.25-inch snow, as shown in Figure 3.23.


(a)

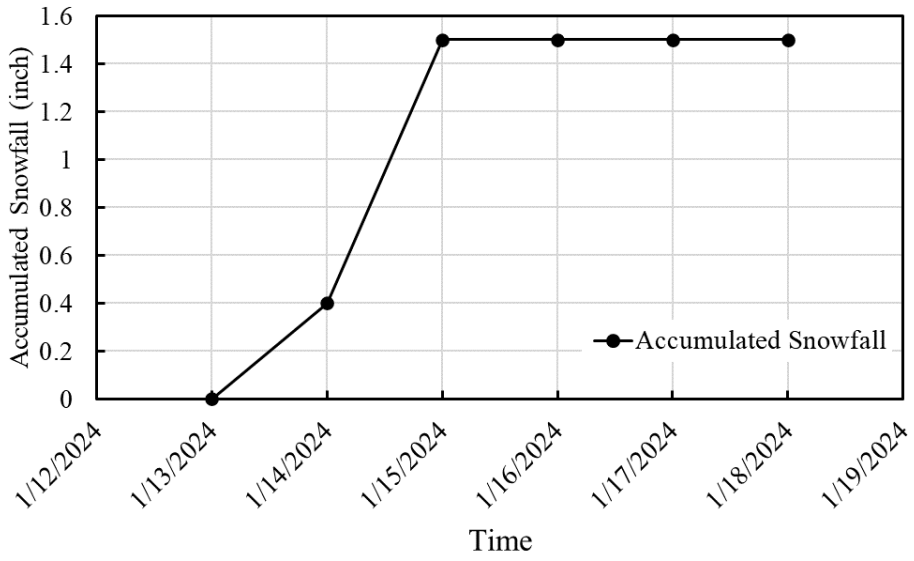


(b)

Figure 3.23 Snow and ice accumulation map: Jan. 13-15, 2024 (Source: National Weather Service, 2024).

Table 3.14 summarizes the five winter tests performed during Jan. 2024. The start and end times are the operating periods during which the geothermal system operates. The minimum and average air temperatures during the freezing period are obtained to characterize the winter events. The heated zone's average and minimum surface temperatures were obtained from sensors installed on the bridge's top surface (Figure 3.24). This sensor was selected as a representative

temperature response of the bridge deck during the coldest winter test period. The average surface heat flux was calculated based on the obtained bridge temperatures. The last column in Table 3.14 describes the geothermal system's operation during each winter test. Table 3.14 shows that during all heating tests, the system could keep the deck surface heat flux above the designed heat flux. Event #1 is selected as an example of the winter tests. A detailed discussion of the system's performance is presented below.

Figure 3.24 shows the temperature variation of the inlet and outlet heat carrier fluid on the bridge deck side. The heat pump output fluid temperature to the bridge deck was 105 °F. The average inlet and outlet fluid temperatures to the bridge span were recorded as 90.8 and 81.5 °F, respectively. Figure 3.24 also compares the surface temperature variation of the externally heated and non-heated zones with that of the ambient temperature data. The temperature data for both zones are obtained from the thermal probes installed on the surface. Before the onset of the system, the heated and non-heated zone deck temperatures are very close to each other and follow the same trend as the ambient temperature. However, after the onset of the circulating pumps, the temperature in the heated zone increases and follows a different trend concerning the non-heated zone. The temperature in the non-heated zone still closely matches the ambient temperature, indicating the monitored data's validity. Overall, the heating system could keep the heated surface temperature above freezing. Although the surface temperature is below freezing at some times in Event #1-3 when the ambient temperature is below 15 °F, no snow/ice formed on the heated bridge surface, as shown in Figure 3.25.

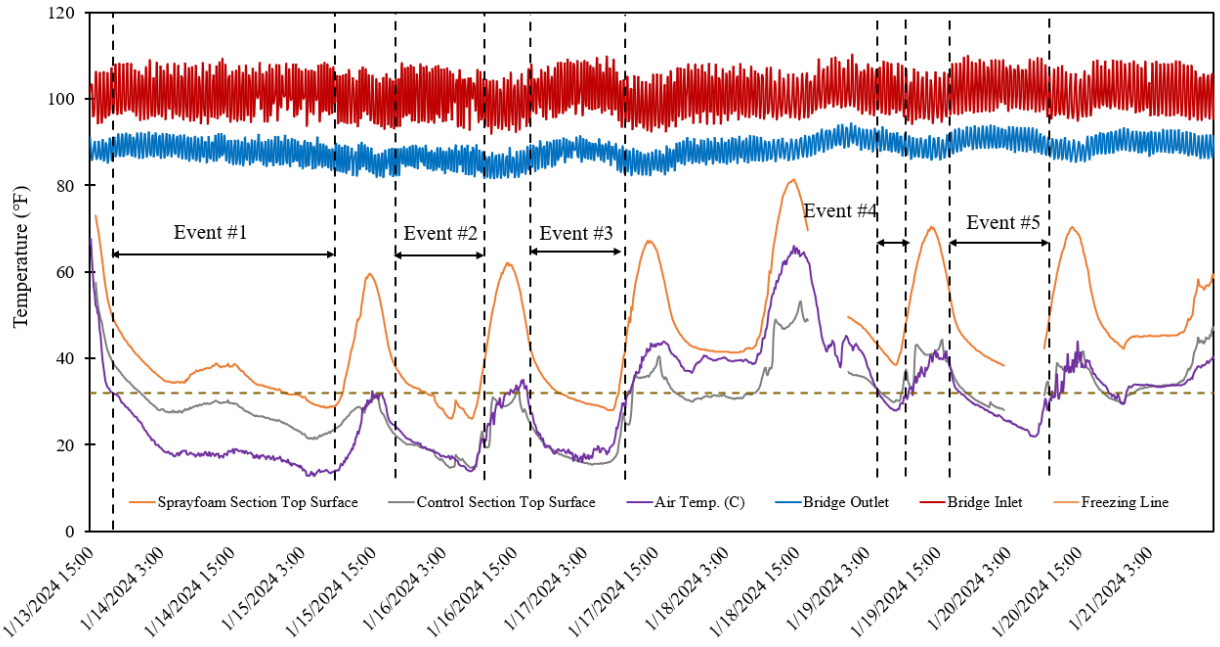


Figure 3.24 Bridge inlet and outlet temperature and bridge deck surface temperature response during the Jan. 2024 winter events.

Table 3.14 Summary of the Jan. 2024 winter tests and performance.

| Event# | Start | End | # Hrs. of freezing | Ave. ambient temp. (˚F) | Minimum ambient temp. (˚F) | Ave. surface temp. (˚F) | Ave. surface heat flux ($W/m^2$) | Test description |
|---|---|---|---|---|---|---|---|---|
| 1 | 1/13/24 18:30 | 1/15/24 15:50 | 45.7 | 17.2 | 12.8 | 37.3 | 312.8 | Full Heating Load (Set inlet: 105 °F) |
| 2 | 1/15/24 17:50 | 1/16/24 14:50 | 21 | 20.9 | 13.9 | 36.9 | 351.2 | |
| 3 | 1/16/24 17:20 | 1/17/24 11:20 | 18 | 21.4 | 16.3 | 33.9 | 342.1 | |
| 4 | 1/19/24 5:00 | 1/19/24 10:30 | 5.5 | 29.9 | 27.9 | 43.1 | 320.4 | |
| 5 | 1/19/24 18:30 | 1/20/24 12:30 | 18 | 27.7 | 21.9 | N/A | N/A | |

### 3.6.2. Heating Performance of the Geothermal Bridge Deicing System

#### 3.6.2.1. Bridge Temperature Response

Winter Event #1 is selected due to the observed snowfall and the lowest temperature of 12.8 °F. This heating test spans from 1/13/2024, 18:30 to 1/15/2024, 15:50. The snow started on 1/14/2024, 18:00, and stopped on 1/15/2024, 8:00 am. The maximum snow accumulation of 1.5 inches occurred across portions of Central TX (Figure 3.24). In this test, the geothermal heating system operated in full heating load (4 heat pumps were on). Figure 3.25 presents the bridge surface status right after snow. No accumulated snow exited on the heated surface of the pilot geothermal bridge (Figure 3.25-a). In contrast, snow formed on the surface of the unheated bridge, which is close to the pilot geothermal bridge (Figure 3.25-b).


(a)


(b)

Figure 3.25 Comparison of bridge surface status between (a) pilot geothermal bridge and (b) unheated bridge, which is close to the pilot bridge.

Figure 3.26 depicts the heat flux on the heated bridge surface during winter Event #1. The heat flux is calculated based on Eq. 1 using temperature data obtained from two thermistors near the bridge surface. The distance between the two thermistors is 0.5 inches.

$$q = -k\frac{\Delta T}{\Delta x} \tag{1}$$

where $q$ is heat flux; $k$ is the concrete thermal conductivity; $\Delta T$ is the temperature difference between two points; and $\Delta x$ is the distance.

During the night, the heating system maintained the heated surface heat flux above 269.1 W/m$^2$, slightly above the design heat flux of 252 W/m$^2$. This means the heating system can prevent snow formation even with the lowest air temperature of 12.8 °F. During the day, the temperature gradient near the deck surface decreased due to the solar radiation and thus the surface heat flux decreased as well.

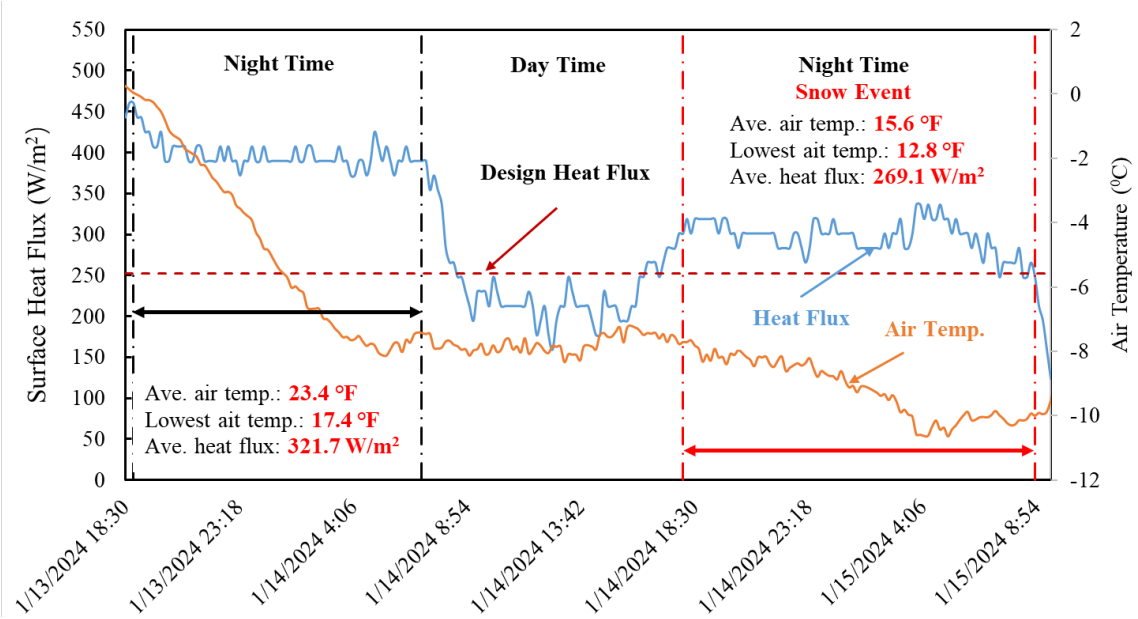


Figure 3.26 Heat flux of the heated bridge surface during Event #1.

### 3.6.2.2. GHE Temperature Response

The GHE provides a consistent heat source to the GSHP, which delivers adequate energy to the bottom of the bridge. The GHE extracts energy from the subsurface when a fluid with an average temperature lower than the subsurface temperature (69.7 °F) is circulated through the u-pipe. As the colder fluid circulates (55 °F) through the u-pipe, the geothermal gradient interacts with the temperature gradient within the fluid and warms it up, thus resulting in energy extraction. Since fluid circulation in the GHEs started on 01/12/2024, a consistently decreasing trend in the temperature has been observed on the installed thermistor strings, which signifies that energy was extracted from the subsurface. Figure 3.27 shows the temperature response at the borehole depth of 50 ft. The extracted energy can be calculated as:

$$Q = c_p m(T_{out} - T_{in}) \quad (2)$$

Where $Q$ is the heat extracted in kJ/hr, $c_p$ is the heat capacity of carrier fluid in kJ/ kg ˚C, $m$ is the mass flow rate of the fluid in kg/hr, $T_{out}$ is the temperature of the circulating fluid exiting, and $T_{in}$ is the temperature of the fluid entering the u-pipe. The heat capacity of the circulating fluid is 4.18 kJ/kg.˚C, and the mass flow rate is 1135 kg/hr (5 gallons per minute). The inlet and outlet temperatures were measured using an Onicon flowmeter. With an inlet temperature of 55˚F (12.77 ˚C) and an outlet temperature of 57 ˚F (13.88 ˚C), the calculated energy extraction is 5266 kJ/hr or 1.46 kW for 1 GHE. Since we have 16 GHEs installed on-site, the average power output of the GHE is 23.36 kW.

The seasonal water table fluctuates between 4-8ft below ground surface. Most of the GHE operation for de-icing the bridge was carried out with most of the GHE submerged in water. Since all the moisture sensors are located below the daily fluctuations, no significant change has been observed in the moisture content of the soil.

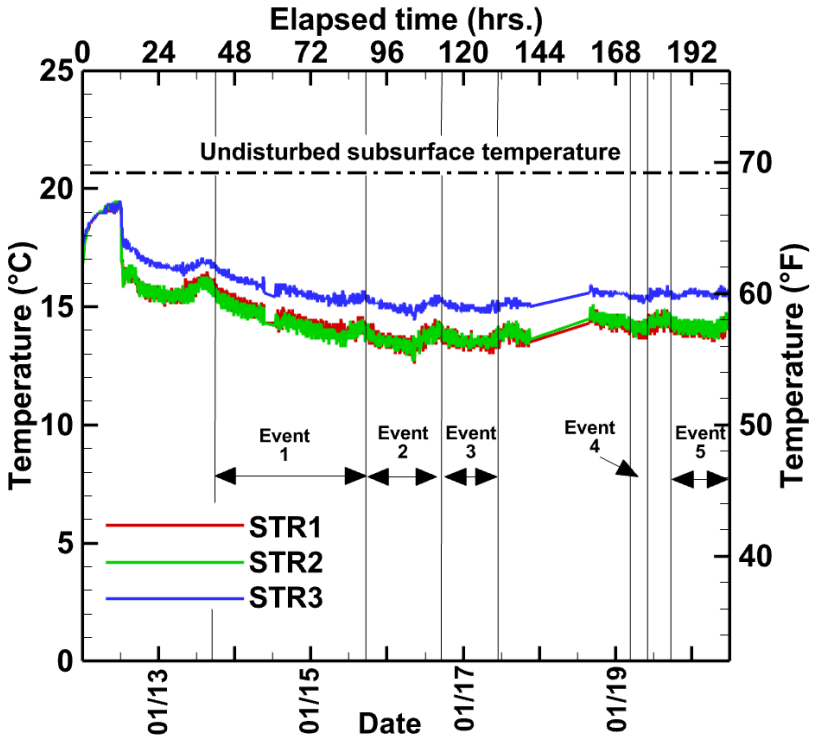


Figure 3.27 Temperature response of the grout and GHE interface at a depth of 50 ft.

### 3.7. Performance of Different Insulations During the Winter Test

There are two insulation materials for the heated bridge: spray foam insulation and geofoam insulation. Among the eight bridge spans, seven were insulated using spray foam, and one span was encapsulated with geofoam. This section compares the performance of the two insulations according to the bridge surface temperature response. Figure 3.28 compares the bridge top surface temperatures at geofoam and spray foam insulated sections. The two temperature curves share the

same trend, and the average temperature difference is approximately 1 °F, indicating that the two insulations have the same capability of preventing heat loss from PEX pipes.

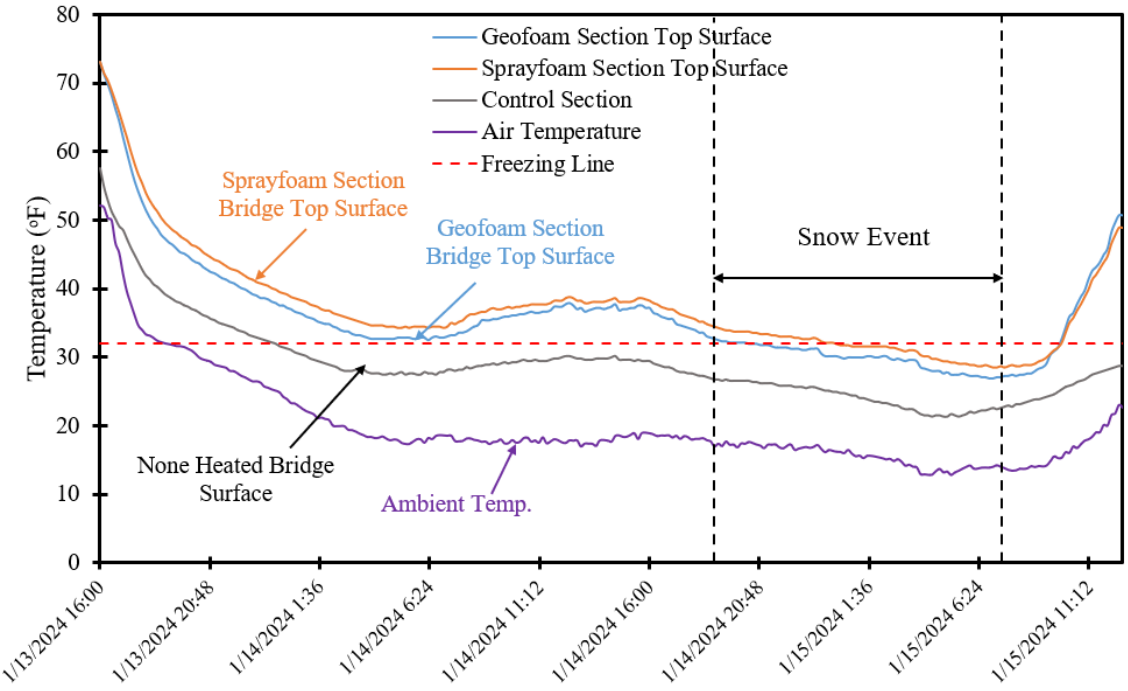


Figure 3.28 Comparison of bridge surface temperature response at spray foam and geofoam insulated sections.

### 3.8. Conclusions

This report documents the deicing tests performed during winter 2023-2024 on the pilot geothermal bridge equipped with a geothermal heat pump de-icing system. The heating performance of the bridge deck and its response to winter events were analyzed. The main findings from these winter tests are summarized as follows:

- During operation, the heating system can provide bridge surface heat flux above 300 W/m2, surpassing the designed surface heat flux of 252 W/m$^2$. Additionally, the GHE's inlet and outlet temperatures are 55˚F (12.77 ˚C) and 57 ˚F (13.88 ˚C), respectively.
- The test results show that the system successfully maintained the heated zone free of snow during the snow event even when the lowest air temperature reached 12.8 °F.
- The 16 GHEs installed on-site provided an average power output of 23.36 kW (4.9 W/ft.).
- Spray foam and geofoam insulations performed similarly in the measured bridge deck surface temperatures; the bridge deck surface of the spray-foam span showed a temperature about 0.5 ˚F higher than that of the geofoam span.

# Chapter 4

# Life Cycle Cost Benefit Analysis

## 4.1. Introduction

Cold-climate conditions significantly impact the functionality of roads, directly affecting the safety and traffic flow of transportation networks. Achieving sustainable transportation necessitates maintaining safe and functional links, with bridges playing a crucial role in road accessibility. Bridges are particularly susceptible to icing and snow accumulation during adverse weather conditions due to their exposure from both the top and bottom surfaces, unlike pavements which are only affected from above. Consequently, de-icing bridge decks becomes a critical issue in snowy and icy regions.

Traditional methods of de-icing, such as the application of road salts and chemicals, have several drawbacks. These substances can be corrosive, leading to the deterioration of bridge materials, including concrete and steel. Corrosion not only compromises the structural integrity of bridges but also increases maintenance costs and reduces the lifespan of the infrastructure. Additionally, road salts and chemicals can have harmful environmental impacts, contaminating nearby water sources and soil. One innovative solution to this problem is using geothermal energy to de-ice bridge decks. Geothermal heat-pump de-icing systems (GHDS) leverage the relatively constant soil temperature to prevent ice formation on bridge surfaces. This technology has been extensively analyzed and studied through experiments, numerical models, and feasibility studies by various research groups. Research has demonstrated the feasibility and promising potential of GHDS, highlighting the key parameters governing the physical processes involved.

While studies have effectively illustrated the technical viability and operational benefits of GHDS, there remains a gap in comprehensive cost and economic feasibility analysis. This analysis is essential to understand the full spectrum of benefits and expenses associated with the implementation of GHDS. This report aims to bridge this gap by conducting a thorough cost-and-benefit analysis of geothermal heat-pump de-icing systems. By evaluating both the monetary value of benefits and the associated costs over the lifecycle of the system, it provides a clearer picture of its economic viability and potential for widespread adoption in cold-climate regions. The primary objective of this report is to assess the economic viability of the GHDS using a life-cycle cost-benefit analysis (LCCBA) for a bridge in Fort Worth, Texas. Additionally, this report aims to demonstrate how GHDS contributes to corrosion prevention, safety enhancement, minimization of travel delays, and corresponding cost savings.

### 4.1.1. Life Cycle Cost Benefit Analysis

In determining total costs of this project, initial installation cost like material, labor and equipment cost and operation cost like electricity consumption and repairs has been considered. The calculation of total benefits is based on corrosion prevention, safety enhancement, and traffic flow enhancement of bridge due to GHDS. The estimation of costs and benefits of the GHDS implemented on the bridge considered in this study is based on available data and reasonable assumptions.

As highway bridges are typically designed for long service lives, the life-cycle cost-benefit analysis is conducted over a 50-year period starting from 2024. Future capital costs are adjusted for the time value of money, and all future expenses are converted to their present value (PV) using a discount rate. The acceptable discount rate in LCCBA typically falls between 3% and 6%. In this study, a discount rate of 5% is selected based on recommendations from Habibzadeh-Bigdarvish et al., (2019). For the LCCBA of this project, the net present value (NPV) is utilized. NPV represents the difference between the present value of cash inflows and outflows over the evaluation period and is calculated using Eq 3.

$$NPV = C_0 + \sum_{t=1}^{T} \frac{C_t}{(1+r)^t} \tag{3}$$

Where, $C_o$ is initial cost of the project, $C_t$ is cash flow in year $t$, $r$ is discount rate and $T$ is total life of the project.

After determining the present values of total costs ($PV_c$) and total benefits ($PV_b$) for the project, the benefit-to-cost ratio (BCR), also known as the profitability index, for the GHDS is calculated using Eq 4. This ratio serves as a measure to assess the economic aspect of the GHDS on bridges. A higher BCR value indicates a more favorable economic and profitable outcome for the project over the long term.

$$BCR = \frac{PV_b}{PV_c} \tag{4}$$

### 4.1.2. Details of Bridge

In the present study, the GHDS is implemented on a bridge located on SH 180 in Fort Worth, near the border of Arlington and Forth Worth in the Tarrant County of Texas (Figure 4.1). The bridge consists of 16 spans and has a length of about 210 ft. It is 48 ft wide with a deck thickness of 20 in. (Figure 4.2). The total bridge pavement area is about 10,500 $ft^2$. However, the middle two lanes (one going in each direction) were selected to be decided as per the scope of the project. Approximately 6,000 $ft^2$ of pavement area was deiced as a part of this project. The traffic volume on this bridge is obtained from the Traffic Count Database System (TCDS) of TxDOT. Although the current average daily traffic is available, the analysis also includes two higher traffic volume scenarios. This accounts for the constant growth in traffic and helps to understand the life cycle

cost-benefit analysis of similar bridges under increased traffic conditions. Table 4.1 provides the details of the bridge considered in this project.

Table 4.1 Details of the bridge.

| Description | Detail |
|---|---|
| Location Coordinates | 32.730049, -97.186797 |
| Number of lanes | 4 |
| Deck Thickness | 20 in. |
| Total Deck Area | 10,450 $ft^2$ |
| Heated Area | 6,000 $ft^2$ |
| Average Daily Traffic | 20,000 vehicles/day |

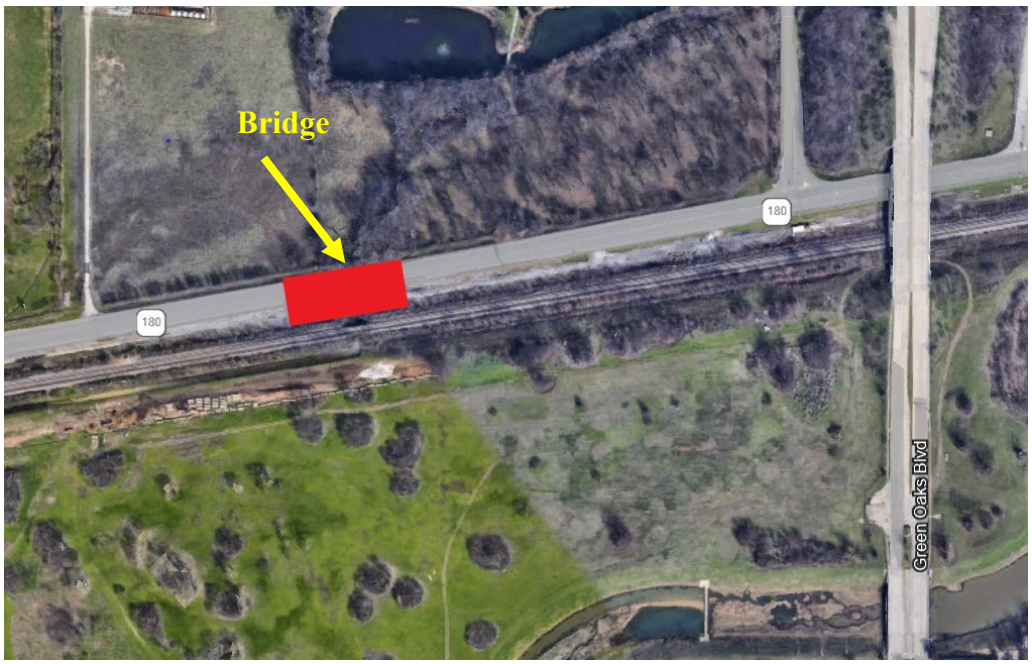

Figure 4.1 Location of test bridge in Tarrant County (Google Earth).

Figure 4.2 Bridge with deck thickness of 20 in.

## 4.2. COST ESTIMATION OF GHDS

### 4.2.1. General

The cost of a geothermal heat-pump de-icing system comprises three main components: initial capital cost, operation cost, and maintenance cost (Figure 4.3). The capital cost includes the total initial expenditure for purchasing materials, equipment, and machinery, as well as installation and labor expenses. Operation costs are calculated based on the energy consumption necessary to keep the system operational, including electricity. Maintenance costs involve regular inspections and any necessary repairs to ensure the system remains in good working condition. Together, these costs provide a comprehensive overview of the financial investment required for the installation and working of geothermal heat-pump de-icing systems. In certain cases, there are additional costs associated with decommissioning geothermal systems. However, this aspect falls outside the scope of this project and is, therefore, not included in the cost analysis study.

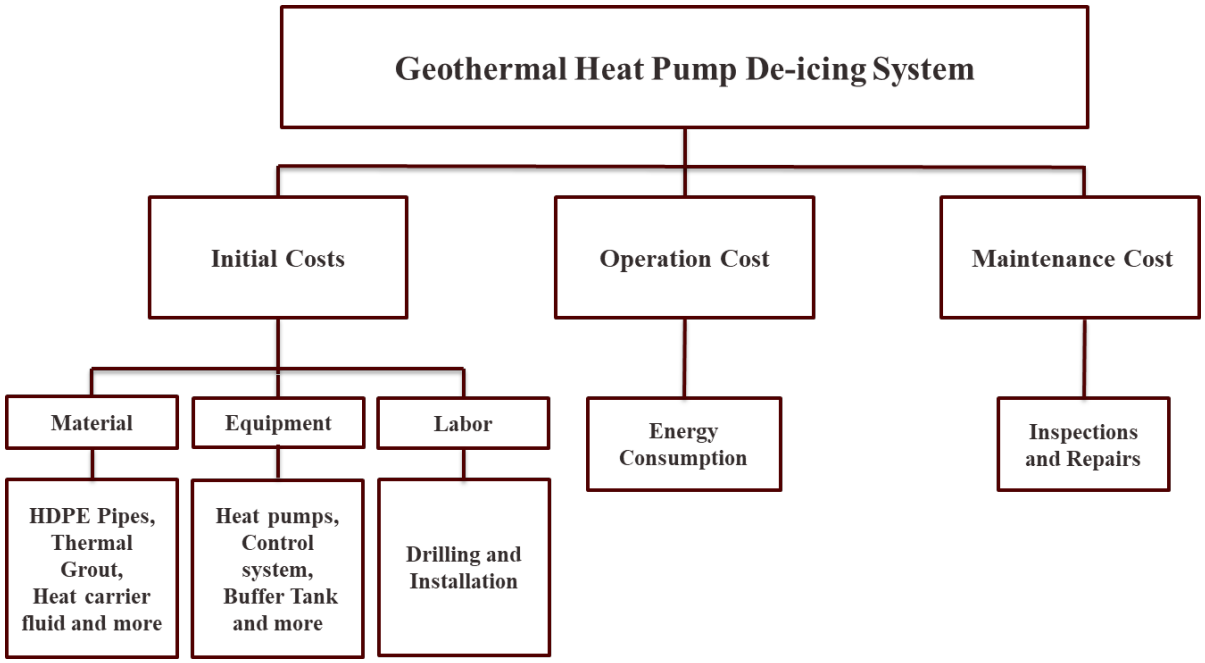


Figure 4.3 Flow chart for cost analysis of a GHDS.

### 4.2.2. Material Cost

The material cost for this project includes a range of expenses associated with various components integral to the geothermal heat pump de-icing system. Specifically, these costs include the expenses for materials used in the construction and implementation of geothermal heat exchangers (GHE), the control room, heating loops installed beneath the bridge deck, and the transmission system of the GHDS. To determine these costs, the quantities of materials required for each component are calculated, ensuring an accurate estimate of the project's total material expenses. The current market prices for these materials are used in our cost analysis, providing a realistic

and up-to-date financial overview. The unit prices for these materials are obtained from quotes provided by relevant vendors and are listed in Table 4.2.

Table 4.2. Approximate unit cost of materials.

| Material | Unit | Price |
|---|---|---|
| HDPE u-pipe | ft | $1.85 |
| HDPE pipe | ft | $0.75 |
| PEX pipe | ft | $0.24 |
| Anti-freeze agent | gallon | $33.00 |
| Thermal Grout | bag | $20.00 |
| Spray Polyurethane Foam (4 in.) * | sq.ft | $5.60 |
| Thermal Mastic | gallon | $115.00 |
| Aluminum Plate | ft | $2.20 |
| Aluminum Fascia | ft | $2.50 |
| Fittings and Connectors | pc | $15.00 |

**This cost includes cost of material, installation and machinery used.*

The required material quantities for this project are determined by considering several critical factors, including the span of the bridge, the design of the GHE, and the distance between the bridge and the GHE. For example, the required length of PEX (cross-linked polyethylene) pipe is determined by analyzing the bridge deck heating loop configuration and the overall span of the bridge. Additionally, the amounts of thermal mastic and spray polyurethane foam required are calculated based on their usage in the bridge heating loop and the total heated area of the bridge.

The volume of thermal grout is calculated based on the depth, diameter, and number of boreholes. Similarly, the amount of antifreeze agent, which is critical for preventing freezing in the heat exchange fluid, is calculated based on the total fluid volume within heating loops. In addition to these calculations, the required length of HDPE (high-density polyethylene) pipe (both header and u-pipe) is determined by considering the total length of the transmission channel and the depth and number of boreholes.

The total material cost for this project is calculated to be $95,000. A breakdown, including the quantities for each item, is presented in Table 1 of the Appendix 4.1. The total material cost is divided into three main categories: GHE, transmission system, and bridge deck heating system. The pie chart in Figure 4.4 shows that the GHE and bridge deck heating system account for nearly equal shares of the total cost. The cost of materials for the transmission system, primarily consisting of HDPE pipes, fittings, and connectors, was the lowest among all components in this project. This cost varies based on the length of the transmission channel, which depends on the distance between the GHE and the bridge deck and may change with the layout of different components of GHDS in a project.

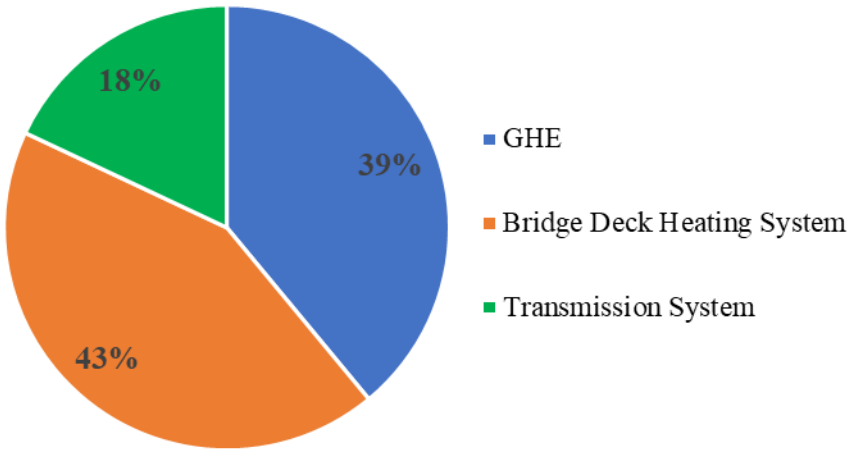


Figure 4.4 Distribution of material cost.

### 4.2.3. Equipment Cost

Equipment cost encompasses the cost of all the equipment installed in the control room to operate the GHD system. It includes expenses for heat pumps, flow centers, expansion tanks, buffer tank, air and dirt separator, and control system. Additionally, it covers the cost of the control room container, which houses all the equipment. The size of the container is determined by the space occupied by the equipment. The unit prices for each piece of equipment used are listed below in the Table 4.3.

Table 4.3 Unit cost of Equipment.

| Equipment | Unit | Price |
|---|---|---|
| Heat Pump | pc | $10,000.00 |
| Flow Center | pc | $1350.00 |
| Expansion Tank | pc | $765.00 |
| Buffer Tank | pc | $1,560.00 |
| Air and Dirt Separator | pc | $3,240.00 |
| Control Center | NA | $1,000.00 |
| Control Room Container | NA | $10,000.00 |

The required capacity of a heat pump in the system is determined by factors such as the thermal load requirements, ground thermal properties, and the efficiency of the GHD system. Based on the required capacity and operational limit provided by the manufacturer, the heat pump quantity can be determined. The quantity of flow centers in this system is determined based on the system's total flow rate requirements and the capacity of individual flow centers. This involved calculating the necessary flow rate to ensure efficient heat exchange and then selecting the appropriate number of flow centers that can collectively meet this demand. Factors such as the size of the heat pump, the length and configuration of the borehole heat exchangers influence the determination of the flow centers needed. The number and size of the expansion tank are calculated

based on the total volume of the geothermal loop system and the anticipated changes in fluid volume due to temperature variations. Similarly, the capacity of the buffer tank is determined by the thermal load requirements. For this system, one air and dirt separator tank and one control system are utilized. The cost of the container or control room, which primarily depends on the size of the control room, can be assumed constant across all similar projects.

The total cost of all equipment used in this project is calculated to be $69,500. A detailed breakdown of this cost is presented in Table 2 of the Appendix 4.1 of this report. It should be noted that this cost does not include the installation expenses of equipment, as those are covered under the labor costs for this project.

### 4.2.4. Labor Cost

The labor cost of this project includes the labor cost of preparing and installing geothermal heat exchangers, transmission pipes, and heating loop installation under the bridge deck. The cost of a geothermal borehole constitutes drilling of the holes, installation of u-pipes, and placement of thermal grout in boreholes. The expenses for pre- and post-drilling activities, such as locating underground utilities, mobilizing the drilling rig to the job site, connecting heat exchangers in each individual bore, and restoring the site, are also added to the labor cost of preparing the geothermal borehole.

The labor cost for ground piping includes the installation of all equipment in the control room and the placement of header pipes and manifolds. Since the installation procedures are nearly identical for all projects, this cost does not vary much with the project size. However, the cost of installing the heating loop under the bridge, which involves securing the PEX pipe loop against the bridge deck along with thermal mastic and spray foam, is dependent on the heated area of the bridge and the loop configuration. Labor costs are calculated based on the hourly rates of drillers and technicians and the estimated time required to complete specific tasks. The unit labor cost for all three categories of work is listed below in Table 4.4.

Table 4.4 Unit cost of labor.

| Item | Unit | Price |
|---|---|---|
| Geothermal Heat Exchanger | ft | $10.00 |
| Transmission System | hr | $25.00 |
| Bridge Deck Heating System | hr | $25.00 |

The total labor cost for this project is calculated to be $88,000. A detailed breakdown, including total drilling footage for GHE and the total number of hours for equipment and bridge loop installation, is presented in Table 2 of the Appendix 4.1 of this report. The total labor cost is divided into three main categories: GHE, transmission system, and bridge deck heating system. The pie chart in Figure 4.5 illustrates the distribution of labor costs among these three categories. It shows that the cost of labor for GHE is more than half of the total cost of labor for this project.

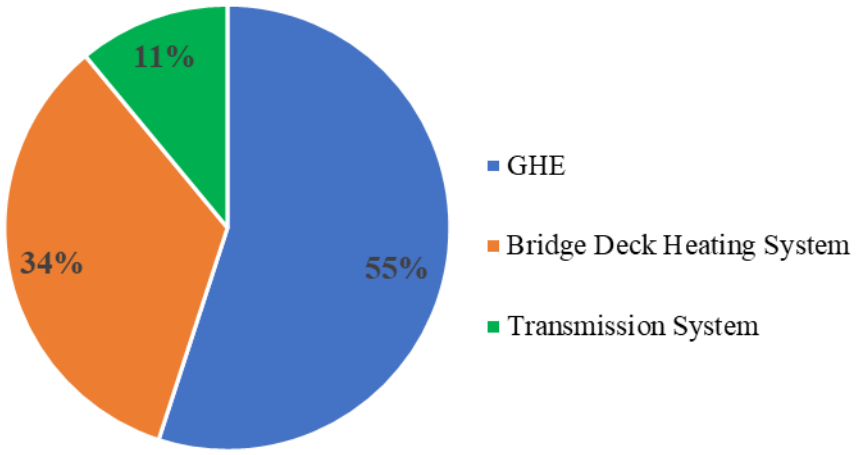


Figure 4.5 Distribution of labor cost.

### 4.2.5. Operation and Maintenance Costs

The operation and maintenance costs of a geothermal heat system are generally low compared to conventional heating and cooling systems. Once installed, these systems require minimal maintenance due to their few moving parts and the durability of the underground components. Routine maintenance primarily involves periodic inspections and checks of the heat pump, electrical connections, and fluid levels in the loop system. Based on a review of similar projects in the literature, the annual operational and maintenance (O&M) cost of this project is estimated to be $8,000. Operational costs of geothermal systems are reduced due to their high efficiency, which can provide significant savings on energy bills. Over the lifespan of the system, these savings often offset the initial installation costs, making geothermal heat systems a cost-effective and sustainable option for deicing bridges.

### 4.2.6. Summary of Cost Estimation

In the LCCBA of this project, all the costs associated with this project are calculated based on the required quantities of material, equipment, and labor and the unit price for each of them. The total initial construction cost of this project is $252,500. Based on the heated area of the bridge, the cost of construction per unit area of this project is $42/ft$^2$. The bar chart in Figure 4.6 provides the breakdown of the unit cost of this project in terms of material, equipment, and labor costs.

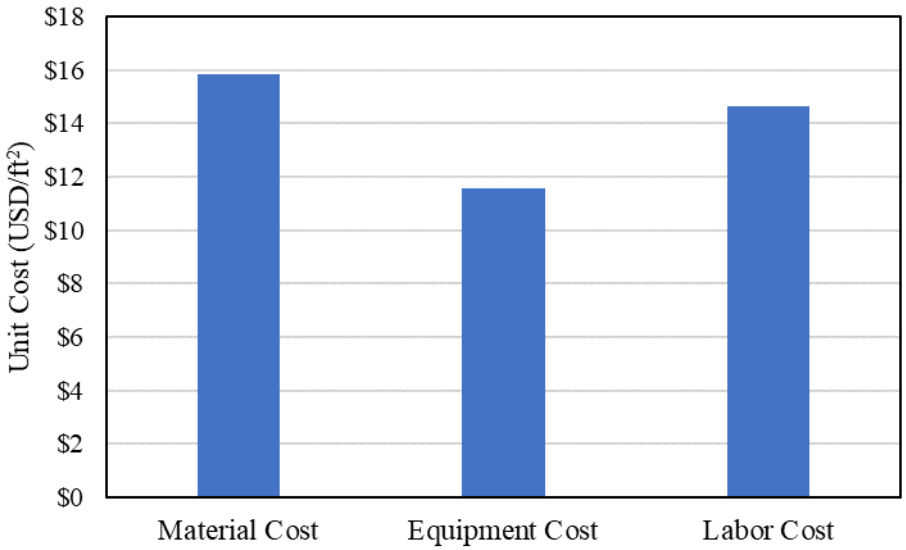


Figure 4.6 Initial unit cost of construction.

## 4.3. Benefit Estimation of GHDS

### 4.3.1. General

The benefits of using a geothermal heat-pump system for de-icing bridges are multifaceted, including corrosion prevention, safety enhancement, improved traffic flow, and environmental advantages. By preventing corrosion, the system extends the lifespan of bridge decks, reducing the need for frequent and costly maintenance and repairs. Safety is significantly enhanced as the system eliminates icy conditions on bridge surfaces, thereby reducing the likelihood of accidents. This improvement in road conditions also leads to better traffic flow, minimizing delays and disruptions caused by hazardous weather or maintenance work. Additionally, geothermal de-icing systems are environmentally friendly, as they negate the need for chemical deicers, which can harm surrounding ecosystems and waterways.

To quantify the benefits of this system, the monetary value of each benefit is estimated using available data and appropriate assumptions. For this project, the life cycle of the bridge is assumed to be 50 years, and all benefits are calculated for this duration. The following sections provide detailed descriptions of each benefit and the methods and assumptions used to estimate their monetary values.

### 4.3.2. Corrosion Prevention

Corrosion poses a significant issue, impacting a wide range of infrastructures and industries. The total annual direct cost of corrosion includes the expenses associated with design, manufacturing, and construction. Indirect costs, on the other hand, cover a broader spectrum, including management, repair, maintenance, rehabilitation, and the loss of productive time. A study by the National Association of Corrosion Engineers (NACE) highlights the growing financial burden of corrosion. According to their research, the annual cost of corrosion exceeded $1 trillion in 2013, effectively doubling since 1998. These statistics provide the nature of corrosion costs, emphasizing the need for new measures and methods to mitigate this issue across various fields, especially in highway infrastructure.

Highway infrastructures, particularly bridges, are highly susceptible to corrosion. The use of de-icing and anti-icing chemicals on roads to clear snow and ice significantly contributes to this problem. While these chemicals effectively improve road safety during winter, they also accelerate the corrosion of highway infrastructures, pipelines, utilities, and vehicles. The structural components of bridges, including the deck, are subject to flexing and seasonal temperature variations. The exposed bottom sides of bridges and the relatively thin concrete cover for embedded reinforcing steel further exacerbate the issue. Cracks in the deck surface allow salt brine from de-icing agents to penetrate, leading to the corrosion of the reinforcing steel. As the steel rebar corrodes, it expands, causing the concrete surface of the bridge deck to delaminate and deteriorate (Vitaliano, D.F., 1992).

The major consequence of using de-icing chemicals is the corrosion of bridge decks, which subsequently necessitates corrosion maintenance activities. However, with the implementation of GHDS, there is no need for repair or rehabilitation of the bridge deck due to corrosion. This benefit is a significant advantage of the GHDS. Table 4.5 provides a schedule of corrosion maintenance scenarios for bridges.

Table 4.5. Corrosion maintenance schedule for a bridge deck

| Event | Percent Deck Damaged (%) | Year of Action |
|---|---|---|
| Routine Maintenance | N/A | N/A |
| Repair/Patch | 2.5 | 25 |
| Rehabilitation Overlay | 10 | 32 |
| Deck Replacement | NA | 50 |

The cost of routine maintenance is not considered as a specific benefit of the GHDS because all bridges require regular maintenance regardless of the ice and snow control methods used. The same reasoning applies to the costs associated with bridge deck replacement. The frequencies of patch repair and rehabilitation overlay are 25 years and 32 years, respectively (Habibzadeh-Bigdarvish et al., 2019). Major repair or patching is conducted when 2.5% of the deck shows delamination and spalling. When 10% of the deck area is spalled and delaminated, it requires rehabilitation with latex-modified concrete.

In order to determine the monetary value of this benefit of GHDS, it is important to obtain the cost of patching and LMC overlaying. Different researchers have suggested the range of agency unit costs for different treatment purposes. Huang et al. (2004) recommended that the costs for patching and concrete overlay in 2004 were \$14.95/ft$^2$ and \$30.00/ft$^2$, respectively. However, in the present study, the present cost for repair/patching and rehabilitation of the bridge deck, considering an interest rate of 5%, are taken as \$22.00/ft$^2$ and \$45.00/ft$^2$, respectively.

The total cost associated with repair/patching and rehabilitation events for this project is calculated by multiplying the unit costs of repairs by the heated area of the bridge deck. Ultimately, the monetary benefit of corrosion prevention is the sum of the present value (PV) of the costs of these maintenance events (Eq. 5).

$$Corrosion\ Prevention\ Benefit = PV_{25th\ year}(patching) + PV_{32nd\ year}(overlaying) \quad (5)$$

Where $PV_{25th}$ year is the present value of patching cost in the 25th year and PV32nd year is the present value of the overlaying cost in the 32$^{nd}$ year.

### 4.3.3. Safety Enhancement

Roadway safety is a major concern when weather conditions affect the road surface, especially for bridges, which are more vulnerable to such conditions. Departments of Transportation (DOTs) are continuously challenged to not only provide a high level of service on roadways but also enhance user safety in a cost-effective manner. According to TxDOT, from 2007 to 2016, there is an annual

average of 4,900 car crashes on Texas roads due to slippery conditions such as ice, snow, and slush. Based on the research of Agent and Deen (1976), a minimum of 8% percent of all crashes happen on bridges. The application of GHD systems can create safe road surfaces, thereby preventing many car crashes due to slippery conditions. Also, it can prevent deck corrosion, eliminating the need for corrosion maintenance activities and work zones areas on the bridge deck. Hence, the costs associated with traffic incidents in this project are estimated based on two factors: icy/snowy road surface conditions and work zones when conventional snow and ice removal systems are used.

The main challenge in this analysis is to determine the average annual number of crashes due to slippery road conditions on the bridge selected for this study. The method adopted by Habibzadeh-Bigdarvish et al. (2019) is used in this analysis to determine this number. As per the method, the total number of crashes on bridges caused by slippery road conditions is divided by the total number of bridges in regions prone to icy road conditions. To identify the regions in Texas prone to icy roads, the annual precipitation map of 2015 and the average daily minimum temperature map for January 2015 are overlaid (Figure 4.7). Areas with precipitation exceeding 28 inches and temperatures below 32°F are selected as high-risk regions for road icing during winter.

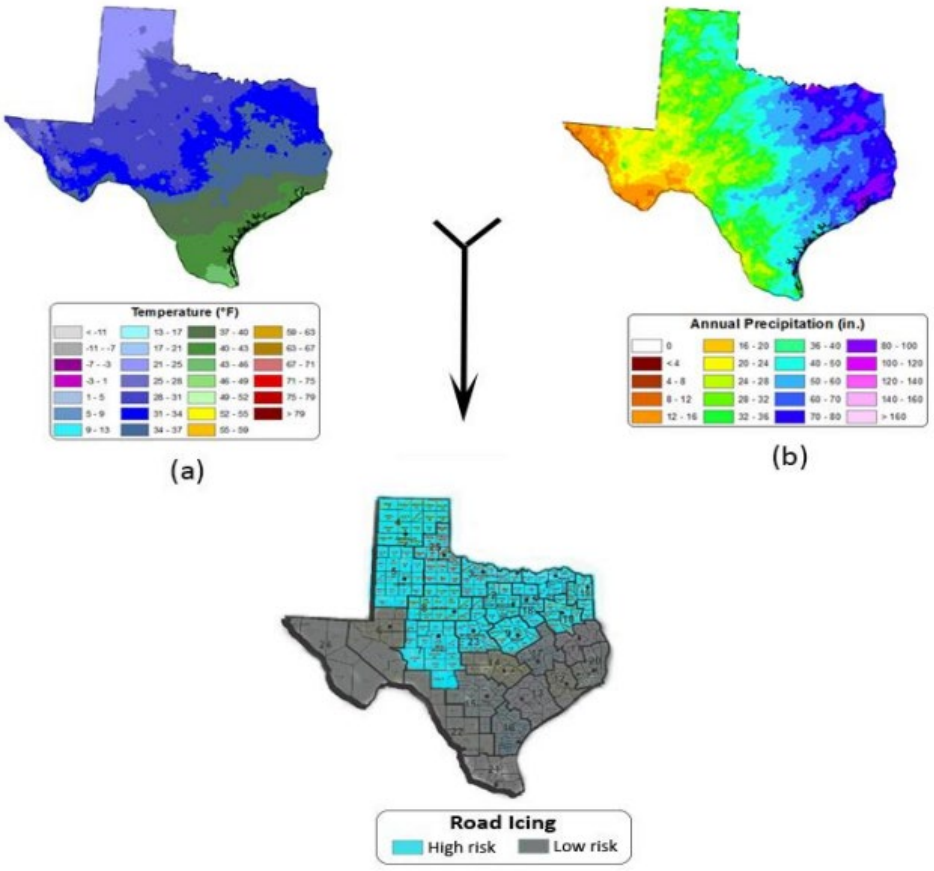


Figure 4.7 (a) Texas average daily minimum temperature map for January 2015, (b) annual precipitation in 2015, and (c) Road icing map (Habibzadeh-Bigdarvish et al., 2019)

Based on the maps in Figure 4.7, counties located in the regions prone to icy roads and their number of bridges are identified. As per TxDOT's (2016) report on Texas bridges, the total number of bridges in these counties is around 17000. Finally, the average annual number of crashes on the bridge in Texas due to slippery road surface conditions is computed by dividing total number of crashes with total number of bridges. A similar method is employed to calculate the number of car crashes occurring in work zones on bridges. Based on TxDOT reports and reasonable assumptions, an average of 1,462 crashes can be expected to occur on bridges in Texas due to work zones. In the present study, the average number of crashes on the bridge due to slippery conditions and work zones are calculated as 0.023 and 0.0018 crashes per year, respectively.

The annual cost of crashes on each bridge is calculated by the product of the average cost of a crash, which is derived from the sample data provided in a report by FHWA and the average annual number of crashes that occur due to work zones and icy roads on each bridge in the regions prone to icy roads.

### 4.3.4. Traffic Flow Enhancement

An essential measure of the effectiveness of traffic-related research is the level of delay. Longer travel delay times lead to increased fuel consumption and time loss, representing both direct and indirect costs. Given the growing trend of delay and congestion on roadways and highways, it is important to implement effective measures to maintain an acceptable level of service. One of the most significant benefits of geothermal bridge deck de-icing systems is the reduction of traffic delays. In this research, the cost of travel delays, which can be mitigated using GHDS, is evaluated in three scenarios:

- Traffic delays caused by work zones on the bridge – Traffic delay time due to work zones refers to the bridge corrosion maintenance activities that slow down traffic during the bridge's operational period.
- Traffic delays due to slippery road surface conditions on the bridge – Icy and snowy road surfaces also cause motorists to decelerate when crossing the bridge.
- Traffic delays resulting from crashes on bridges - This involves traffic congestion caused by car crashes on the bridge.

The average traffic volume on the bridge, obtained from TCDS of TxDOT, is 20,000 vehicles/day. However, the present study also estimates the expected benefits for traffic volume of 40,000 and 60,000 vehicles per day on the same bridge. Table 4.6 provides assumed traffic percentages for different types of travel on the bridge under consideration.

Table 4.6 Traffic data of the bridge.

| Type of Travel | % of Average Daily Traffic (vehicle/day)) |
|---|---|
| Personal travel | 85 |
| Business travel | 10 |
| Truck Travel | 5 |

To calculate the monetary value of travel delay, the unit cost of travel time is multiplied by the estimated delays for personal, business, and truck travel caused by the work zone, slippery conditions, and crashes. The unit cost for travel time, which depends on the type of vehicle, average occupancy of the vehicle, and gross annual income of occupants, is obtained from Habibzadeh-Bigdarvish et al. (2019). Table 4.7 provides the unit cost of travel time for personal, business, and truck travel.

Table 4.7 Hourly travel time value per vehicle.

| Type of Travel | Travel Time Value |
|---|---|
| Personal travel | $44.60/hr |
| Business travel | $34.35/hr |
| Truck Travel | $19.84/hr |

As actual hourly traffic volume data during events of crash, slippery condition, and work zone is unavailable, traffic delay times for these different events are assumed. Through a review of online sources and consideration of typical durations for various activities/events, delay times have been determined as shown in the Table 4.8. The total cost of traffic delays for due to work zones (repair and rehabilitation) is calculated for one life cycle of bridge whereas, the cost of delays due to slippery conditions and crashes is calculated annually.

Table 4.8 Travel delay scenario due to different events.

| Event | Duration | Delay Time | Delay (Veh-hr/day) |
|---|---|---|---|
| Repair/patching | 5 days | 1 min | 0.016 |
| Rehabilitation | 30 days | 3 min | 0.033 |
| Snow/Ice Conditions | 60 hours/year | 1 min | 0.0083 |
| Car Crash | 4 hours/year | 30 mins | 0.083 |

### 4.4. Results and Discussions

#### 4.4.1. Results

The initial cost of this project, as detailed in Chapter 2, is $243,500 and incurred once at the start of the life cycle. For this study, referencing similar projects in the literature, the annual operational and maintenance (O&M) cost is estimated at $8,000. The present value of the O&M cost is calculated for this project using a discount rate of 5% over a 50-year life period. A summary of all project costs, including their present value, is presented in Table 4.9. Figure 4.8 illustrates that 37% of the total present value of the GHDS cost is attributed to its operation and maintenance cost, while 63% is associated with the initial construction.

Table 4.9 Summary of cost and present their values.

| Cost of GHDS | Value | Present Value |
|---|---|---|
| Initial cost | $252,500 | $252,500 |
| Annual operational and maintenance cost | $8,000 | $146,000 |
| Total present value of cost | | **$398,500** |

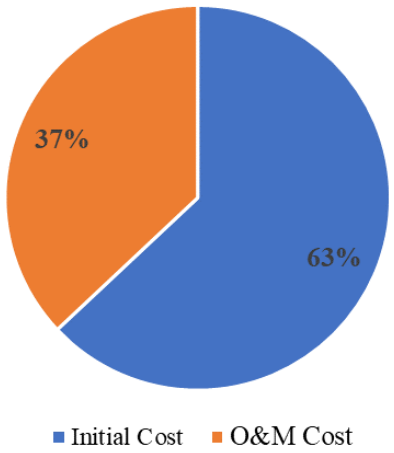


Figure 4.8 Distribution of costs of GHDS over the entire life cycle.

The monetary value of all GHDS benefits is computed using the methods and assumptions outlined in section 3. Over the entire life cycle of the bridge, GHDS delivers benefits totaling approximately $402,000 through corrosion prevention. This saving arises from averting the expenses linked with repairing, patching, and rehabilitating the corroded bridge deck, actions typically required in the 25th and 32nd years of its life cycle due to conventional use of chemicals for de-icing. Furthermore, this technology saves an annual recurrent cost of $3,500 by ensuring safe road surface conditions. This calculation involves multiplying the average annual number of crashes due to slippery roads and work zone areas by the cost of each crash. The crash cost, approximately $150,000, corresponds to the mean comprehensive cost per crash for severity levels B or C and a speed limit of 50 mph or higher in 2020 (Habibzadeh-Bigdarvish et al., 2019). In

terms of traffic flow enhancements, considering present average daily traffic to be 20,000 vehicle/day, the GHDS system generates annual savings of $35,000 by preventing delays caused by slippery road surfaces. Furthermore, it also helps save $1,700 annually by preventing traffic delays resulting from accidents due to slippery conditions. Over its entire life cycle, the system achieves a total saving of $917,000 by eliminating traffic delays associated with work zones. Table 4.10 provides the expected value of GHDS benefits for different traffic volumes.

Table 4.10 Summary of GHDS benefits for different traffic volumes.

| **Benefit of GHDS** | **Monetary value of benefit** | | |
|---|---|---|---|
| | **20,000 vehicles/day** | **40,000 vehicles/day** | **60,000 vehicles/day** |
| Corrosion Prevention (over entire life cycle) | $402,000 | $402,000 | $402,000 |
| Annual savings from enhanced safety | $3,500 | $3,500 | $3,500 |
| Annual delay cost of snow and icy bridge deck | $35,000 | $70,000 | $105,000 |
| Annual delay cost due to car crashes | $1,700 | $3,400 | $5,100 |
| Traffic delay cost due to repair/patching (over entire life cycle) | $70,000 | $140,000 | $210,000 |
| Traffic delay cost due to rehabilitation (over entire life cycle) | $847,000 | $1,694,000 | $2,540,000 |

The present value of all these benefits is calculated using Eq. 3. Table 4.11 summarizes all present monetary values of the benefits for the GHDS in this study. It's evident that the major benefit of the GHDS implementation in this project is the cost-saving from enhancements in traffic flow. Results show that the present value of benefits significantly grows with an increase in average traffic volume. This growth is attributed to higher benefits from traffic flow enhancement due to high traffic volume. Considering the present average daily traffic of $20k for this bridge, the total present value of GHDS benefits is computed as $1,027,500. Based on the present value of costs and benefits, the benefit-to-cost ratio is calculated for all three traffic volumes using Eq. 4 and is tabulated in Table 4.12.

Table 4.11 Present value of GHDS benefits for different traffic volumes.

| Benefit of GHDS | Present value of benefit | | |
|---|---|---|---|
| | **20,000 vehicles/day** | **40,000 vehicles/day** | **60,000 vehicles/day** |
| Corrosion Prevention (over entire life cycle) | $95,500 | $95,500 | $95,500 |
| Annual savings from enhanced safety | $64,000 | $64,000 | $64,000 |
| Annual delay cost of snow and icy bridge deck | $639,000 | $1,278,000 | $1,917,000 |
| Annual delay cost due to car crashes | $31,000 | $62,000 | $93,000 |
| Traffic delay cost due to repair/patching (over the entire life cycle) | $21,000 | $42,000 | $63,000 |
| Traffic delay cost due to rehabilitation (over the entire life cycle) | $177,000 | $354,000 | $531,000 |
| Total present value of benefits | **$1,027,500** | **1,895,500** | **$2,763,500** |

Table 4.12 Summary of LCCBA for different traffic volumes.

| Cost/Benefit Category | Average Daily Traffic | | |
|---|---|---|---|
| | **20,000 vehicles/day** | **40,000 vehicles/day** | **60,000 vehicles/day** |
| Total present value of costs | $398,500 | $398,500 | $398,500 |
| Total present value of benefits | $1,027,500 | $1,895,500 | $2,763,500 |
| Net Present Value | $638,000 | $1506,000 | $2,374,000 |
| Benefit to Cost Ratio (BCR) | **2.5** | **4.7** | **6.9** |

### 4.4.2. Summary

The present report aims at conducting a life cycle cost-benefit analysis of a geothermal heat pump bridge deck deicing system on a service bridge in Fort Worth, Texas. All the expenses and benefits were estimated, and the cost-to-benefit ratio was computed for different traffic volumes. The total initial construction cost of the pilot geothermal project is estimated at $252,500. The cost of construction per unit heating deck area of this project is $42/ft$^2$. The findings highlight that despite significant initial construction, operation, and maintenance costs, the GHDS yields substantial savings in corrosion prevention and safety enhancement, notably in reducing traffic delay times. Furthermore, the system's features make it environmentally friendly, although the monetary value of this environmental benefit isn't assessed in this study. It's important to acknowledge that this analysis pertains to a bridge with a deck thickness of 20 inches, which has notably inflated the initial cost. However, for bridges with thinner decks and higher traffic volumes, the benefits are expected to far outweigh the project costs, suggesting GHDS as a dependable alternative to conventional methods of de-icing bridge decks.

## APPENDIX 4.1

## Cost estimation for the GHDS implementation on the bridge

Table 1 Estimated quantities and price of material for this project

| Material | Unit | Price | Quantity | Total Price |
|---|---|---|---|---|
| HDPE u-pipe | ft | 1.85 | 9900 | 18315 |
| HDPE Header Pipe | ft | 0.75 | 2500 | 1875 |
| PEX pipe | ft | 0.24 | 7100 | 1704 |
| Anti-freeze agent | gallon | 33.00 | 300 | 9900 |
| Thermal Grout | bag | 20 | 450 | 9000 |
| Spray Polyurethane Foam (4") | sq.ft | 5.6 | 3600 | 20160 |
| Thermal Mastic | gallon | 115 | 16 | 1840 |
| Aluminum Plate | ft | 2.2 | 5800 | 12760 |
| Fittings and Connectors | pc | 15 | 1000 | 15000 |
| Aluminum Fascia | ft | 2.5 | 1800 | 4500 |

Table 2 Estimated quantities and price of equipment for this project

| Equipment | Unit | Price | Quantity | Total Price |
|---|---|---|---|---|
| Heat Pump | pc | $10,000.00 | 4 | 40000 |
| Flow Center | pc | $1,350.00 | 9 | 12150 |
| Expansion Tank | pc | $765.00 | 2 | 1530 |
| Buffer Tank | pc | $1,560.00 | 1 | 1560 |
| Air and Dirt Separator | pc | $3,240.00 | 1 | 3240 |
| Control Center | pc | $1,000.00 | 1 | 1000 |
| Control Room Container | NA | $10,000.00 | 1 | 10000 |

Table 3 Estimated quantities and price of labor for this project

| Labor | Unit | Price | Quantity | Total Price |
|---|---|---|---|---|
| Geothermal Borehole | ft | $10.00 | 4800 | 48000 |
| Transmission System | hr | $25.00 | 1200 | 30000 |
| Bridge Deck Heating System | hr | $25.00 | 400 | 10000 |

# Chapter 5

# Deicing Operation Manual for the Pilot Geothermal Bridge

## 5.1. Introduction

A 28-ton geothermal heat pump system (GHPS) was installed to deice a pilot bridge on SH 180 in the Dallas/Fort Worth Metroplex in North Texas. The bridge consists of 8 spans and has 2 lanes on each bound. It is 200 ft. long by 48 ft. wide, and the bridge deck is 18 in. thick. The total bridge deck area is 9,600 $ft^2$; however, the bottom surface of the deck, which would be used to install the hydronic heating loops, has an area of about 8,650 $ft^2$. Consequently, a vertical ground loop heat exchanger (GLHE) with 16 vertical boreholes (300 ft. deep) was constructed in the field. The GHPS consists of a vertical GLHE, 4 heat pumps, 10 circulating pumps, 1 dirt-air separator, 2 expansion tanks, 1 storage tank, and 1 heat pump control. The installation of the entire heating system was completed before winter 2023.

The objective of the control system is to run the deicing system efficiently and effectively under different winter weather conditions. The system can be operated for bridge deicing in heat pump or bypass mode. The heat pump mode involves all four heat pumps and the GLHE during bridge deicing, while the bypass mode only relies on GLHE to heat the bridge. The original control design was one Tekmar 670 as the control module to control all heat pump and water pump units automatically. However, the implementation of Tekmar 670 was delayed. Instead, an alternative control using four Tekmar 519 was implemented for snow-melting operations in the winter of 2023. In this alternative control, each heat pump was controlled by one Tekmar 519 directly. The drawback of this alternative is that the system is operated manually.

This chapter outlines the control system for the pilot bridge deicing system using Tekmar 519, including the control module, control algorithm, and operation procedure. This report also provides a recommendation for a Tekmar 670 system and its control algorithm.

## 5.2. Control Algorithm

The heating system for the pilot bridge includes 4 heat pumps, 10 circulating pumps, 2 expansion tanks, and 1 storage tank, which are located in the control room, as shown in Figure 5.1. The control module (Tekmar 519) only controls heat pumps during the heating stage. The circulating pumps are controlled by four power switches, meaning that they need to be manually turned on or off.

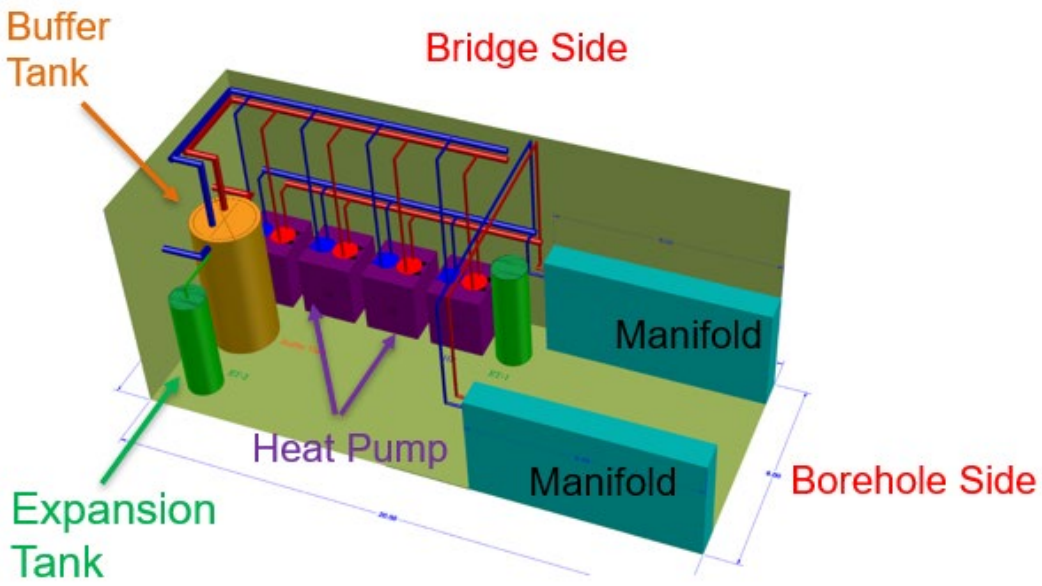


Figure 5.1 Schematic of the equipment inside the control room.

In terms of making the system economically viable, the controller may eventually be the most important part of the geothermal deicing system. The previous control system used in the mockup bridge geothermal deicing system relied on simple control strategies since only one heat pump and two flow centers were involved. The new pilot bridge deicing system utilized a total of 4 heat pumps and 10 flow centers, creating a complex flow system. Therefore, each heat pump was paired with one thermostat (Tekmar 519) to control the operation of the heat pump. Tekmar 519 operates on a temperature sensor attached to the inlet pipe to the bridge to detect the heat pump output temperature. The flow centers were controlled manually using electrical switches.

For the current pilot bridge heating system, there are two heating modes, namely, heat pump mode and bypass mode. The heat pump mode involves heat pumps, GLHE, and the Tekmar 519 control module. The control module controls the heat pump operation based on the set temperature. For example, if the set temperature is 100 °F when the detected heat pump output temperature (via temperature sensors attached to the inlet pipes to the bridge loop) is less than 100 °F, Tekmar 519 will turn on the heat pump. If the detected temperature is larger than 100 °F, the control will shut off the heat pump. In this mode, the circulating pumps keep running. The bypass mode operates by circulating the heat carrier fluids from GLHE directly to the hydronic loops underneath the bridge, bypassing heat pumps. Therefore, the heat pumps and control module do not participate in this mode, and only circulating pumps keep running to transfer heat from GLHE to the bridge surface. The detailed operation steps for the 2023 winter event are shown in the appendix.

### 5.3. Control System of Geothermal Heating System

As shown in Figure 5.2, an example thermostat (Tekmar 519) was wired to the heat pump to control its operation. Moreover, the thermostat was controlled by an external thermistor attached to the inlet pipe to the bridge deck to measure the inlet heat carrier fluid temperature. However, it

should be noted that the whole system, including the 10 circulating pumps, was turned on and off manually, and four thermostats only controlled four heat pumps when the power supply was active. The system was completed before the 2023 winter events.

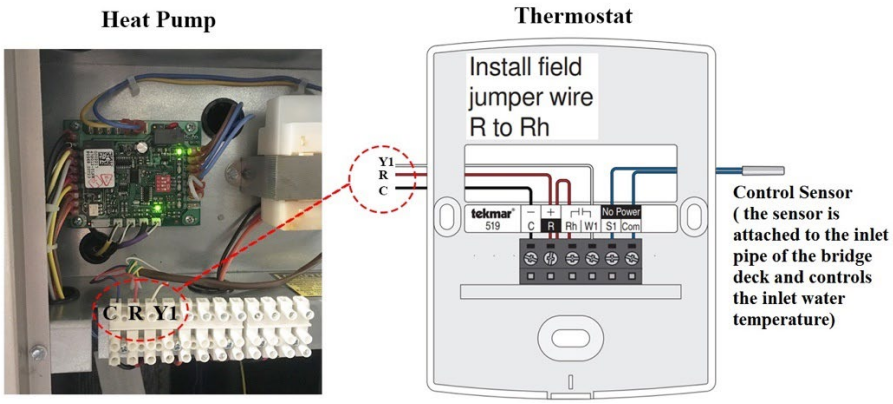


(a)

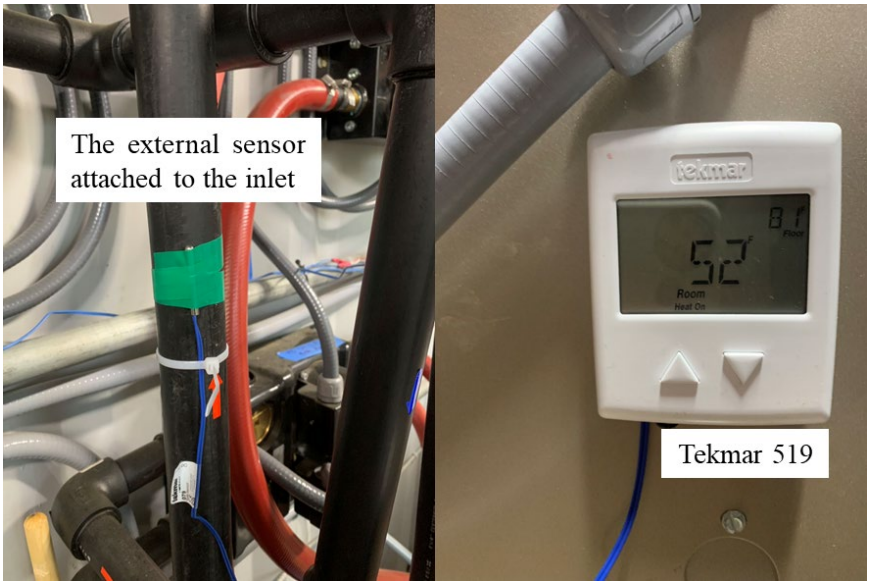


**(b)**

Figure 5.2 Control system: a) wiring diagram of the heat pump and thermostat; b) Tekmar 519 thermostat and control sensor attached to the inlet pipe.

### 5.4. Operation Procedures of Control System

During the deicing/snow-melting operation, the power switches for the heat pumps and circulating pumps are first turned on. Then, the four Tekmar 519 thermostats are set to the desired temperature, which controls the heat fluid temperature supplied to the bridge loop inlet and is monitored by the thermocouple from Tekmar 519. The thermostat then oversees the operation of the heat pumps, continuously monitoring the heat pump output temperature to avoid overheating. Detailed operation procedures for the heating system can be found in the appendix.

## 5.5. System Inspection, Maintenance, and Monitoring

### 5.5.1. Regular Inspections

To uphold the optimal functionality of our geothermal deicing system, we've implemented an accurate schedule for regular inspections. This proactive approach involves systematically assessing all components of the system on a predefined timeline. During these inspections, trained personnel examine every aspect of the system, from the PEX piping and insulation materials to the control room equipment and overhang HDPE pipes. Any signs of wear, damage, or malfunction are promptly identified and addressed to ensure uninterrupted and efficient operation. By conducting regular inspections, we can detect potential issues early on, preventing minor problems from escalating into major disruptions. This proactive maintenance strategy is instrumental in maintaining the reliability and effectiveness of our geothermal deicing system, ultimately enhancing the safety and functionality of the bridge infrastructure.

### 5.5.2. Maintenance Procedures

We've developed thorough maintenance processes to handle the upkeep of crucial geothermal deicing system components in addition to routine inspections. This covers regular upkeep for valves, tanks, pumps, and other necessary machinery. These maintenance processes are competently carried out by trained staff, guaranteeing that every operation is completed with care and precision. We can reduce the chance of unplanned failures, stop wear, and tear, and extend the life of components by following a planned maintenance schedule. Furthermore, ongoing training programs are in place to keep personnel up to date on the latest maintenance techniques and best practices. This ensures that our team is well-equipped to maintain the proper functionality of the geothermal deicing system and respond effectively to any maintenance needs that may arise.

### 5.5.3. Monitoring System Performance

To optimize the performance of our geothermal deicing system, we've implemented a robust monitoring system that tracks various parameters in real-time. This includes monitoring temperature levels, flow rates, pressure readings, and energy consumption data. By continuously monitoring system performance, we can promptly identify any deviations from expected norms and take corrective action as needed. This may involve adjusting settings, fine-tuning operational parameters, or addressing any underlying issues that may be affecting system performance. The use of real-time data allows us to make informed decisions to optimize the efficiency and effectiveness of the geothermal deicing system. By leveraging this monitoring system, we can ensure that the system operates at peak performance levels, providing reliable deicing capabilities for the bridge infrastructure while maximizing energy efficiency.

## 5.4. Safety Compliance

### 5.4.1. Safety Measures

Ensuring the safety of all personnel involved in construction and maintenance activities is paramount. We prioritize safety at every stage of the project, from planning to execution. Comprehensive safety protocols are established and strictly adhered to, minimizing the risk of accidents and injuries. Proper training is provided to all personnel involved in the project, equipping them with the knowledge and skills necessary to perform their tasks safely and effectively. This includes training on handling equipment, emergency procedures, and hazard recognition. Regular safety briefings and toolbox talks reinforce the importance of safety and promote a culture of awareness and accountability. By prioritizing safety, we create a work environment where personnel can confidently carry out their responsibilities, knowing that their well-being is safeguarded. This commitment to safety not only protects individuals but also contributes to the overall success and efficiency of the project.

### 5.4.2. Environmental Compliance

Environmental responsibility is integral to our approach to construction and operation. We are committed to adhering to all environmental regulations and guidelines, ensuring compliance with local, state, and federal requirements. Throughout the project lifecycle, we take proactive measures to minimize our environmental impact and follow best practices for sustainability. This includes implementing erosion and sediment control measures, managing construction waste responsibly, and employing eco-friendly construction materials whenever feasible. During operation, we continue to prioritize environmental compliance, implementing measures to reduce energy consumption, minimize emissions, and protect natural habitats. Regular monitoring and assessment ensure that our operations remain in accordance with environmental regulations and contribute to the preservation of the environment. By adhering to environmental compliance standards and embracing sustainable practices, we demonstrate our commitment to being responsible for the environment while delivering high-quality infrastructure that meets the needs of the community.

## 5.5. Conclusions

This report presents the control module, control algorithm, and operational procedures of the control system for the geothermal heating system. This report also details the operation manual for the control system. The objective of the control system is to ensure that 4 heat pumps work smoothly during winter events. During 10 days of operation, the control system worked smoothly during the Jan. 2024 winter event.

## 5.6. Recommendations

Although the current Tekmar 519 demonstrated its feasibility in controlling the pilot bridge geothermal heating system, the drawback of this system is that all circulating pumps need to be

manually turned on/off. An automatic control system that operates on its own depending on the weather conditions is ideal for the operation of the deicing system. Therefore, the research team recommends using Tekmar 670 to automate the operation of the current deicing system. The Tekmar 670 system can automatically control the operation of heat pumps and circulating pumps and automatically shut off the system based on the detected bridge surface temperature.

The control algorithm for Tekmar 670 developed by the research team is shown in Figure 5.3. It is able to operate the heating system based on slab temperature, outdoor (ambient) temperature, and temperature set points. The algorithm needs users to set warm weather shutdown (WWSD) and cold weather shut-off (CWSO) temperatures. The heating system will be idling when outdoor and slab temperature sensors detect temperatures below WWSD. The control automatically starts the heating system to preheat bridge decks to shorten the time to melt snow or ice. During the idling operation, the system remains in idling status if the ambient and slab temperatures are above freezing. Otherwise, the melting operation initiates when moisture is detected on slab surfaces. When the surface is dry, the system will continue heating the bridge for additional time and then shut off. In addition, to protect the heating system, the system will shut off automatically if the outdoor and slab temperatures are under CWSO during heating.

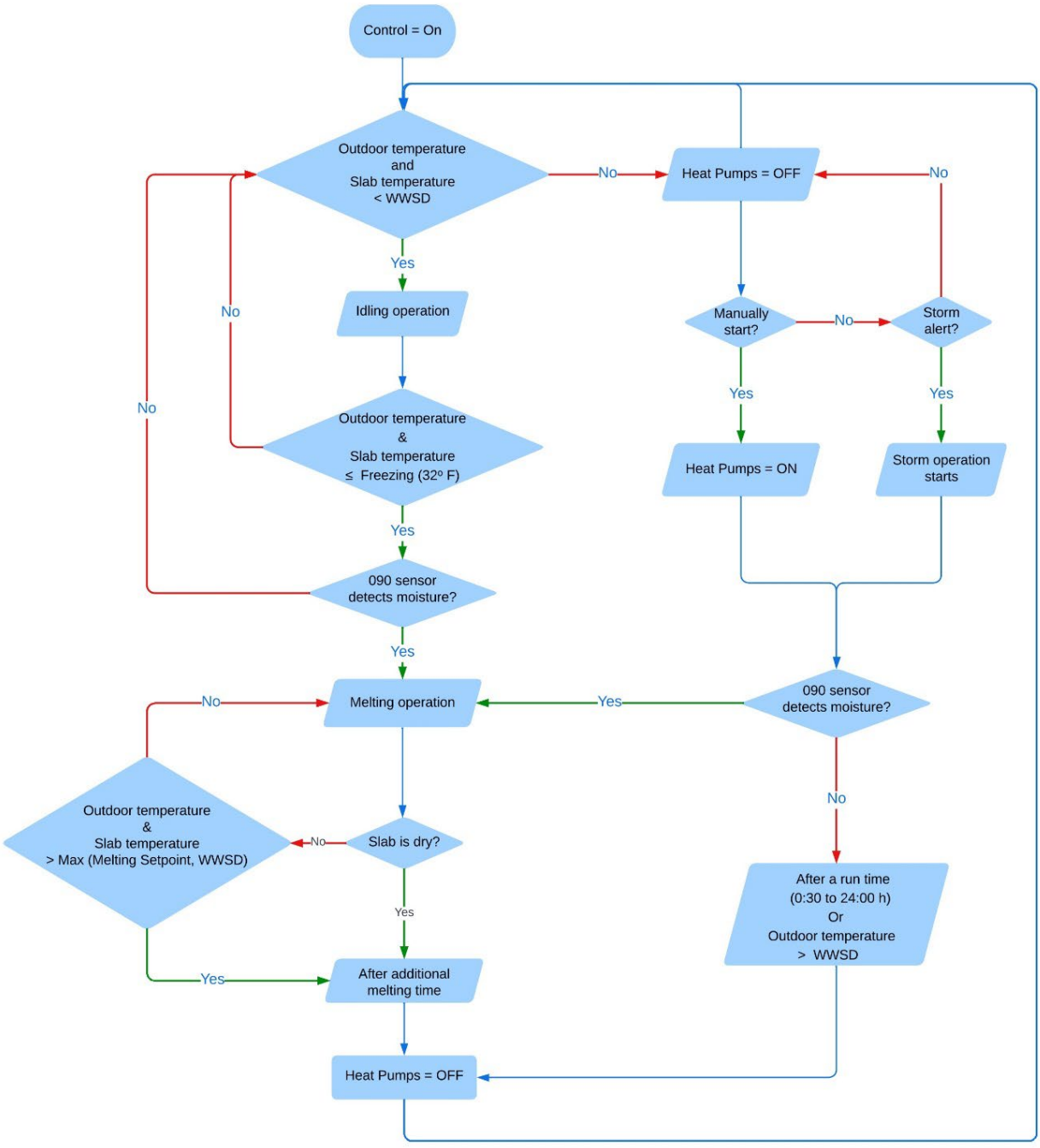


Figure 5.3 Proposed Tekmar 670 Control Algorithm for the Geothermal Deicing System.

**APPENDIX 5.1: Deicing Operation Manual**

**Bridge Deicing Operation Example: Heat Pump Mode**

**(Operation based on Tekmar 519 Thermostat)**

**Step 1: Valve check**

1.1. Ensure all system valves are switched to the right position, as shown below (labeled ***V1, V2, V3, and V4***)

***V-1***

***V-2***

***V-3***

***V-4***

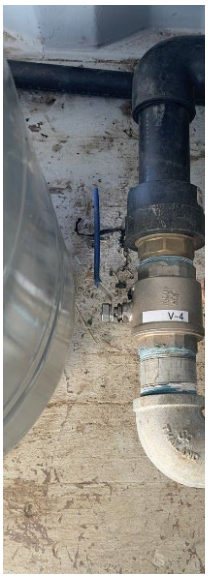

1.2. Check and set all the manifold balancing valves and ball valves.

- **Balancing valves set to 5.0 GPM:** the 5.0 GPM setting is achieved by rotating the valve until the number 5.0 is aligned with the indicator on the dial. This controls the flow rate to ensure it matches the required setting of 5.0 gallons per minute.
- **The red valves are set to open.** The red handle of the ball valve is turned clockwise until it is in line with the pipe.

***Manifolds***


***Manifold Balancing Valves***


1.3. Verify the closure of the two bypass valves (V-Bypass) to ensure that the arrow mark stays in the position shown in the photo.

V-Bypass


1.4. Check the ball valves installed on the inlet and outlet pipes for each bridge span to ensure they are open. Also, check that the flow control valve, as shown below, is set to maximum.

Taco flow setter (maximum) and ball valve (open) for the bridge heating panel

**Step 2: Power Supply**

2.1. Turn on switches for heat pumps and circulating pumps on the electrical panel located at the back of the control room.

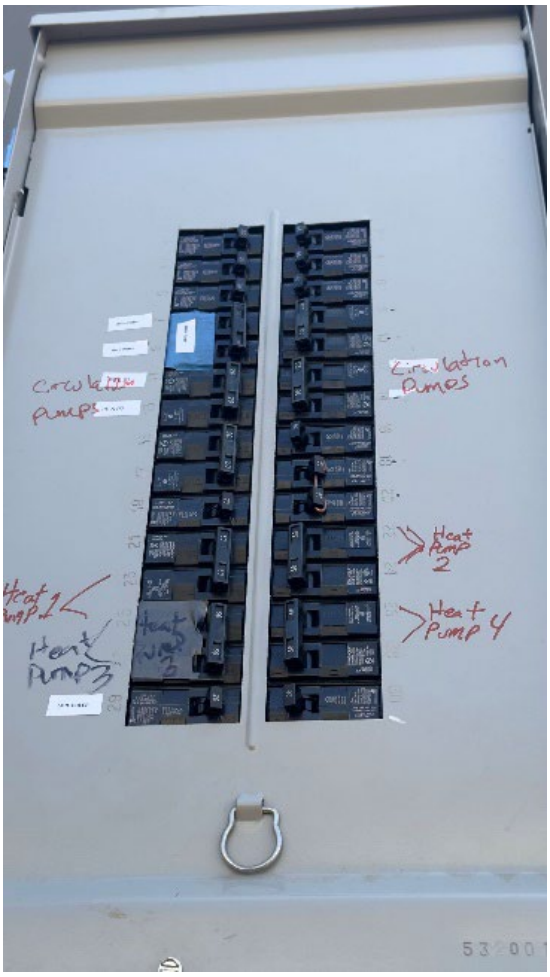


2.2. Turn on the circulating pumps using switches located inside the control room

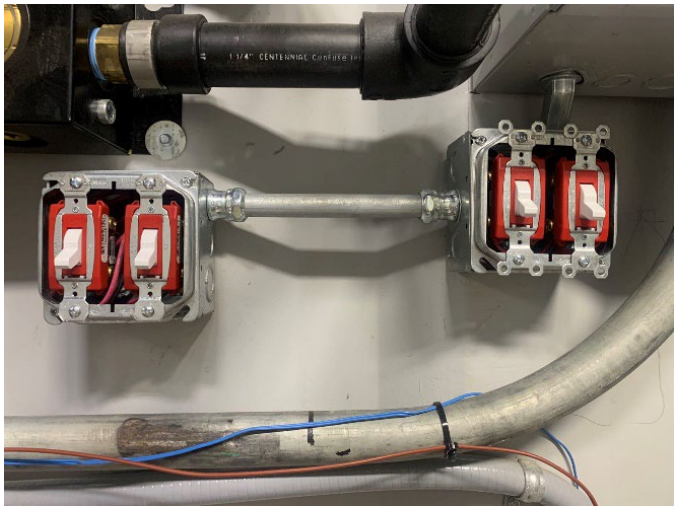

**Step 3: Temperature Setting on Tekmar 519**

3.1. Use the two triangle buttons below the display on the thermostat to set the heat pump's desired output temperature. The maximum setting temperature allowed is 105 °F. For mild winter events (air temperature is between 27 °F to 32 °F), 95 °F is the suggested thermostat setting temperature. If the air temperature is below 27 °F, the setting temperature is 105 °F. However, in most cases, setting thermostat temperatures to 105 °F is probably not the most energy-efficient temperature. Note: The Number 81 shown in the thermostat interface means the setting temperature. The number 52 shown in the thermostat interface indicates the heat pump output fluid temperature measured by the thermocouple attached to Tekmar 519.

Tekmar 519 thermostat


**Step 4: Monitoring the Operation Status of Heat Pumps and Circulating Pumps**

4.1. Once you have finished setting the temperature on the Tekmar 519, stay on site for 10-15 minutes until the heat pump output temperature reaches the set temperature and no overheating occurs.

- Note: For example, as shown in the thermostat interface, the setting temperature is 81 °F, and the output fluid temperature is 52 °F. The heat pump will start working, and the number 52 will blink and increase to 81. When the output fluid temperature reaches 81°F, the heat pump will stop, meaning that no overheating occurs.

**Step 5: Monitoring the Working Status of Bridge Heating Panels**

5.1. Visually check the operation status of the bridge heating panels underneath the bridge to ensure no leakage occurs.

**Step 6: Turn off the Heat Pump and Circulating Pump**

6.1. When the weather forecast indicates the winter event has passed and the air temperature for the next few days is greater than 32 °F, the system can be shut off.

6.2. First, turn off switches that control circulating pumps, as shown in Step 2.2.

6.3. Then turn off the switches on the electrical panel, as shown in Step 2.1.

6.4. Ensure all valves, as shown in Step 1, are set to close.

**Startup Sequence for Bypass Mode without Heat Pumps**

**(for bridge heating or summer recharging)**

**Step 1: Valve Check**

1.1. Ensure that all manifold valves, the bypass valve (labeled V-Bypass), and four buffer tank valves (labeled V-1, V-2, V-3, and V-4) are at the right position, as shown in the photos.

- Note: Please pay attention to the orientation of the Bypass valve. It is considered open when the arrow on the valve is parallel to the pipe.
- Note: Please make sure that all the manifold flow setters have been set at 5 GPM.

***V-Bypass*** ***V-1*** ***V-4*** ***V-Manifolds*** ***Manifold Flow setter***





- Note: Two flushing vales (V-Flushing) must be in the position as shown in the photo.

***V-Flushing***

**Step 2: Power Supply**

2.1. Confirm a stable power supply to the main pump (behind the Buffer Tank) and bypass flow pump (manual Switch labeled Bypass).

***Main Pump***

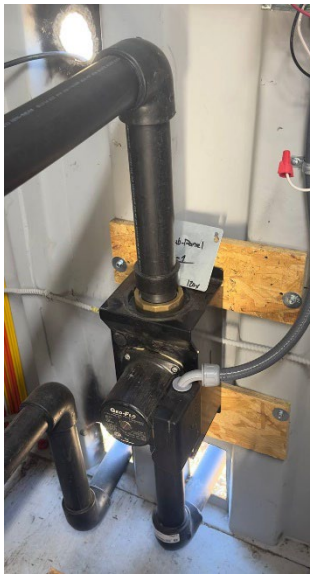

***Bypass Flow Pump***

***Manual Switch***


**Step 3: Monitoring circulation pump working status, pressure, and temperature**

3.1. Ensure proper water flows through the loop.

3.2. Monitor the pumps for any unusual noises or vibrations.

3.3. Continuously monitor the system's pressure and temperature gauges to ensure they are within the recommended operating range.

3.4. Promptly address any abnormal readings.

**Step 4: Check for leaks**

4.1. Inspect the entire system for any signs of leaks.

4.2. Address any identified leaks immediately.

**Step 5: Turn off the circulating pump**

5.1. When the weather forecast indicates the winter event has passed and the air temperature for the next few days is larger than 32 °F, the system can be shut off during a mild winter event.

5.2. First, turn off switches that control circulating pumps, as shown in Step 2.1.

5.3. Ensure valves V-1 and V-4, as shown in Step 1, are set to close.

# REFERENCES


Agent, K. R., & Deen, R. C. (1976). Highway accidents at bridges. Journal of the Transportation Research Board, Transportation Research Record (601).

Amatya, B. L., Bourne-Webb, P. J., Amis, T., Soga, K., and Laloui, L. (2012). "Thermo-mechanical behaviour of energy piles." *Géotechnique*, 62(6), 503-519.

American Society of Heating, R., and Engineers, A.-C. (1995). *1995 ASHRAE Handbook: Heating, ventilating, and air-conditioning applications*, American Society of Heating, Refrigerating and Air-Conditioning Engineers.

Andersson, O., Ekkestubbe, J., and Ekdahl, A. (2013). "UTES (Underground Thermal Energy Storage)—Applications and Market Development in Sweden." *J. Energ. Pow. Eng*, 7, 669.

Andersson, O., Ekkestubbe, J., and Ekdahl, A. (2013). "UTES (Underground Thermal Energy Storage)â€”Applications and Market Development in Sweden." *J. Energ. Pow. Eng*, 7(Journal Article), 669.

Balbay, A., and Esen, M. (2010). "Experimental investigation of using ground source heat pump system for snow melting on pavements and bridge decks." *Scientific Research and Essays*, 5(Journal Article), 3955-3966.

Balbay, A., and Esen, M. (2013). "Temperature distributions in pavement and bridge slabs heated by using vertical ground-source heat pump systems." *Acta Scientiarum. Technology*, 35(Journal Article), 677-685.

Bonte, M., Stuyfzand, P. J., Hulsmann, A., and Van Beelen, P. (2011). "Underground Thermal Energy Storage: Environmental Risks and Policy Developments in the Netherlands and European Union." *Ecology and Society*, 16(1).

Bourne-Webb, P. J., Soga, K., Amis, T., Davidson, C., Payne, P., and Amatya, B. (2009). "Energy pile test at Lambeth College, London: geotechnical and thermodynamic aspects of pile response to heat cycles." *Géotechnique*, 59(3), 237-248.

Boyd, T. L. (2003). "New snow melt projects in Klamath Falls, OR." *Geo-Heat Center Quarterly Bulletin*, 24, 12-15.

Brun, G. (1965). "La régularisation de l'energie solaire par stockage thermique dans le sol." *Revue Général de Thermique, 44, August.*

Brun, G. (1967). "Le stockage thermique dans le sol en vue de la regularisation de l'energie solaire." *Comptes*, 13, 39-44.

Cheng, Q., Mingzhi, L., Chunwu, S., and Xianying, L. (2005). "Performance test of ground source heat pump systems in summer and heat transfer model." *Hv & Ac*, 3, 001.

Chiasson, A., and Spitler, J. D. (2000). "A modeling approach to design of a ground-source heat pump bridge deck heating system." *Transportation Research Record: Journal of the Transportation Research Board*, 1741(Journal Article), 207-215.

Chowdhury, M. (2019) *Analytical and numerical modeling of externally heated geothermal bridge deck*. MS thesis, Arlington, TX: University of Texas at Arlington.

Clesson, J. a. H. (1981). "Model studies of duct storage systems." *Dept. of Mathematical Physics. Lund Inst. of Technology, Lund, Sweden.*

Cress, M. D. (1995). "Heated bridge deck construction and operation in Lincoln, Nebraska." (Journal Article), 448-454.

Desmedt, J., Hoes, H., and Van Bael, J. "Status of underground thermal energy storage in Belgium." *Proc., 10th International Conference on Thermal Energy Storage, New Jersey, USA*.

Dickinson, J. S., Buik, N., Matthews, M. C., and Snijders, A. (2009). "Aquifer thermal energy storage: theoretical and operational analysis." *Geotechnique*, 59(Journal Article), 249-260.

Donnelly, D. E. (1981). "GEOTHERMAL ENERGY FOR HIGHWAY SNOW AND ICE CONTROL." internal-pdf://3783037501/Geothermal Energy for Highway Snow and Ice Con.pdf.

Eugster, J. W. "Road and bridge heating using geothermal energy. overview and examples." *Proc., Proceedings European Geothermal Congress*.

Faccini, E. C. (1976). "Heat transfer simulation of the geothermal heating of bridge decks using heat pipes." 45, University of Wyoming.

Federal Highway Administration (FHWA) (2005). Highway economic requirements system state version, technical report. Washington

Gaine, K., and Duffy, A. (2010). "A life cycle cost analysis of large-scale thermal energy storage technologies for buildings using combined heat and power." *Proceedings of Renewable Energy Conference 2010*.

Gaine, K., and Dufy, A. "A life cycle cost analysis of large-scale thermal energy storage technologies for buildings using combined heat and power." *Proc., Renewable Energy Research Conference 2010 Zero Emission Buildings NTNU*.

Griffin, R. G. (1982). "Highway Bridge Deicing Using Passive Heat Sources." *Publication No. FHWA-CO-82-7, Colorado Dept. of Highways. Springfield, VA* internal-pdf://2777906954/Highway Bridge Deicing Using Passive Heat Sour.pdf.

Gustafson, G. (1985). "Heat Storage in Caverns, Tanks and Pits." *An Overview of Swedish Experiences. Proc. Enerstock'85, Toronto, Canada.* , 525-531.

Habibzadeh-Bigdarvish, O., Yu, X., Lei, G., Li, T., & Puppala, A. J. (2019). Life-Cycle cost benefit analysis of Bridge deck de-icing using geothermal heat pump system: A case study of North Texas. Sustainable cities and society, 47, 101492

Habibzadeh-Bigdarvish, O., Yu, X., Li, T., Lei, G., Banerjee, A. and Puppala, A.J., 2021. A novel full-scale external geothermal heating system for bridge deck de-icing. Applied Thermal Engineering, 185, p.116365.

Hasnain, S. M. (1998). "Review on sustainable thermal energy storage technologies, Part I: heat storage materials and techniques." *Energy Conversion and Management*, 39(Journal Article), 1127-1138.

Heloasz, Z., and Ostaficzuk, S. (2001). "How to use waste heat and geothermal energy for de-snowing and de-icing in Poland-concepts and problems." *Proceedings of International Scientific Conference*, 149-154.

Hoyer, M. C. W., M.; Kanivetsky, R. and Holm, T. R. (1985). "Short-term aquifer thermal energy storage (ATES) test cycles, St. Paul, Minnesota U.S.A." *Proceedings, Enerstock 85, Toronto Canada*, 75-79.

Huang, Y. H., Adams, T. M., & Pincheira, J. A. (2004). Analysis of life-cycle maintenance strategies for concrete bridge decks. Journal of Bridge Engineering, 9(3), 250–258

Iris, P. a. V., P (1988). "An example of heat pumps on aquifer for collective dwellings: comments after 5 years of operation." *Proceedings, Jigastock 88, Versailles, France.[IV88]*.

Iwamoto, K., Nagasaka, S., Hamada, Y., Nakamura, M., Ochifuji, K., and Nagano, K. "Prospects of snow melting systems (SMS) using underground thermal energy storage (UTES) in Japan." *Proc., The Second Stockton International Geothermal Conference*.

Jahansson, B. a. N., B (1980). "The borehole heat store - a plant for seasonal heat storage." *Report A nr.39. TULEA 1980:14. Div. of Water Res. Eng., Lulea University of Technology, Sweden (in Swedish)*.

Jiang, C., Zheng, J., Liu, J., Wu, L., and Jin, Y. (2011). "Studies review of the technology for snow and ice control for winter road maintenance." *ICTE 2011*, 3245-3254.

Johnston, I. W., Narsilio, G. A., and Colls, S. (2011). "Emerging geothermal energy technologies." *KSCE J Civ Eng*, 15(4), 643-653.

Hurley, Mark; Habibzadeh-Bigdarvish, Omid; Lei, Gang; Yu, Xinbao (2024): Laboratory study of a hydronic concrete deck heated externally in a controlled sub-freezing environment. In Energy and Built Environment 5 (1), pp. 9–23. DOI: 10.1016/j.enbenv.2022.07.003.

Kaller, R. (2007). "Dimensioning of deicing and some melting systems suppiled by geothermal energy."

Kamimura, S., Kuwabara, K., and Umemura, T. "Pavement snow-melting system utilizing shallow layer geothermal energy." *Proc., Snow Engineering: Recent Advances and Developments. Proceedings of the Fourth International Conference on Snow Engineering.*, 409.

Kannberg, L. D. (1985). "Aquifer thermal energy storage in the United States." *Proceedings Enerstock '85, Toronto Canada*(3-8).

Kilkis, I. B. (1994). "Design of embedded snow-melting systems: heat transfer in the slab-a simplified model." *ASHRAE Transaction*, 1(Journal Article), 434-441.

Knellwolf, C., Peron, H., and Laloui, L. (2011). "Geotechnical Analysis of Heat Exchanger Piles." *Journal of Geotechnical and Geoenvironmental Engineering*, 137(10), 890-902.

Laloui, L. (2010). "Advances in Energy Piles analyses." *MITTEILUNGEN der GEOTECHNIK SCHWEIZ PUBLICATION de la GÉOTHECHNIQUE SUISSE*, 23.

Laloui, L., Nuth, M., and Vulliet, L. (2006). "Experimental and numerical investigations of the behaviour of a heat exchanger pile." *International Journal for Numerical and Analytical Methods in Geomechanics*, 30(8), 763-781.

Lee, K. S. (2010). "A review on concepts, applications, and models of aquifer thermal energy storage systems." *Energies*, 3(Journal Article), 1320-1334.

Lei, G., Yu, X., Li, T., Habibzadeh-Bigdarvish, O., Wang, X., Mrinal, M., and Luo, C. (2020). "Feasibility study of a new attached multi-loop CO2 heat pipe for bridge deck de-icing using geothermal energy." Journal of Cleaner Production, 275, 123160.

Chowdhury, M. (2019) Analytical and numerical modeling of externally heated geothermal

Liu, C. L., F.; Ma, L. P. and Cheng, H. M. (2010). "Advanced materials for energy storage." *Advanced Materials*, 22, E28-E62.

Liu, X. (2005). "Development and experimental validation of simulation of hydronic snow melting systems for bridges." DOCTOR OF PHILOSOPHY, Tongji University.

Liu, X., and Spitler, J. D. "A simulation tool for the hydronic bridge snow melting system." *Proc., 12th International Road Weather Conference*.

Liu, X. B., Rees, S. J., and Spitler, J. D. (2003). "Simulation of a geothermal bridge deck anti-icing system and experimental validation." (Journal Article).

Liu, X. B., Rees, S. J., and Spitler, J. D. (2007). "Modeling snow melting on heated pavement surfaces. Part II: Experimental validation." *Applied Thermal Engineering*, 27(Journal Article), 1125-1131.

Lund, J. W. (1999). "Reconstruction of a pavement geothermal deicing system." *Geo-Heat Center Quarterly Bulletin*, 20(Journal Article), 14-17.

Lund, J. W., and Freeston, D. H. (2001). "World-wide direct uses of geothermal energy 2000." *Geothermics*, 30(Journal Article), 29-68.
Mangold, D., and Schmidt, T. (2007). "The next generations of seasonal thermal energy storage in Germany." *Weiterentwicklung der Erdbecken Wärmespeichertechnologie (Development of Pit Thermal Energy Storage Technology*.
Manonelles, J. J. (2014). "Large-scale underground thermal energy storage." *University of de Lieida*.
Margen, P. H. (1959). "Thermal Storage in Rock Chambers." *Nuclear Engineering (Great Britain) 4, p. 259.*
Mathey, B. (1975). "Le stockage de chaleur dans les nappes souterrains (Application à l'Energie Solaire)." *IPEN-EPF Lausanne et CHYN Uni Neuchâtel, Nov.* .
McCartney, J. S., Sánchez, M., and Tomac, I. (2016). "Energy geotechnics: Advances in subsurface energy recovery, storage, exchange, and waste management." *Computers and Geotechnics*, 75, 244-256.
Meyer, C. F. a. T., D. K. (1974). "Heat storage wells - an answer to energy conservation and thermal pollution." *Water Well Journal*, 25, 35-41.
Minsk, L. D. (1999). "Heated bridge technology: report on ISTEA Sec. 6005 program."Washington, DC 20590, internal-pdf://4282711904/Heated Bridge Technolog - a reprot by FHWA.pdf.
Molz, F. J. P., A. D.; Andersen, P. F.; Lucido, V. D., and Warman, J. C. (1979). "Thermal energy storage in a confined aquifer: experimental results." *Water Resources Research*, 15(6), 1509-1514.
Morita, K., Bollmeier, W., and Mizogami, H. (1992). "Analysis of the results from the downhole coaxial heat exchanger (DCHE) experiment in Hawaii." *Transactions - Geothermal Resources Council*.
Morita, K., and Tago, M. (2000). "Operational Characteristics of the Gaia Snow-Melting System in Ninohe, Iwate, Japan, Development of a Snow-Melting System Which Utilizes Thermal Functions." *World Geothermal Congress*.
Nagai, N., Miyamoto, S., Nishiwaki, M., and Takeuchi, M. (2009). "Numerical simulation of snow melting on pavement surface with heat dissipation pipe embedded." *Heat Transferâ€"Asian Research*, 38(Journal Article), 313-329.
Nielsen, K. (2003). "Thermal energy storage-a state of the art." *A report within the research program"Smart Energy-Efficient Buildings" at NTNU and SINTEF*.
Nordell, B. (1994). "Borehole heat store design optimization. ." *PhD thesis, Lulea University of Technology, Sweden, pp.196.*
Nordell, B. (2000). "Large-scale thermal energy storage." *Proceedings of Winter Cities*(Journal Article), 1-10.
Nordell, B. (2012). "Underground Thermal Energy Storage (UTES)." *LuleÃ¥ University of*(Journal Article).
Nordell, B., Grein, M., and Kharseh, M. (2007). "Large-scale utilisation of renewable energy requires energy storage." *International confernce for renewable energies and sustainable development (ICRESD_07), UniversitÃ© Abou Bakr BELKAIDâ€"TLEMCEN, Algeria, May*(Journal Article), 21-24.
Nordell, B., and Hellström, G. (2000). "High temperature solar heated seasonal storage system for low temperature heating of buildings." *Solar Energy*, 69(6), 511-523.

Ohga, H. a. M., K. "Energy performance of borehole thermal energy storage systems." *Proc., Seventh International IBPSA Conference, Brazil*, 1009-1016.

Olgun, C. G., and Bowers, G. A. "Numerical modelling of ground source bridge deck deicing."

Paksoy, H. O., Andersson, O., Abaci, S., Evliya, H., and Turgut, B. (2000). "Heating and cooling of a hospital using solar energy coupled with seasonal thermal enegy storage in an aquifer." *Renewable Energy*, 19, 117-122.

Penrod, E. B. G., O. W.; Jones, C. D.; Collier, H. E. and Batey, R. N. (1949). "Earth Heat Pump Research." *University of Kentucky Bulletin 14, December, Lexington KY.* .

Ramsey, J. W., Hewett, M. J., Kuehn, T. H., and Petersen, S. D. (1999). "Updated design guidelines for snow melting systems." *ASHRAE Transactions*, 105(Journal Article), 1055.

Rees, S. J., Spitler, J. D., and Xiao, X. (2002). "Transient analysis of snow-melting system performance." *ASHRAE Transactions*, 108(Journal Article), 406-423.

Rosenberg, J. E. (2010). "Centrifuge modeling of soil-structure interaction in thermo-active foundations." M.S. 1481159, University of Colorado at Boulder, United States -- Colorado.

Sanner, B. (2001). "Shallow geothermal energy." *Geo-Heat Center Bulletin*, 22(Journal Article), 19-25.

Sanner, B., Kabus, F., Seibt, P., and Bartels, J. "Underground thermal energy storage for the German Parliament in Berlin, system concept and operational experiences." *Proc., Proceedings world geothermal congress*, 1-8.

Schaetzle, W. J. B., E. C.; Jackins, G. A. and Miller, E. B. (1981). "Free-cooling applications using annual aquifer thermal energy storage." *Proceedings, International Conference on Seasonal Thermal Energy Storage and Compressed Air Energy Storage, Seattle WA*, 1, 310-319.

Skogsberg, K. (2005). "Seasonal snow storage for space and process cooling." *Architecture and Infrastructure, Luleå University of Technology. Luleå: Luleå University of Technology*, 1402-1544.

Socaciu, L. G. (2011). "Seasonal sensible thermal energy storage solutions." *Leonardo Electronic Journal of Practices and Technologies*(19), 49-68.

Spitler, J. D. (2000). "GLHEPRO -- A Design Tool For Commercial Building Ground Loop Heat Exchangers." *Proceedings of the Fourth International Heat Pumps in Cold Climates Conference, Aylmer, Québec.*

Stephen, C. J., and James, W. R. (2003). "Smart Control of a Geothermally Heated Bridge Deck." (Journal Article).

Suryatriyastuti, M. E., Mroueh, H., and Burlon, S. (2012). "Understanding the temperature-induced mechanical behaviour of energy pile foundations." *Renewable and Sustainable Energy Reviews*, 16(5), 3344-3354.

Swanson, H. N. (1980). "Evaluation of geothermal energy for heating highway structures."

Tsang, C. F. L., M. J. and Witherspoon, P. A. (1976). "Numerical modelling of cyclic storage of hot water in aquifers." *Symposium on Use of Aquifer Systems for Cyclic Storage of Water. Fall Annual Meeting of American Geophysical Union, San Francisco CA.*

Wadivkar, O. (1997). "An Experimental And Numerical Study Of The Thermal Performance Of A Bridge Deck De-Icing System." Master of Science Thesis, Oklahoma State University, Stillwater, OK.

Wang, H., Zhao, J., and Chen, Z. (2008). "Experimental investigation of ice and snow melting process on pavement utilizing geothermal tail water." *Energy Conversion and Management*, 49(Journal Article), 1538-1546.

Wong, B. S., A.; McClung, L. "Recent inter-seasonal underground thermal energy storage applications in Canada." *Proc., EIC Climate Change Technology, 2006 IEEE,* IEEE, 1-7.

Yoshitake, I., Yasumura, N., Syobuzako, M., and Scanlon, A. (2011). "Pipe Heating System with Underground Water Tank for Snow Thawing and Ice Prevention on Roads and Bridge Decks." *Journal of Cold Regions Engineering*, 25(2), 71-86.

Yu, X., Hurley, M. T., Li, T., Lei, G., Pedarla, A., and Puppala, A. J. (2020). "Experimental feasibility study of a new attached hydronic loop design for geothermal heating of bridge decks." Applied Thermal Engineering, 164, 11450.

Yu, L., Jun, Z., Xingguo, L., Qiang, Z., and Jun, Z. (2004). "A heat transfer model and the experiments for vertical spiral geothermal heat pump." *Acta Energiae Solaris Sinica*, 25, 690-694.

Yu, Y., and Ma, Z. (2005). "Heat transfer model of underground heat exchangers in ground-coupled heat pump systems."

Yukie, K., and Masayoshi, K. "Introduction of Practical Use of Snow Mound." *Proc., Proceedings of llth International Conference on Thermal Energy Storage, Effstcck.*

Texas Department of Transportation (TxDOT) (2016). Report on Texas bridges as of September 2016https://ftp.dot.state.tx.us/pub/txdot-info/library/reports/gov/ bridge/fy16.pdf.

Texas Department of Transportation (TxDOT) (2017). Texas motor vehicle crash statistics (19 October 2018).

Vitaliano, D.F., (1992). An economic assessment of the social costs of highway salting and the efficiency of substituting a new deicing material. Journal of Policy Analysis and Management, 11(3), 397-418.

Zhang, J., Das, D., Peterson, R., and Goering, D. (2007). "Comprehensive evaluation of bridge anti-icing technologies-final report." *Alaska Department of Transportation and Public Facilities*.

Zhang, J., Das, D. K., and Peterson, R. (2009). "Selection of effective and efficient snow removal and ice control technologies for cold-region bridges." *Journal of Civil, Environmental, and Architectural Engineering*, 3(Journal Article), 1-14.

Zhou, Y., Zhang, Xu, and Chen, P. (2001). "Heat Transfer and Reasonable Distance Analysis for Vertical U-tubes Used in GSHP [J]." *Journal of Donghua University, Natural Science*, 5, 002.

Zizzo, R. (2009). "Designing an optimal urban community mix for an aquifer thermal energy storage system." *Master Thesis, University of Toronto*.

Zwarycz, K. (2002). "Snow melting and heating systems based on geothermal heat pumps at Goleniow Airport, Poland." (Journal Article), 431.